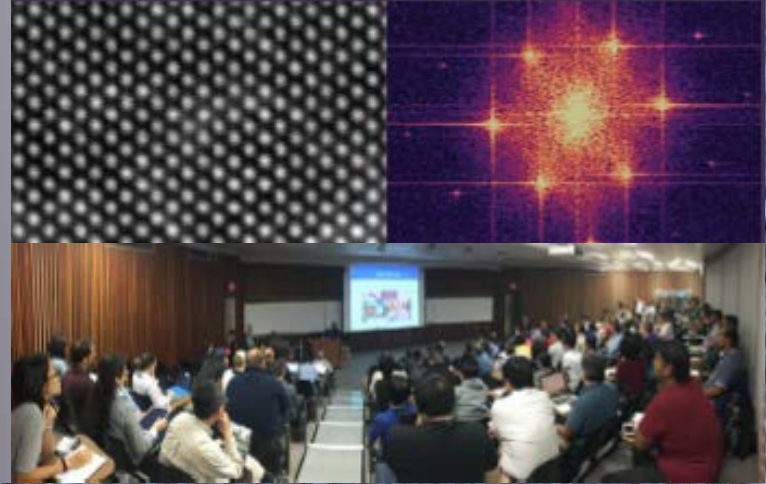


June 4 - 5, 2019

AMC

Advanced Materials
Characterization Workshop



Transmission Electron Microscopy

Jim Mabon, Wacek Swiech, CQ Chen and Honghui Zhou

Materials Research Laboratory
University of Illinois

amc.mrl.illinois.edu

 Materials
Research Laboratory

© 2019 University of Illinois Board of Trustees. All rights reserved.





1. Introduction to TEM

2. Basic Concepts

3. Basic TEM techniques

Diffraction

Bright Field & Dark Field TEM imaging

High Resolution TEM Imaging

4. Scanning Transmission Electron Microscopy (STEM)

5. Aberration-corrected STEM / TEM & Applications

6. Microspectroscopy & spectromicroscopy

X-ray Energy Dispersive Spectroscopy

Electron Energy-Loss Spectroscopy

EFTEM and Spectrum Imaging

7. Introduction to a New S/TEM: Themis Z

8. Summary





Why Use Transmission Electron Microscopy?

Optical Microscope



Resolution

$$d = \frac{\lambda}{2A_N}$$

A_N is 0.95 with air
up to 1.5 with oil

Resolution limit: ~200 nm

Transmission Electron Microscope (TEM)



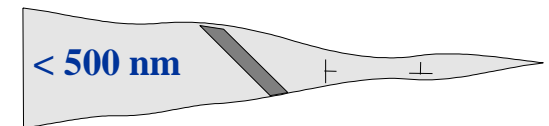
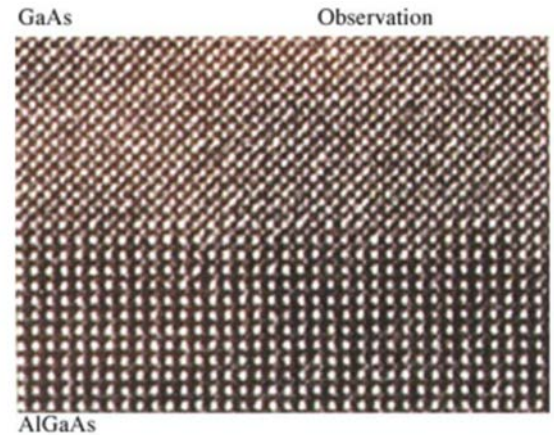
$$\lambda = h / (2mE_k)^{1/2} \sim (1.5 / U)^{1/2} \text{ [nm]}$$

200 keV electrons: $\lambda = 0.0027 \text{ nm}$

$$R = 0.66(C_s \lambda^3)^{1/4}$$

Resolution limit: ~0.15 nm
(uncorrected)

High Resolution TEM

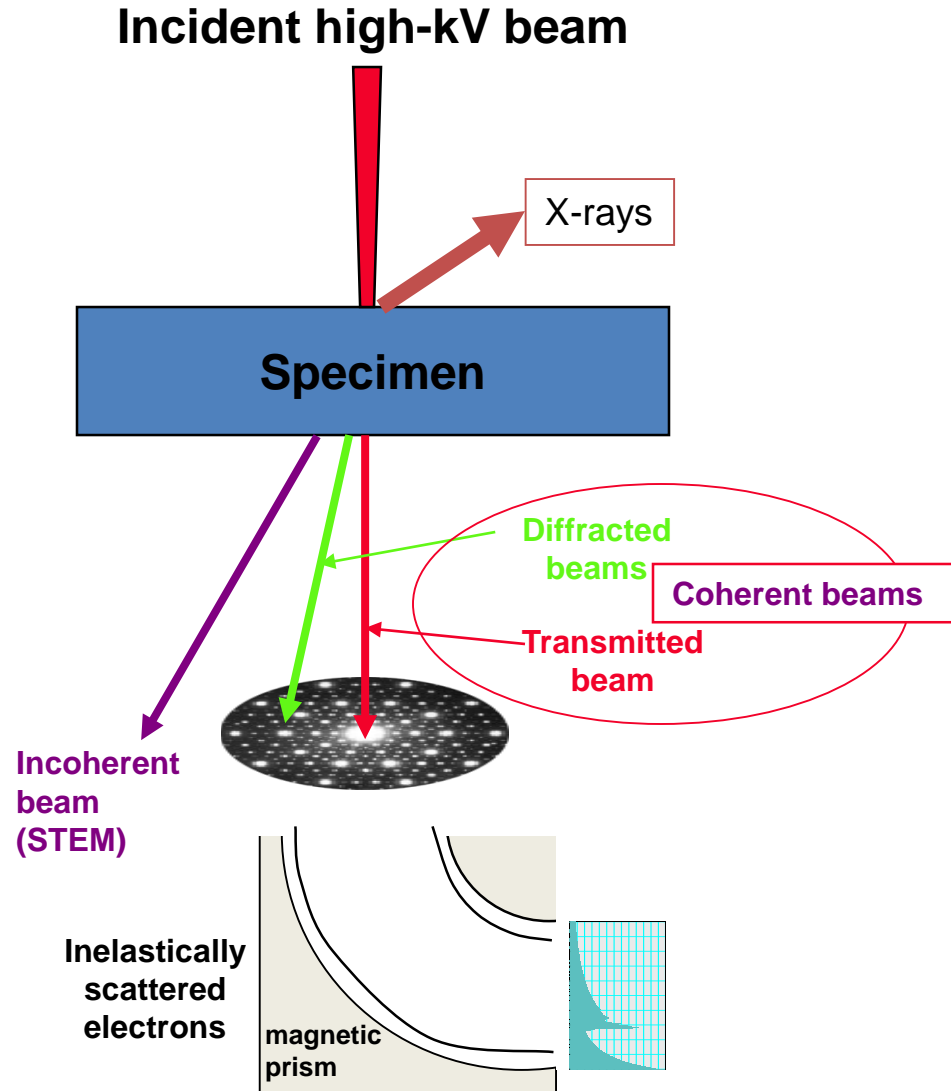
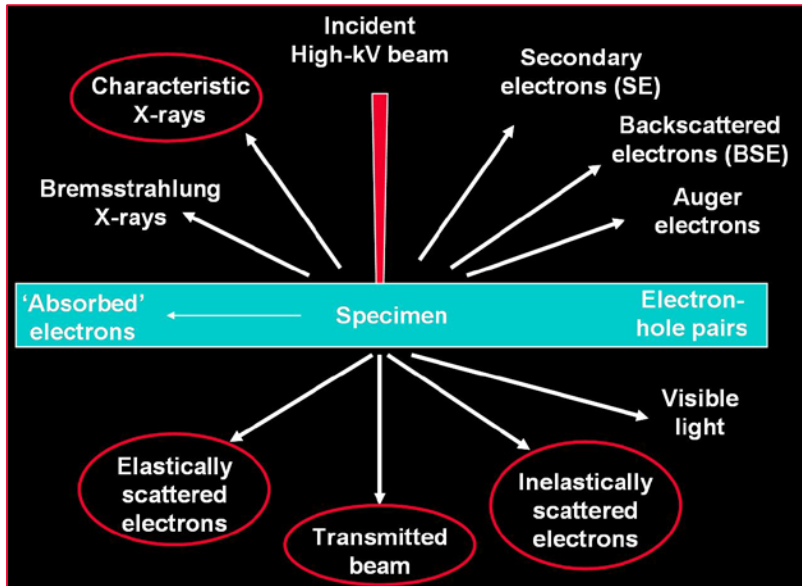


- Sample thickness requirement:
- Thinner than 500 nm
- High quality image: <20 nm

TEM is ideal for investigating thin foil, thin edge, and nanoparticles



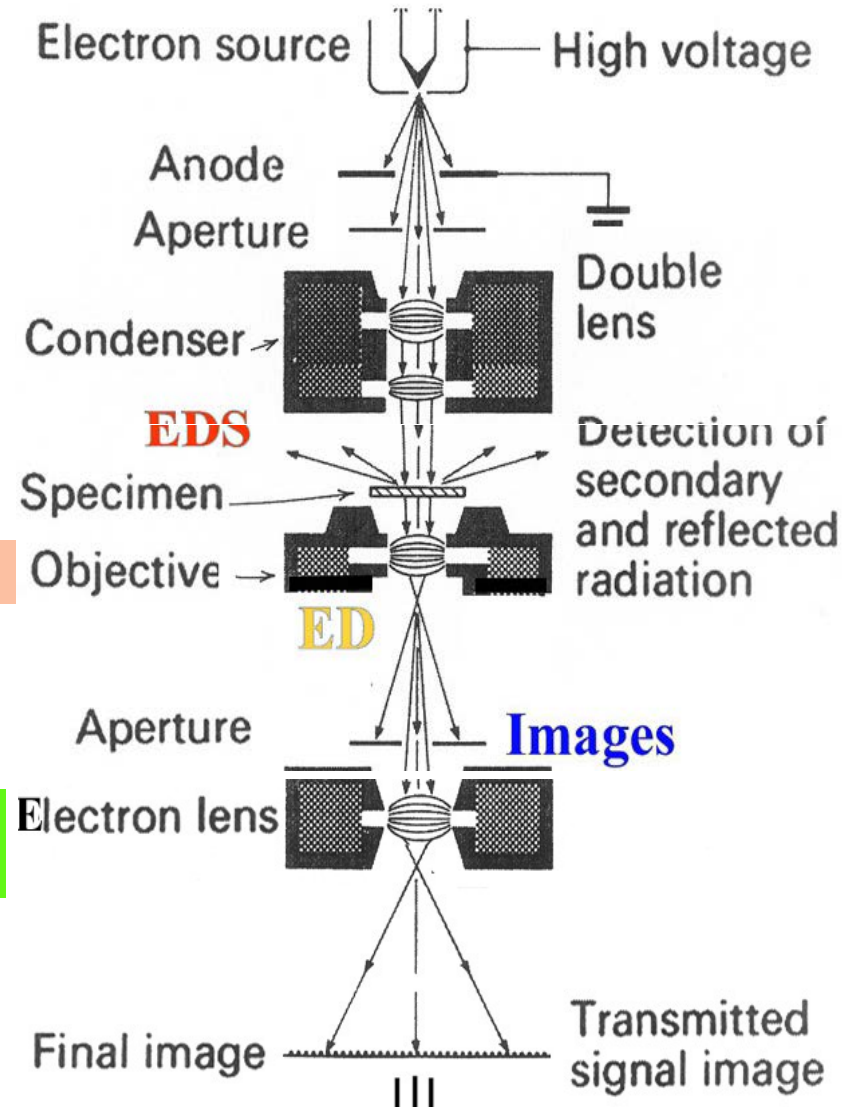
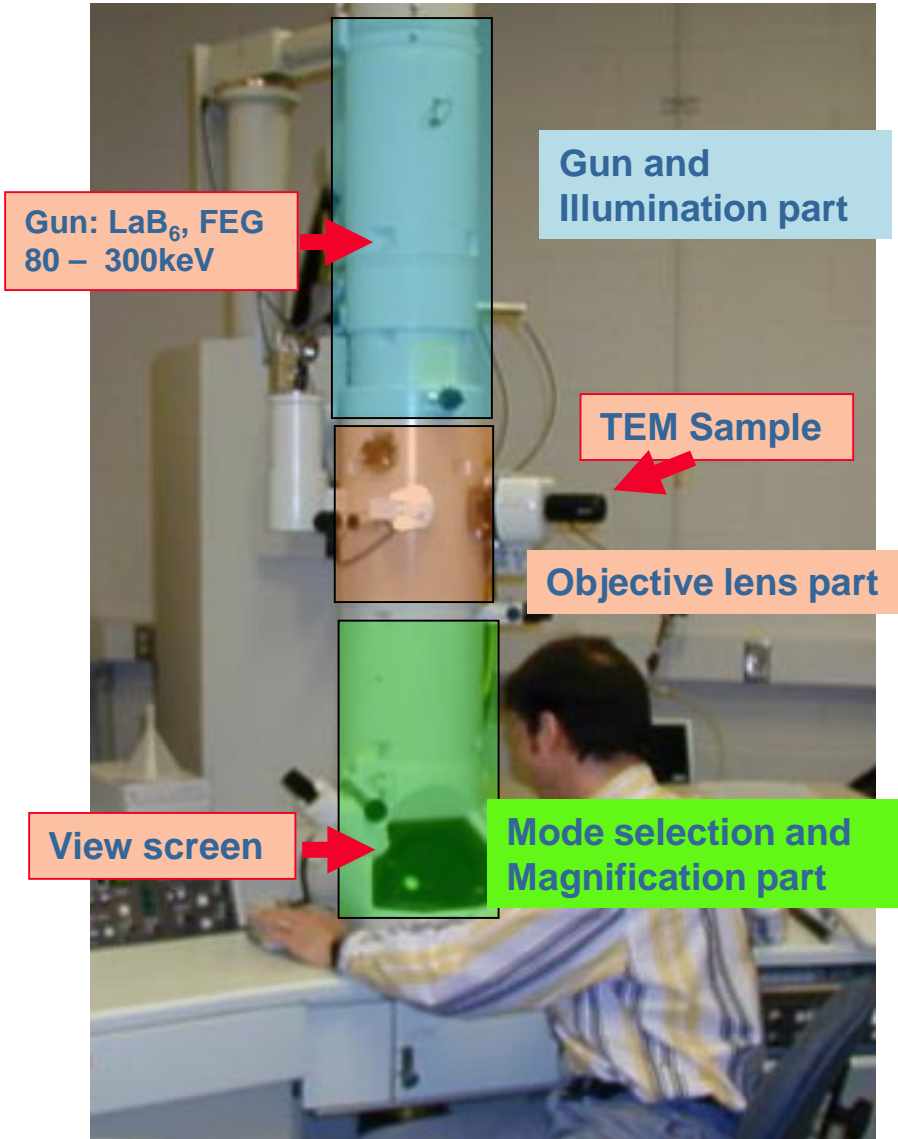
1. Transmitted electrons (beam)
2. Diffracted electrons (beams)
(Elastically scattered)
3. Coherent beams
4. Incoherent beams
5. Inelastically scattered electrons
6. Characteristic X-rays



TEM can acquire images, diffraction patterns, spectroscopic and chemically sensitive images **at resolution of 50 – 1000 of picometers.**



Structure of a TEM

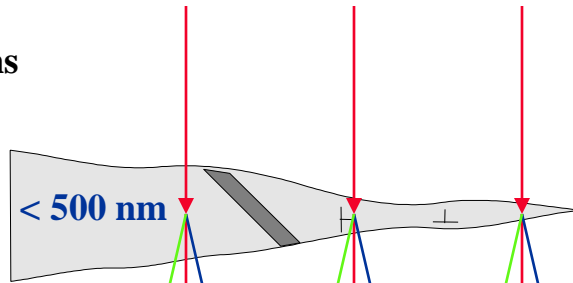




How does a TEM Obtain Image and Diffraction?

Incident Electrons

Sample



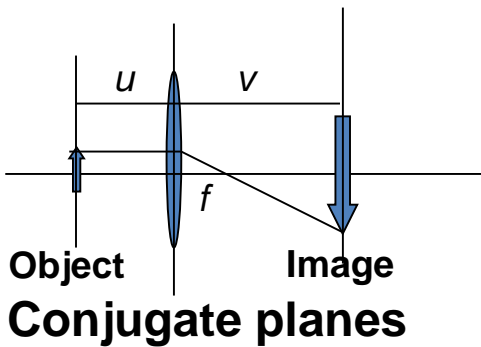
Objective Lens



Back Focal Plane



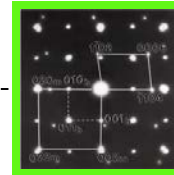
First Image Plane



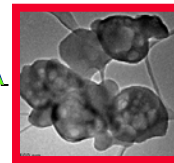
$$\frac{1}{u} + \frac{1}{v} = \frac{1}{f}$$

$$\text{Mag.} = v/u$$

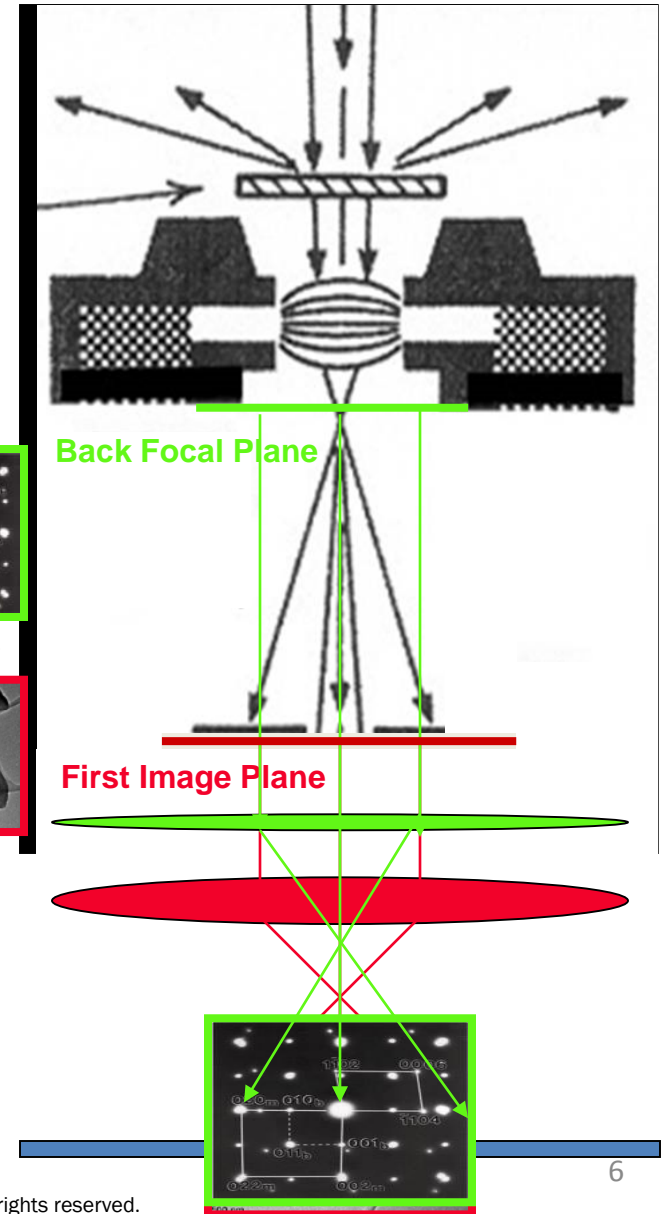
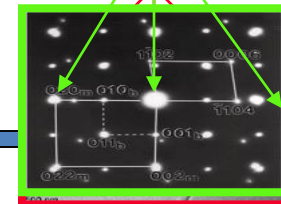
Structural info



Morphology

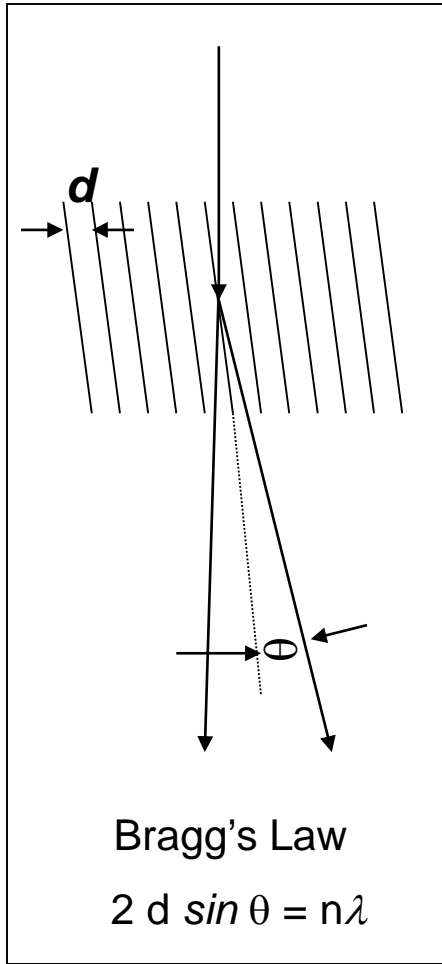


View Screen

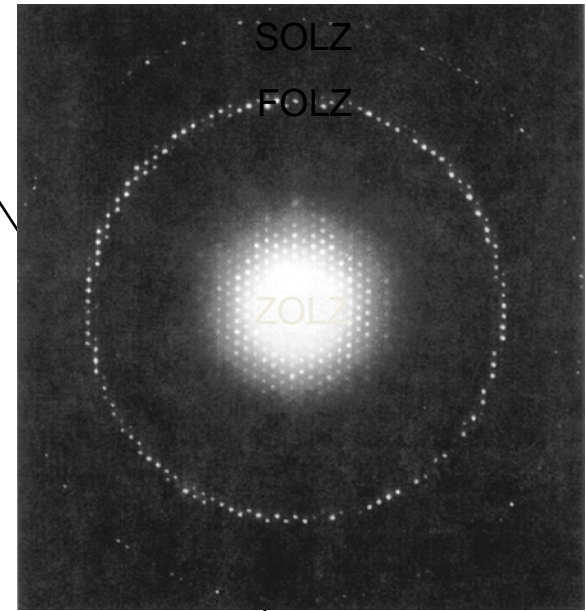




Electron Diffraction I

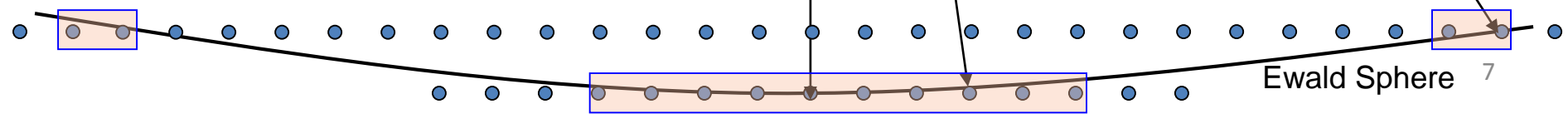


Wavelength
X-rays: about 0.1nm
Electrons: 0.0027nm,
@ 200kV



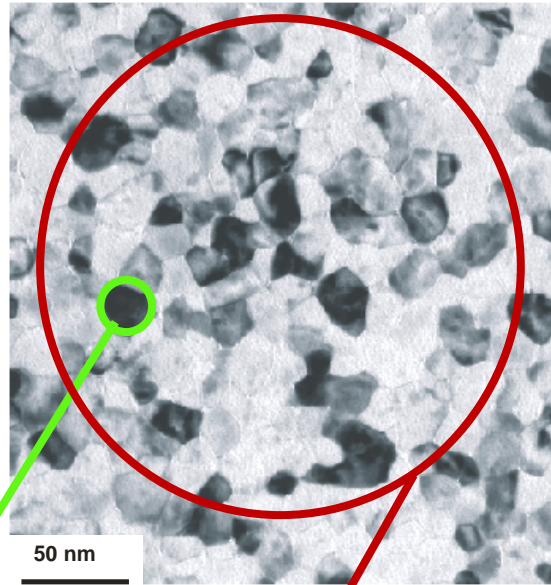
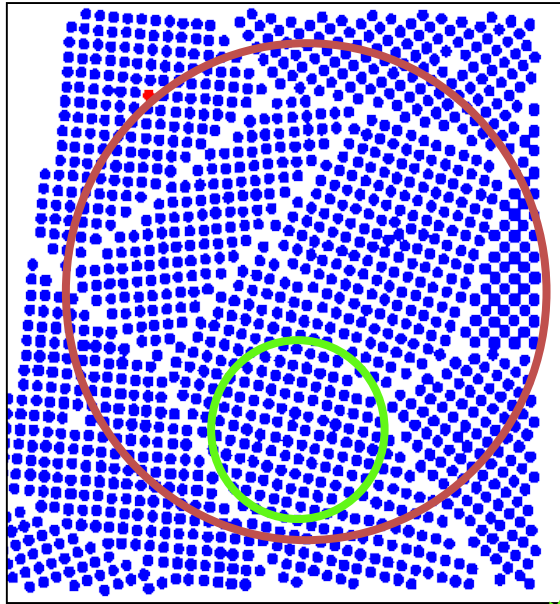
Zero-order Laue Zone (ZOLZ)
First-order Laue Zone (FOLZ)
....
High-order Laue Zone (HOLZ)

λ is small, Ewald sphere ($1/\lambda$) is almost flat

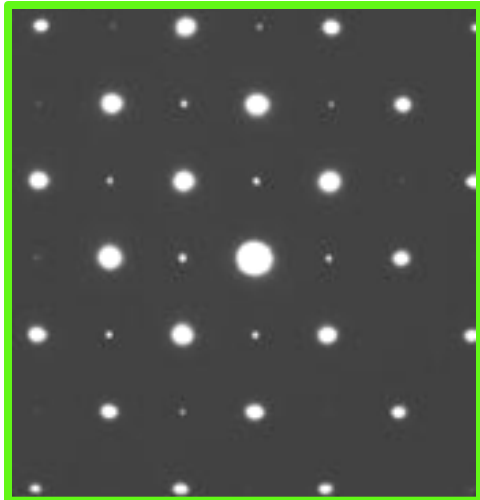




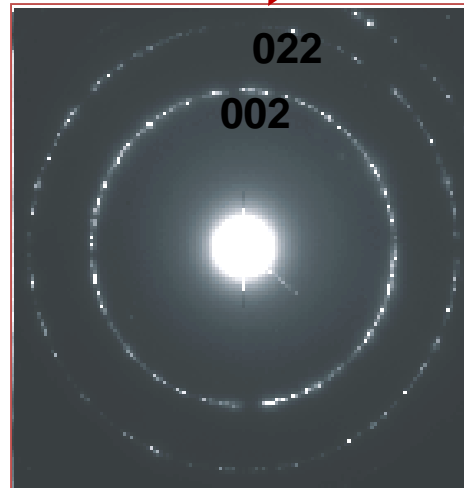
Electron Diffraction II



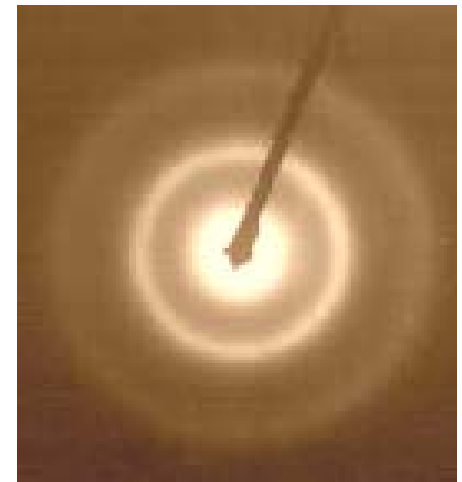
Diffraction patterns from single grain or multiple grains



Single crystal



Polycrystal



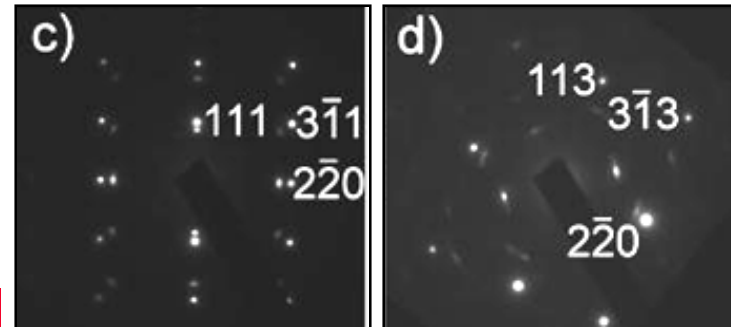
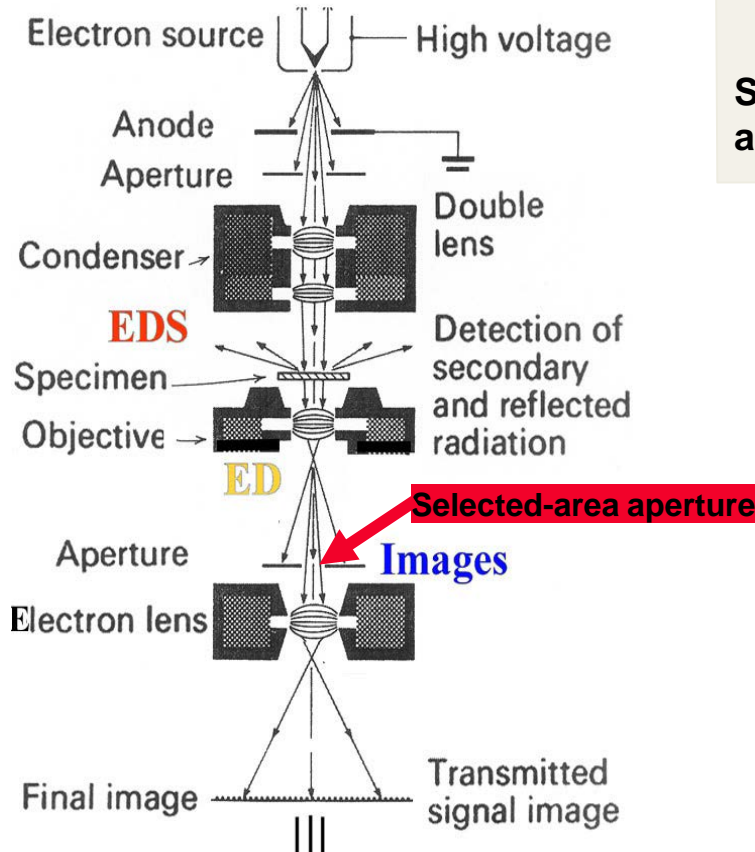
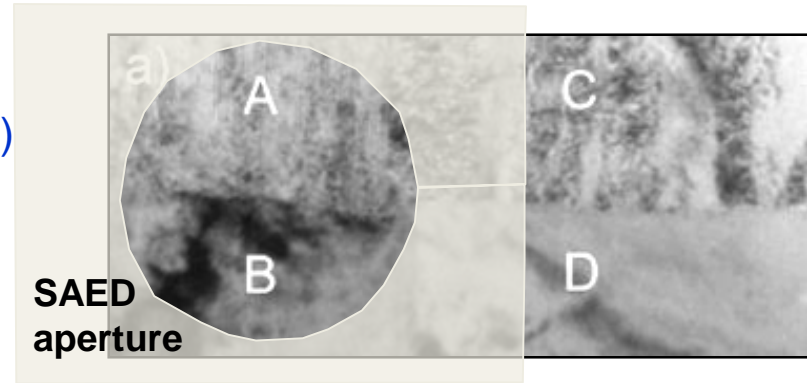
Amorphous



Example of SAED

Major Diffraction Techniques

- 1) Selected-Area Electron Diffraction (SAED)
- 2) NanoArea Electron Diffraction (NBED)
- 3) Convergent Beam Electron Diffraction (CBED)



Selected Area Electron Diffraction (SAED)

1. Illuminate a large area of the specimen with a parallel beam.
2. Insert an aperture in the first image plane to select an area of the image.
3. Focus the first imaging lens on the OL Back Focal Plane

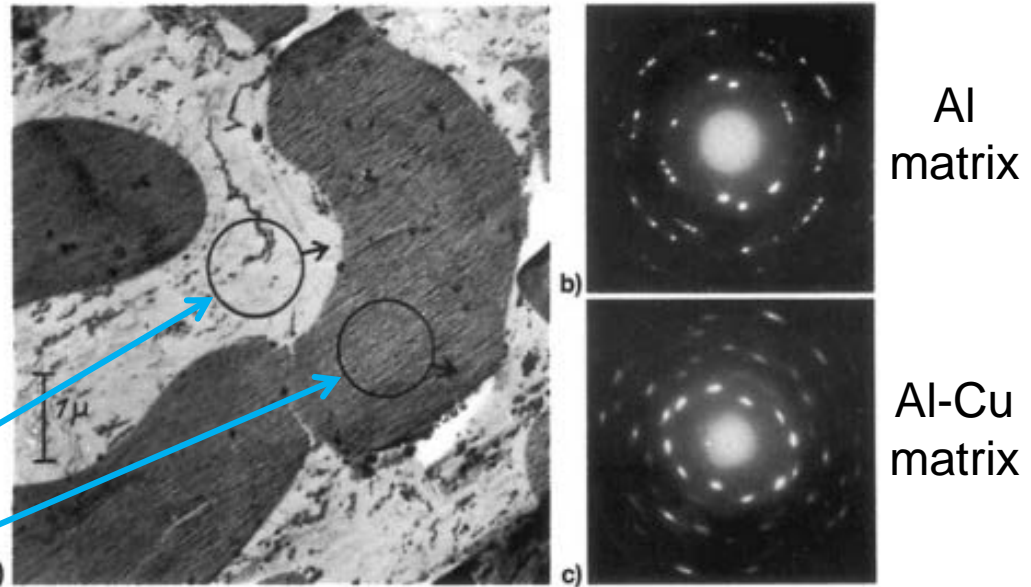
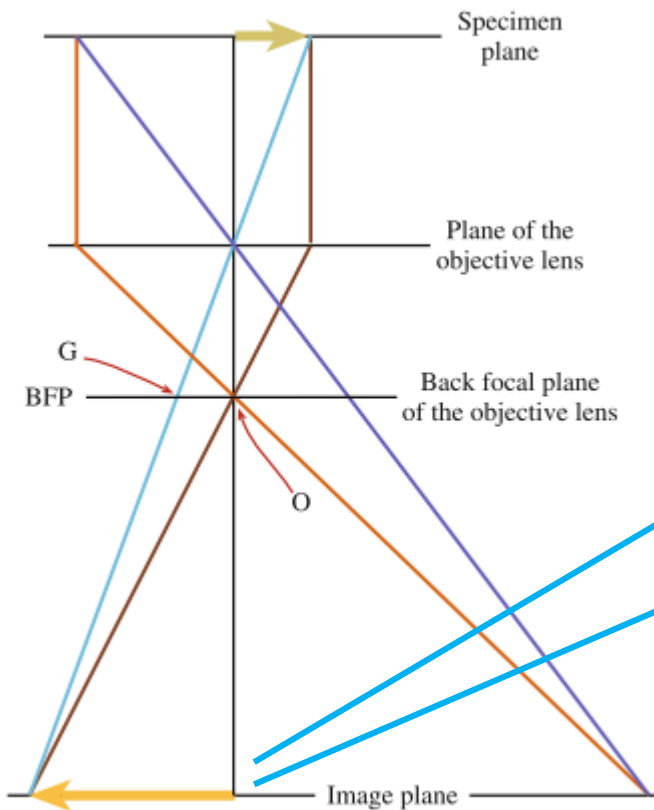


Fig. 8.1. Example of a selected-area electron diffraction (SAED) from a thin section of an Al-Cu eutectic cut with a microtome. (b) (Al matrix) and (c) (AlCu₂) contain the SAED pattern of the circles indicated in (a).

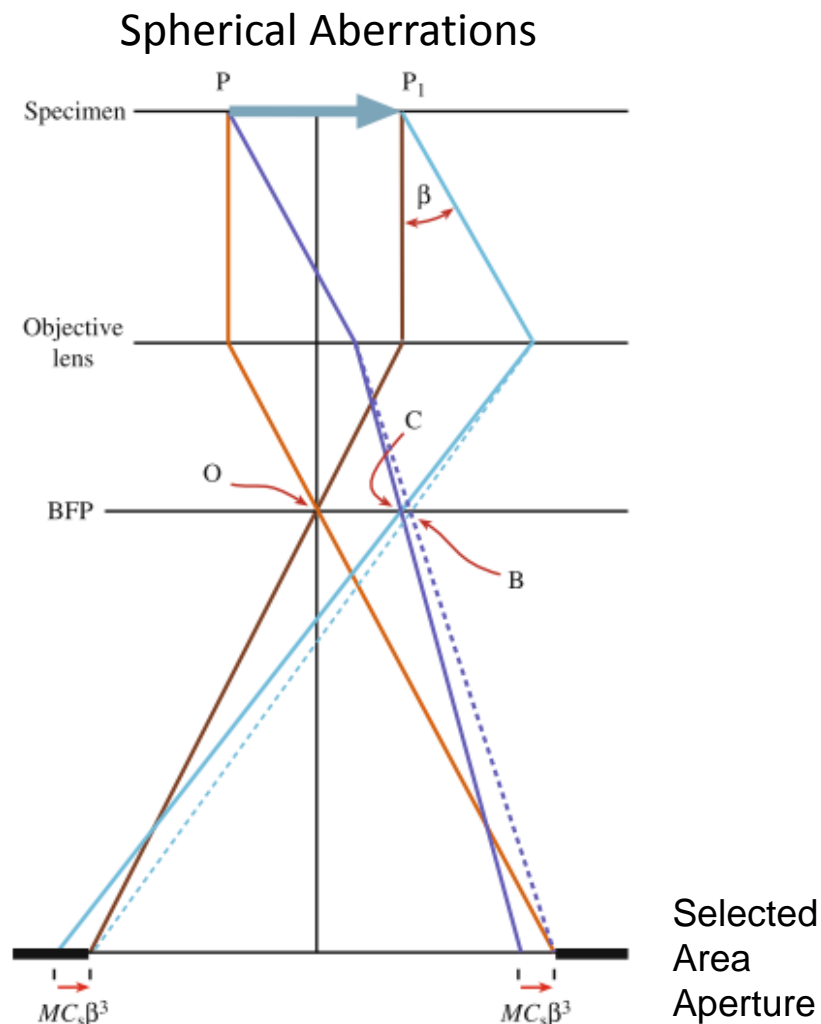
L. Reimer and H. Kohl, *Transmission Electron Microscopy, Physics of Image Formation*, 2008.

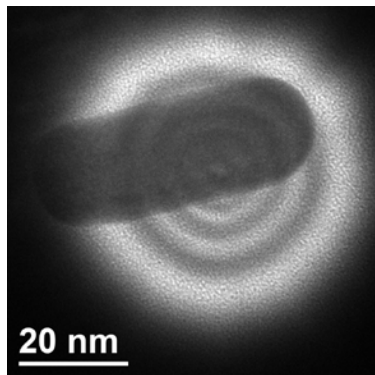
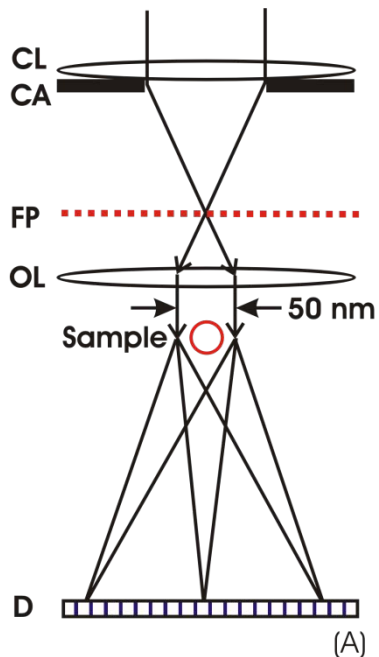
Advantages

1. Can observe a large area of specimen with a bright beam
2. Since the image plane is magnified, can easily select an area with an aperture → A 50 μm aperture can select a 2 μm area
3. Useful to study thick films, bulk samples, and in-situ phase transformations

Disadvantages

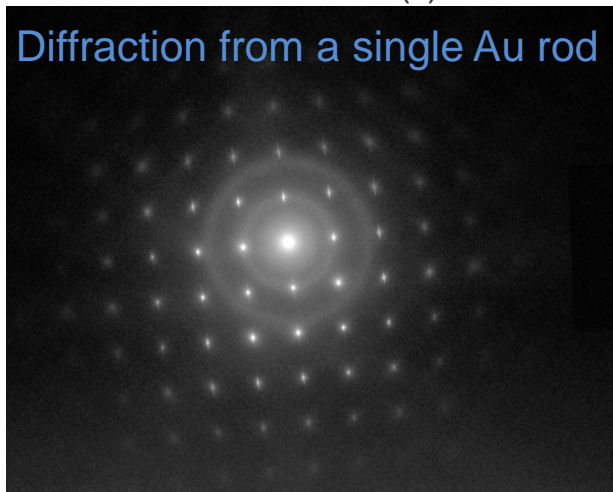
1. Cannot select an area less than $\sim 1 \mu\text{m}$ due to spherical aberrations and precision in aperture position
2. Difficult to record diffraction from individual nanoparticles or thin films





55 nm nano-probe

Diffraction from a single Au rod



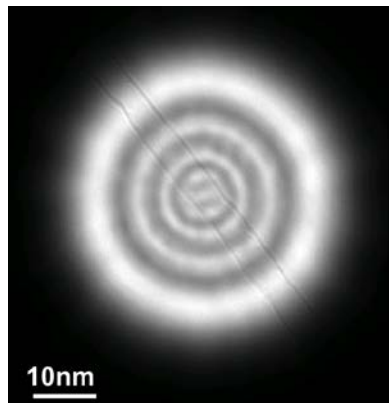
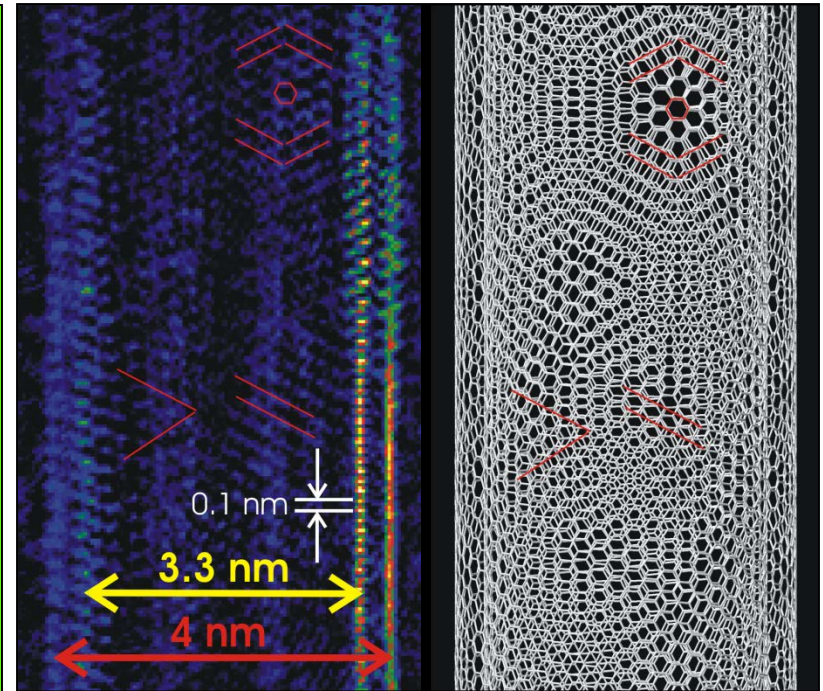
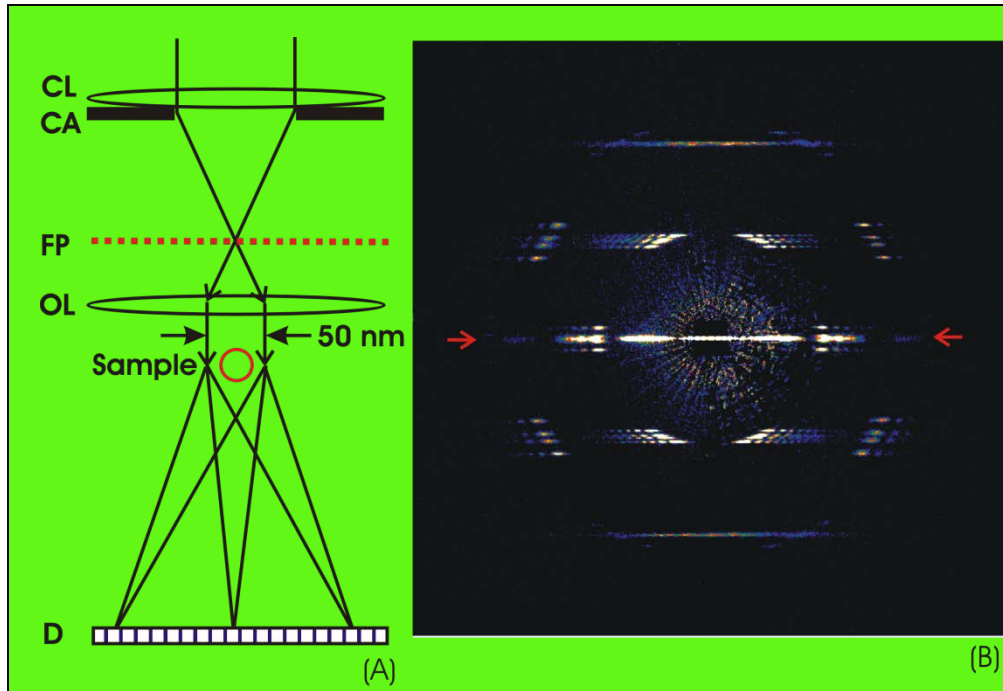
A. B. Shah, S. Sivapalan, and C. Murphy

Technique

1. Focus the beam on the front focal plane of the objective lens and use a small condenser aperture to limit beam size
2. A parallel beam without selection errors \rightarrow A $10 \mu\text{m}$ aperture can form a $\sim 50 \text{ nm}$ probe size
3. Useful to investigate individual nanocrystals and superlattices

Disadvantages

1. Very weak beam – *difficult to see and tilt the sample*
2. More complex alignment than conventional TEM
3. High resolution images are difficult to obtain \rightarrow Need to switch between NAED and TEM modes)



5 μm condenser aperture → 30 nm

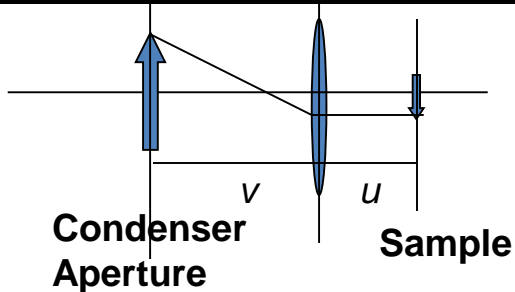
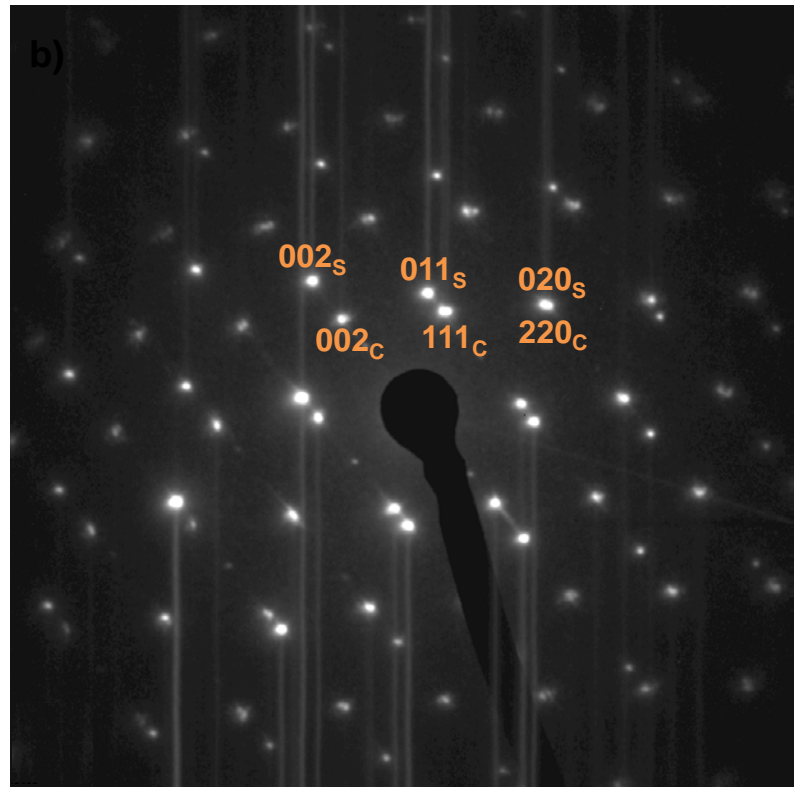
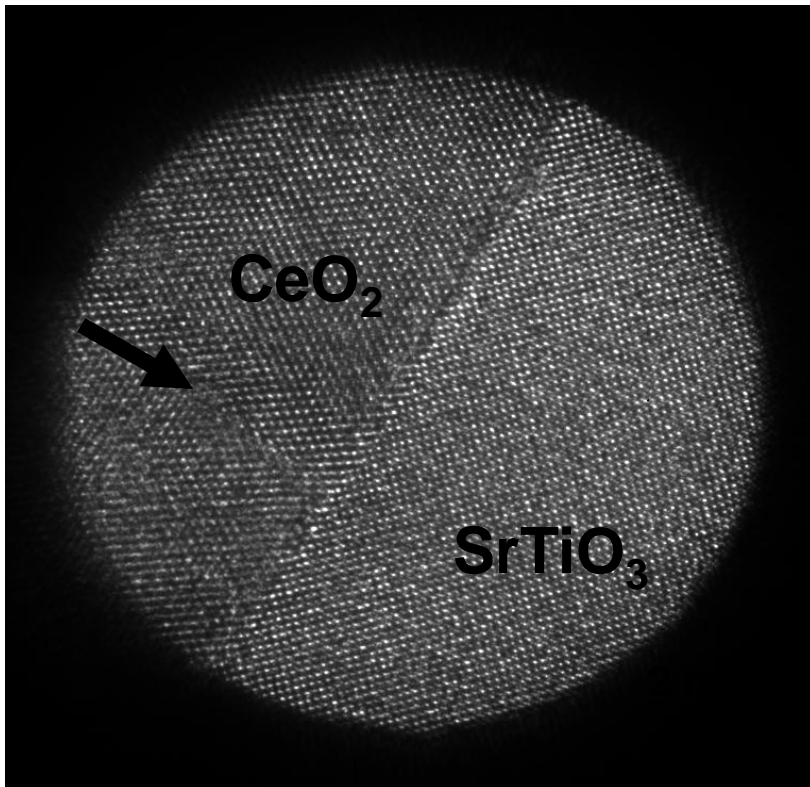
M. Gao, J.M. Zuo, R.D. Twesten, I. Petrov, L.A. Nagahara & R. Zhang,
Appl. Phys. Lett. 82, 2703 (2003)

J.M. Zuo, I. Vartanyants, M. Gao, R. Zhang and L.A. Nagahara,
Science, 300, 1419 (2003)

This technique was developed by CMM



Aperture-Beam Nanoarea Electron Diffraction



20 μm condenser aperture \rightarrow 20 nm probe size

Conjugate planes

This technique was developed by CMM

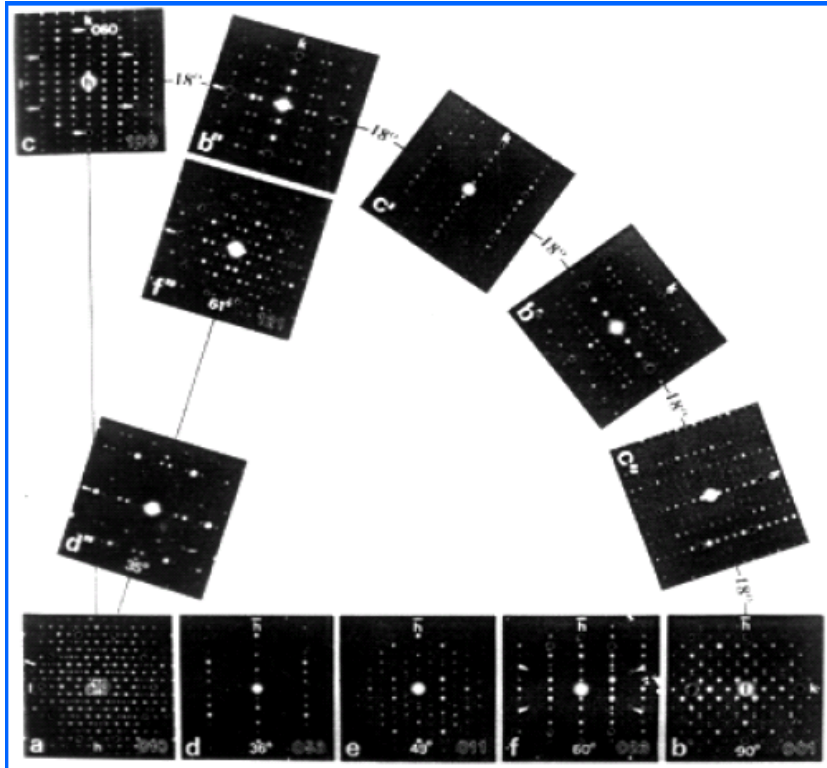




Applications of Electron Diffraction

Tilting sample to obtain 3-D structure of a crystal

Lattice parameter, space group, orientation relationship



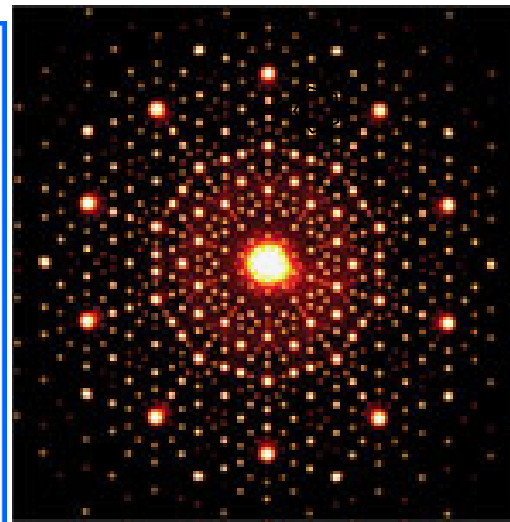
To identify new phases, TEM has advantages:

- 1) Small amount of materials
- 2) No need to be single phases
- 3) Determining composition by EDS or EELS

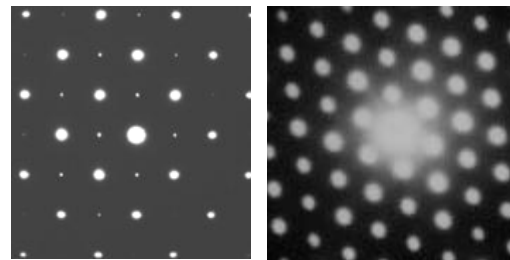
Disadvantage: needs experience

New materials discovered by TEM

Quasi-crystal

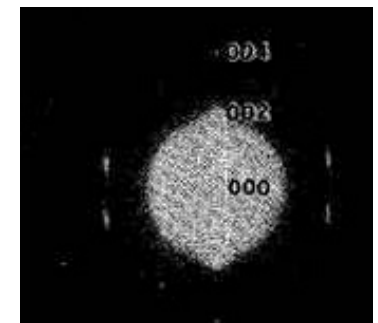


5-fold symmetry



1, 2, 3, 4, 6-fold symmetry
No 5-fold for a crystal

Carbon Nanotube

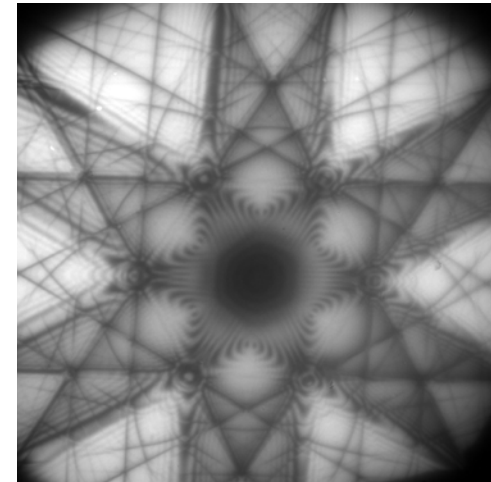
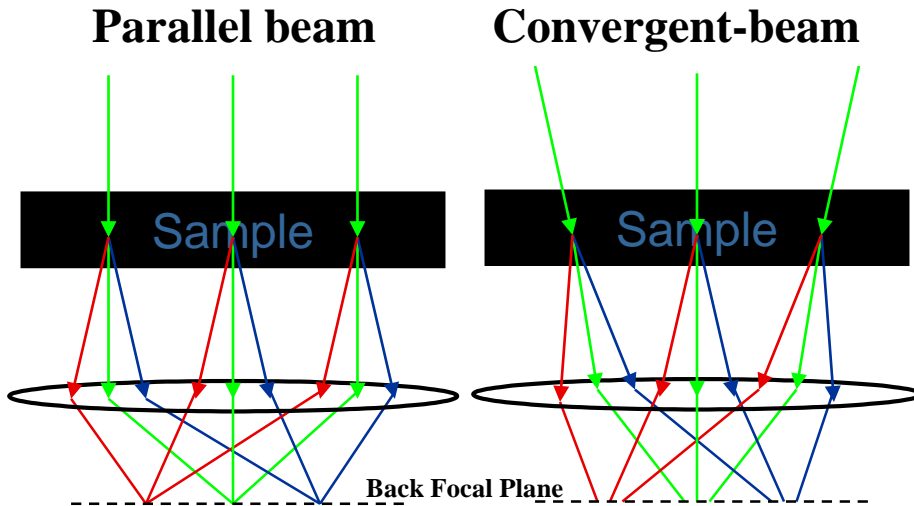


Helical graphene sheet

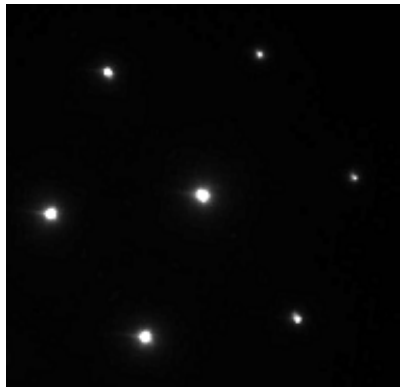
More advanced electron diffraction techniques¹⁵



Convergent Beam Electron Diffraction (CBED)

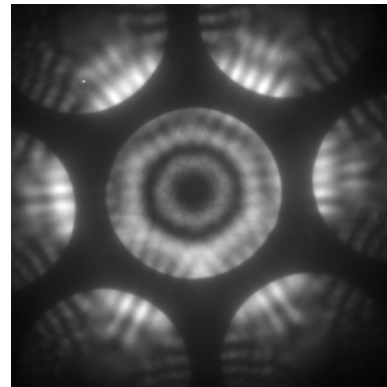


Large-angle bright-field CBED

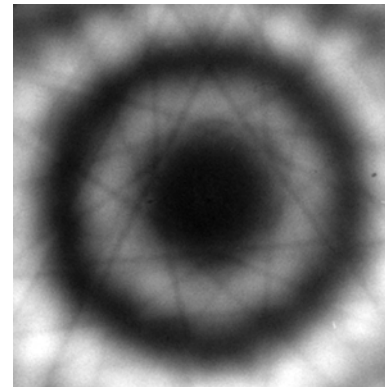


SAED

1. Point and space group
2. Lattice parameter (3-D) strain field



CBED

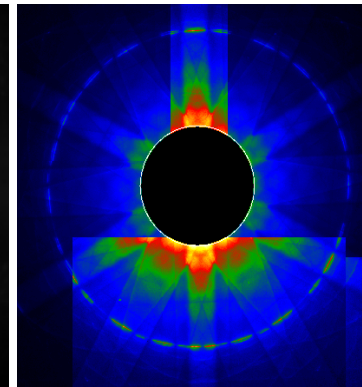


Bright-disk

3. Thickness
4. Defects



Dark-disk

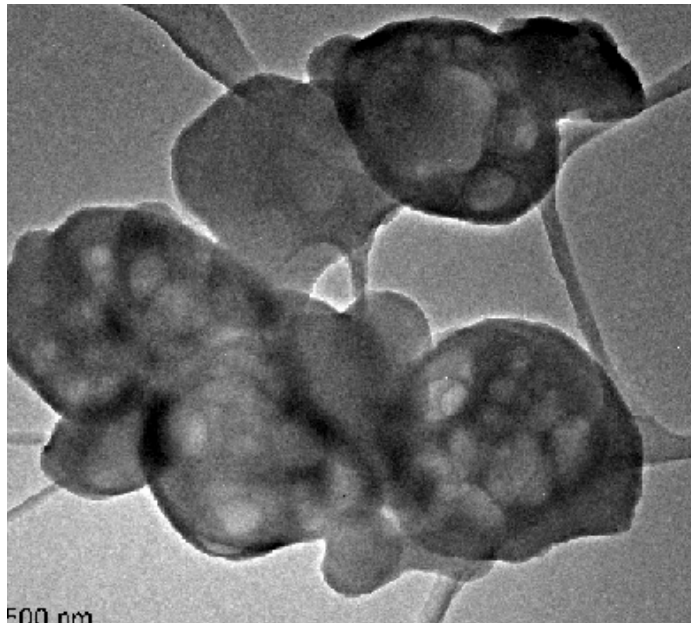


Whole-pattern



Major Imaging Contrast Mechanisms:

1. Mass-thickness contrast
2. Diffraction contrast
3. Phase contrast
4. Z-contrast (S-TEM)



Mass-thickness contrast

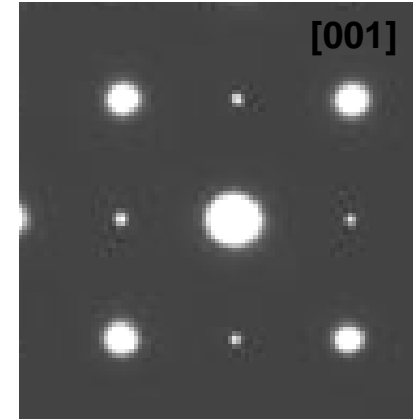
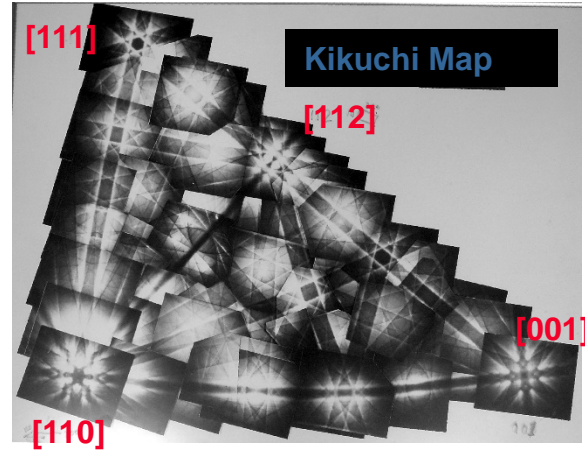
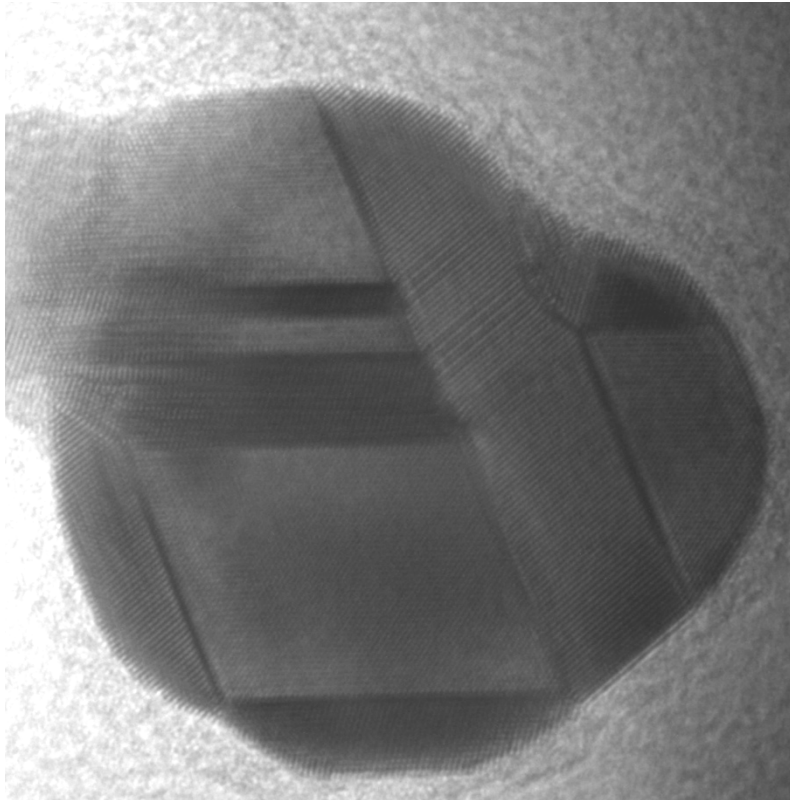
- 1) Imaging techniques in **TEM** mode
 - a) Bright-Field TEM (Diff. contrast)
 - b) Dark-Field TEM (Diff. contrast)
 - c) Weak-beam imaging
hollow-cone dark-field imaging
 - d) Lattice image (Phase)
 - e) High-Resolution Electron Microscopy (Phase)

Simulation and interpretation

- 2) Imaging techniques in **Scanning Transmission Electron Microscope (STEM)** mode
 - 1) Z-contrast imaging (Dark-Field)
 - 2) Bright-Field STEM imaging
 - 3) High-resolution Z-contrast imaging (Bright- & Dark-Field)
- 3) **Spectrum imaging**
 - 1) Energy-Filtered TEM (**TEM** mode)
 - 2) EELS mapping (**STEM** mode)
 - 3) EDS mapping (**STEM** mode)

I. Diffraction Contrast Image: Contrast related to crystal orientation

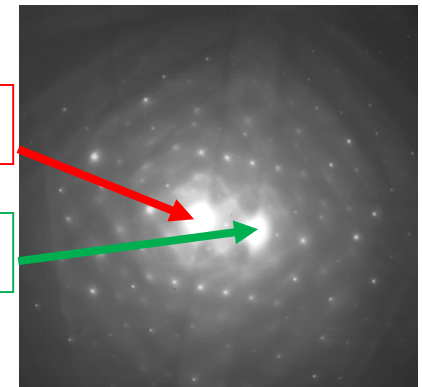
Phase Contrast Image



Two-beam condition

Transmitted beam

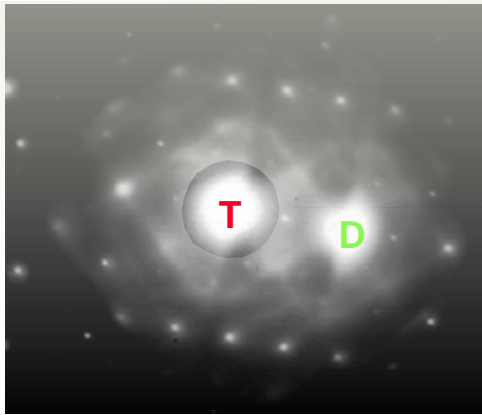
Diffacted beam



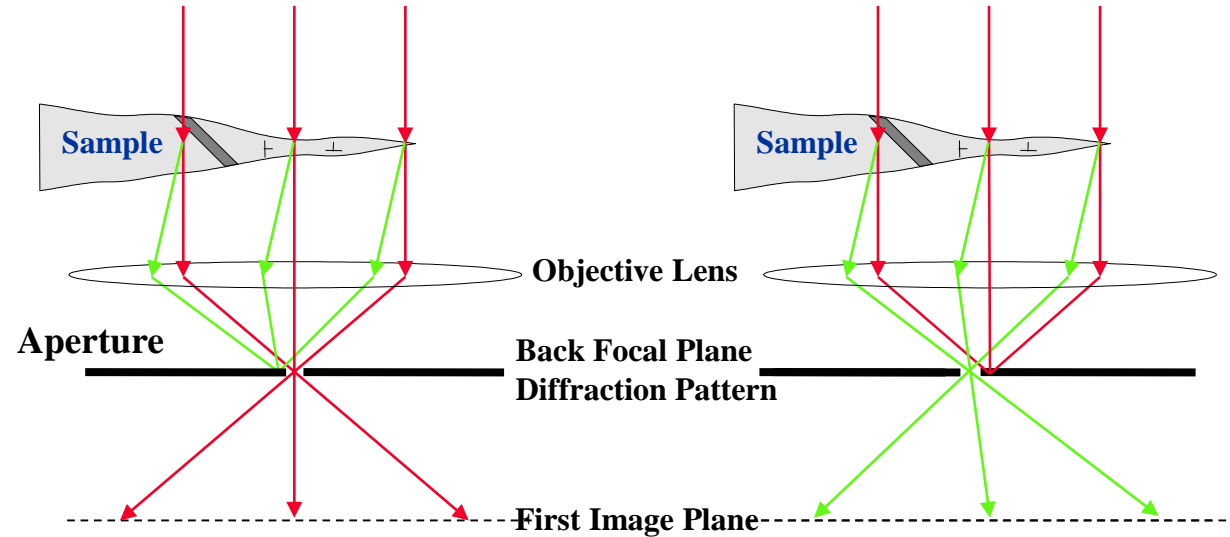
Application:

Morphology, defects, grain boundary, strain field, precipitates

II. Diffraction Contrast Image: Bright-field & Dark-field Imaging

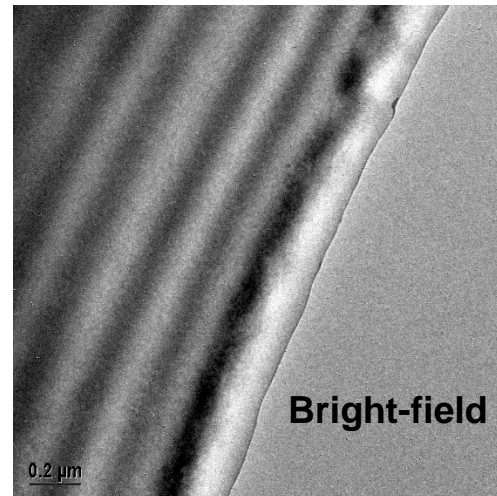


Two-beam condition

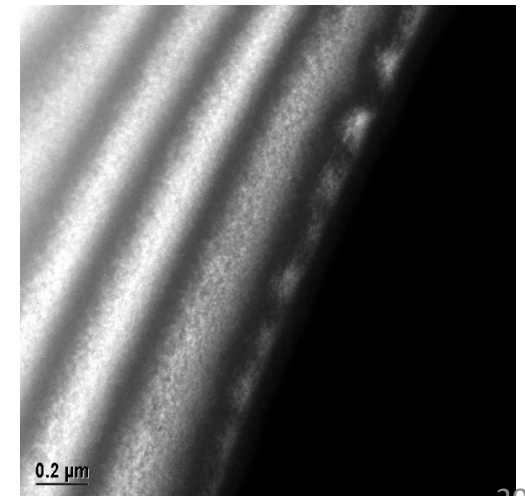


Bright-field Image

Dark-field Image

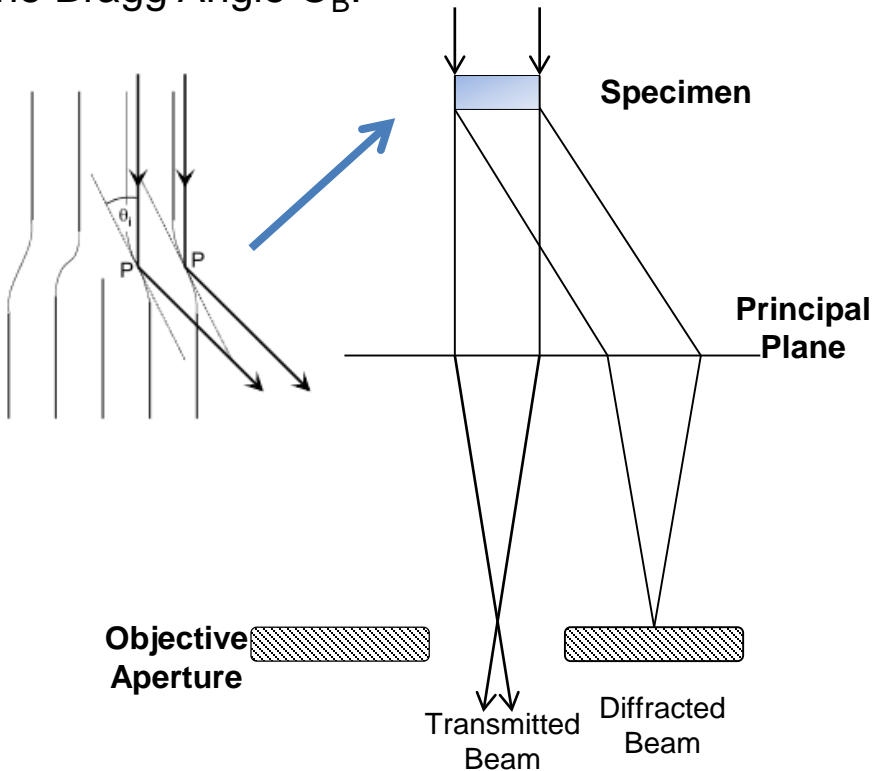


Bright-field

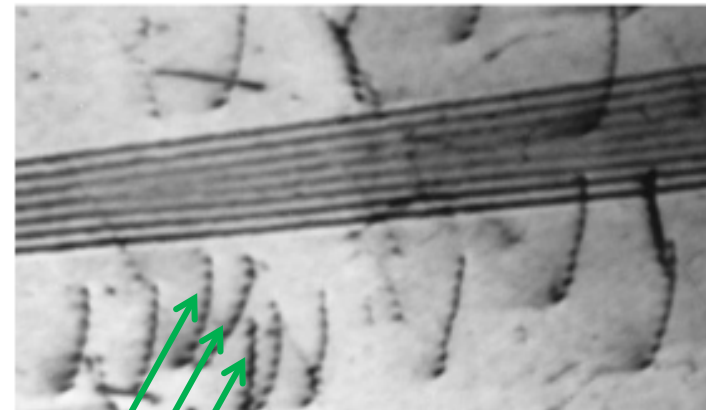


II. Diffraction Contrast Imaging

At edge dislocation, strain from extra half plane of atoms causes atomic planes to bend. The angle between the incident beam and a few atomic planes becomes equal to the Bragg Angle Θ_B .



Dislocations & Stacking Faults Bright Field Image



Near dislocations, electrons are strongly diffracted outside the objective aperture

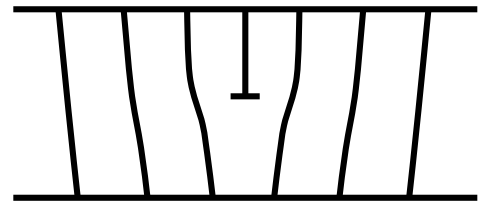
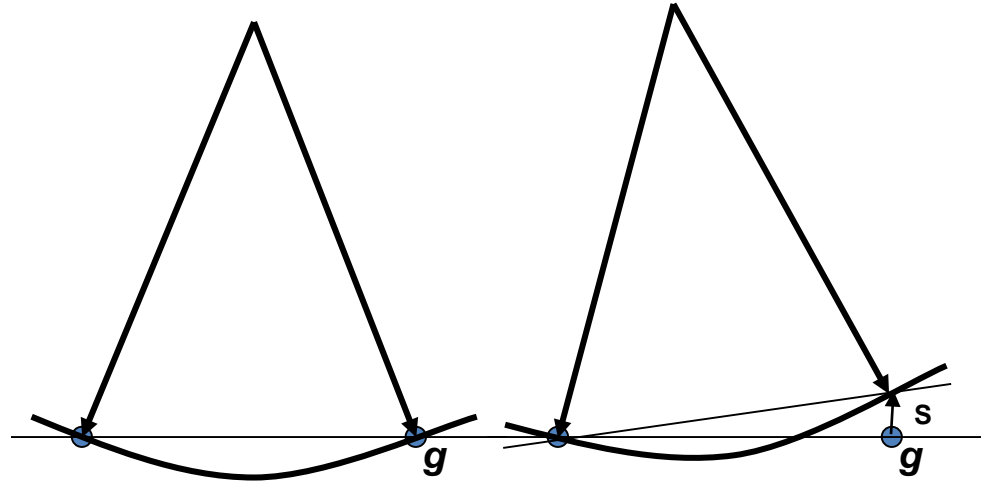
R. F. Egerton, *Physical Principles of Electron Microscopy*, 2007.



Weak-beam Dark Field Imaging

High-resolution dark-field imaging

“Near Bragg Condition”



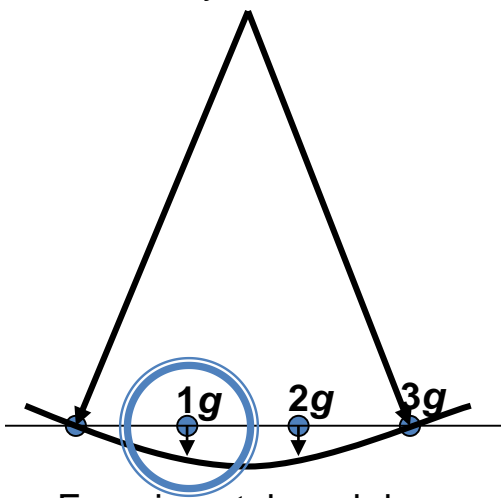
Planes do not satisfy Bragg diffraction

Possible planes satisfy Bragg diffraction

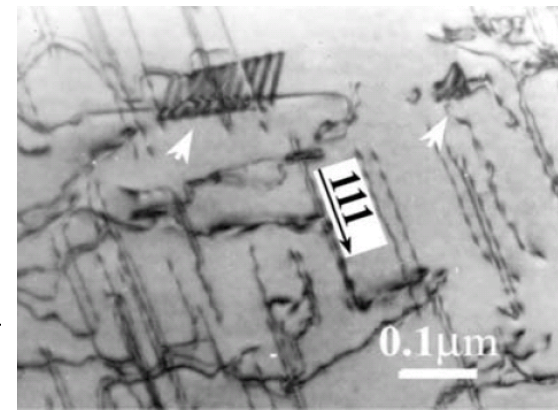
Taken by I. Petrov

Exact Bragg condition

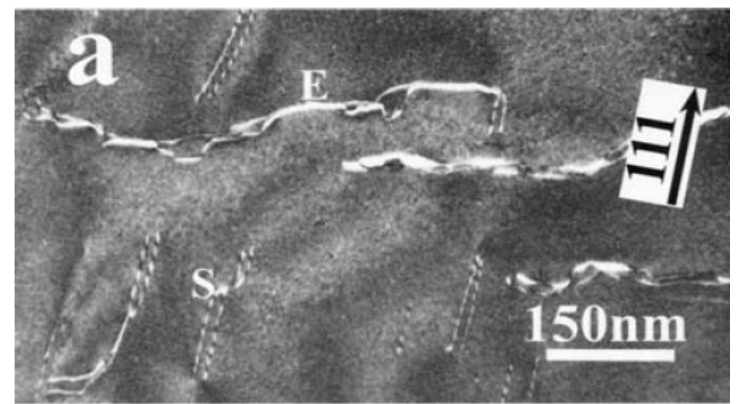
Weak-beam means Large excitation error



Experimental weak-beam



Bright-field



Weak-beam

Dislocations can be imaged as 1.5 nm narrow lines



II. Diffraction Contrast Image

Two-beam condition for defects

Howie-Whelan equation

$$\frac{d\phi_0}{dz} = \frac{\pi i}{\xi_g} \phi_g \exp\{2\pi i(sz + \mathbf{g} \cdot \mathbf{R})\}$$

Dislocations

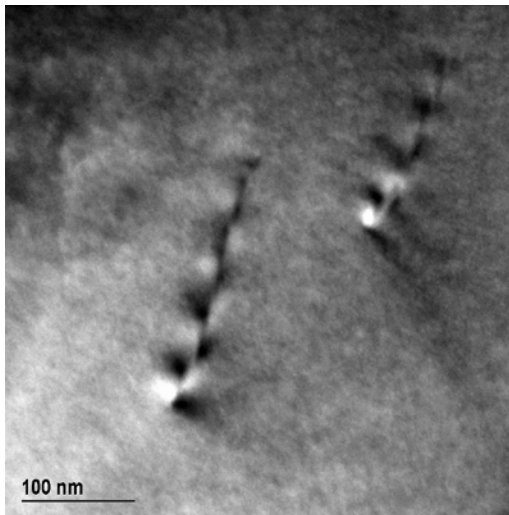
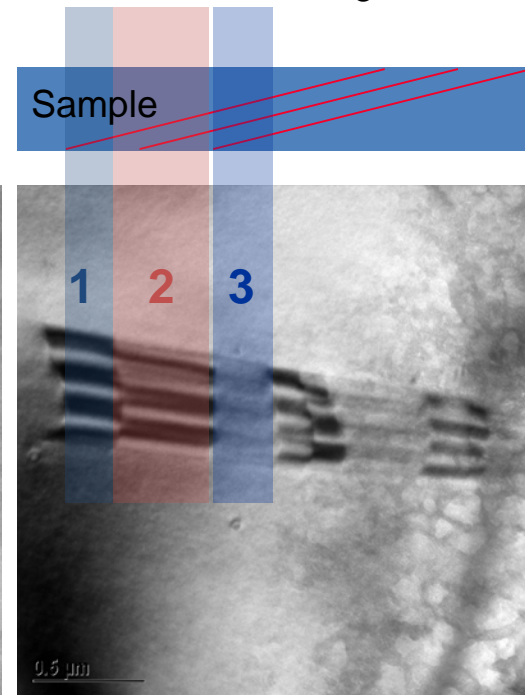
Use $\mathbf{g} \cdot \mathbf{b} = 0$ to determine Burgers vector \mathbf{b}

Stacking faults

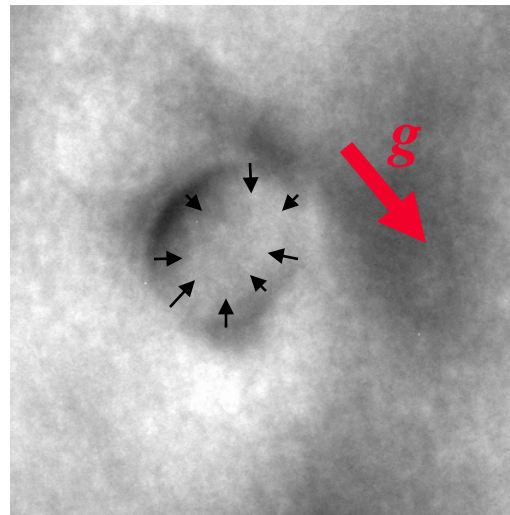
Phase = $2\pi \mathbf{g} \cdot \mathbf{R}$

Each stacking fault changes phase $\frac{2}{3}\pi$

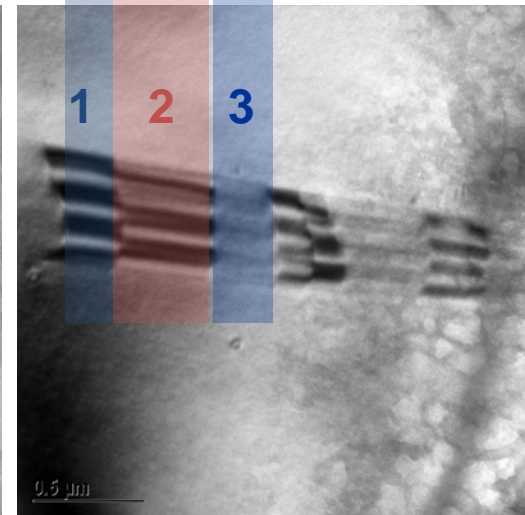
Diffraction contrast images of typical defects



Dislocations

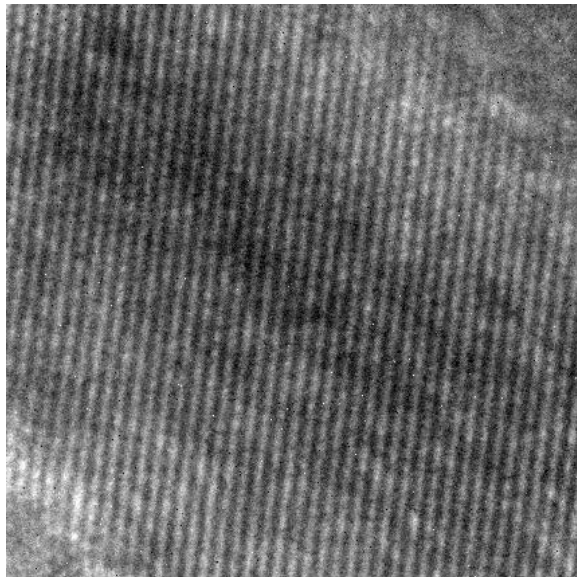
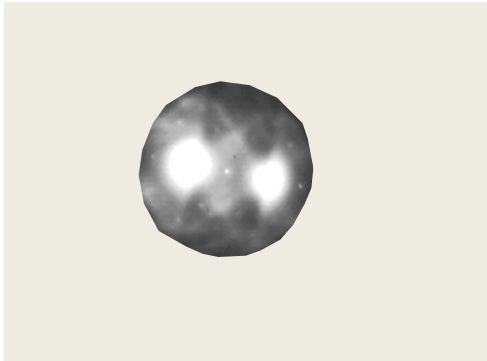


Dislocation loop



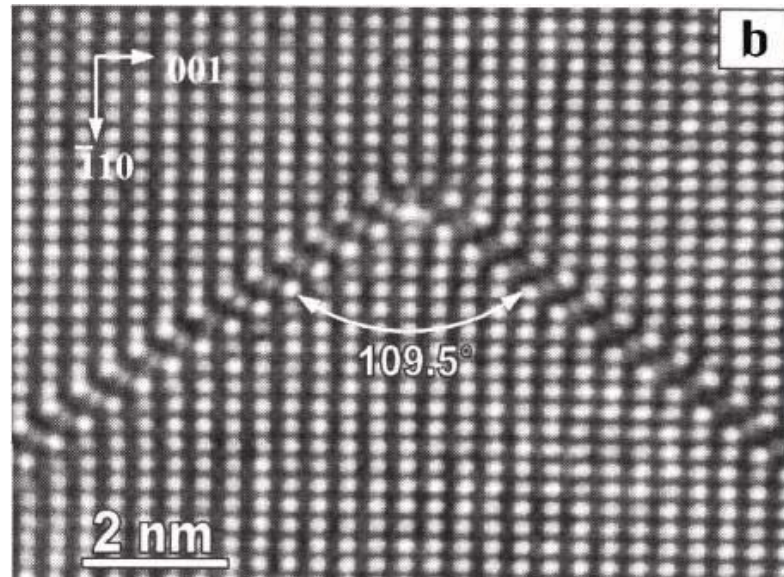
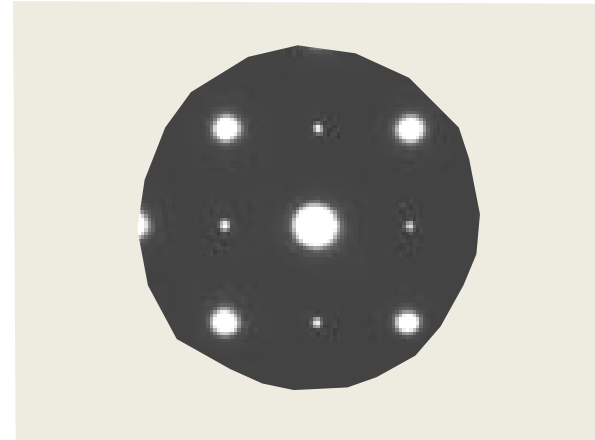
Stacking faults

Two-beam condition



M. Marshall

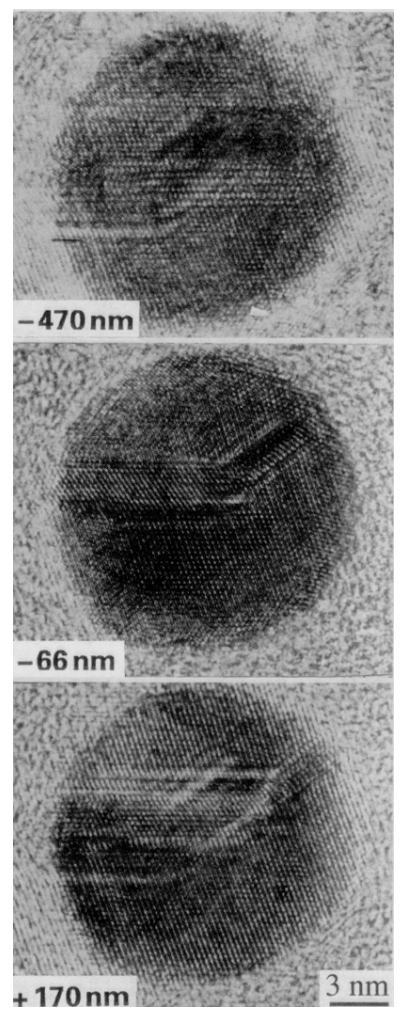
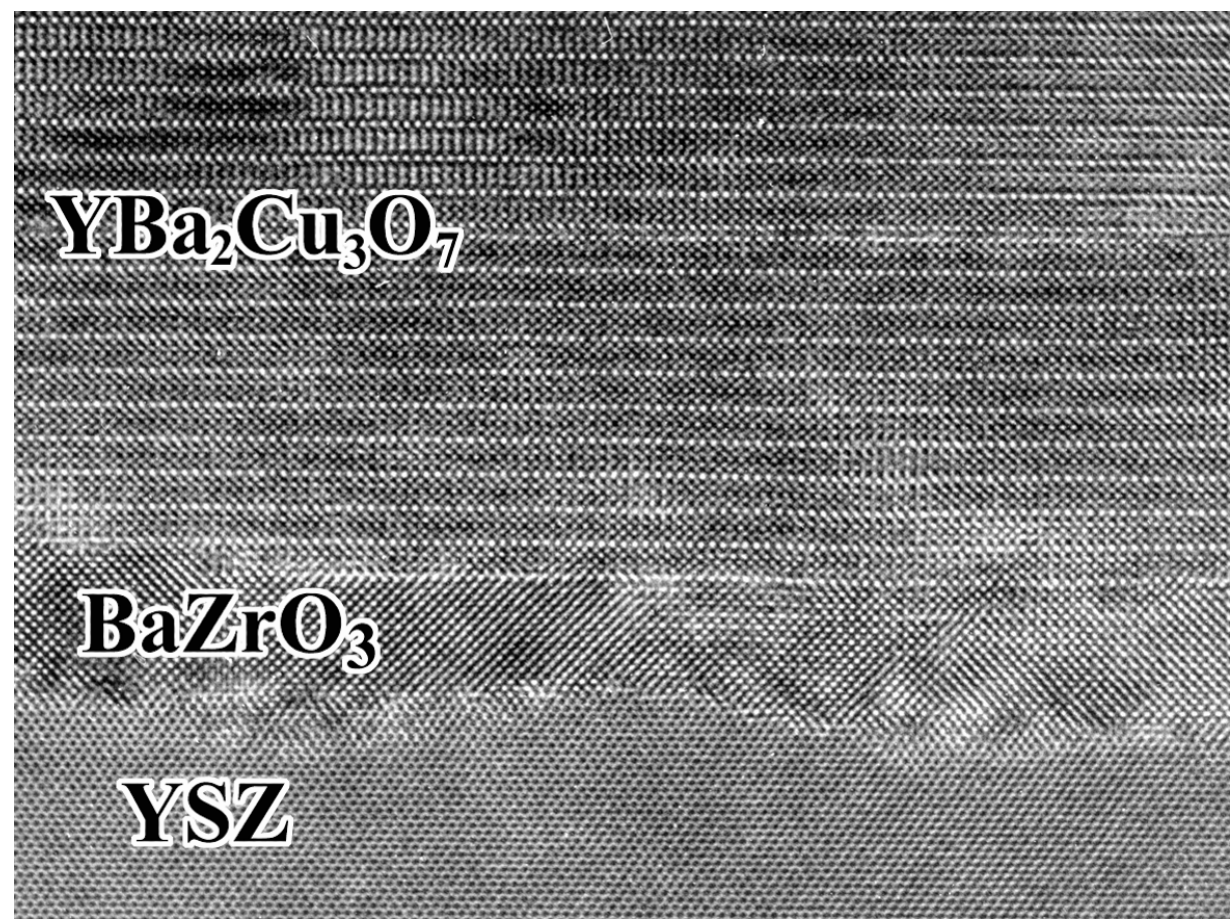
Many-beam condition



C.H. Lei

Delocalization effect from a Schottky-emission gun (S-FEG)
From a LaB₆ Gun

S-Field-Emission Gun



Lattice image of film on substrates



High Resolution Transmission Electron Microscopy (HRTEM)

$$f(x,y) = \exp(i\sigma V_t(x,y))$$

$$\sim 1 + i\sigma V_t(x,y)$$

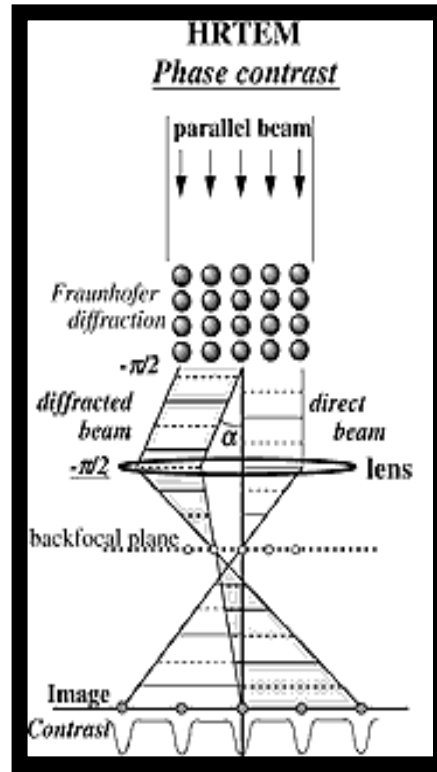
$V_t(x,y)$: projected potential

Scherzer defocus

$$\Delta f_{sch} = -1.2 (C_s \lambda)^{\frac{1}{2}}$$

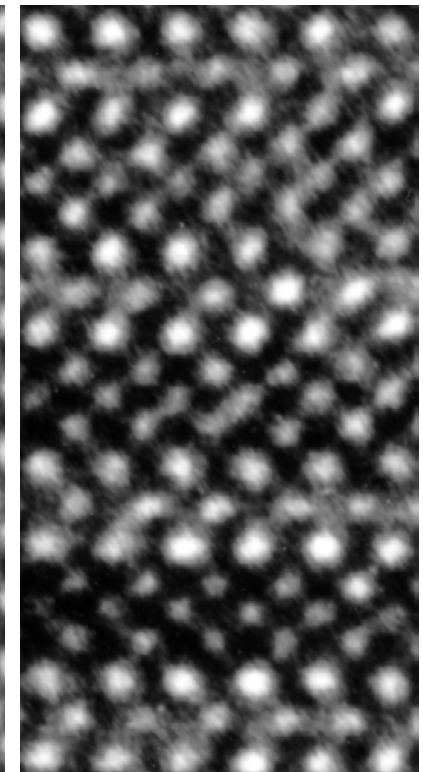
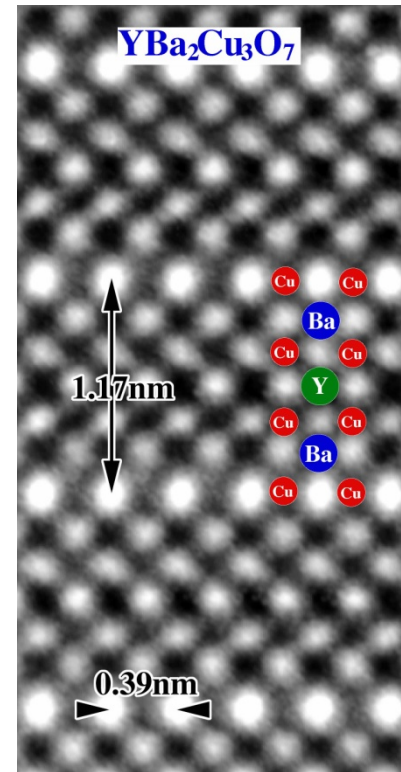
Resolution limit

$$r_{sch} = 0.66 C_s^{\frac{1}{4}} \lambda^{\frac{3}{4}}$$



$1 \Delta f_{sch}$

$2 \Delta f_{sch}$



1 Scherzer Defocus:

Positive phase contrast "black atoms"

2 Scherzer Defocus: ("2nd Passband" defocus).

Contrast Transfer Function is positive

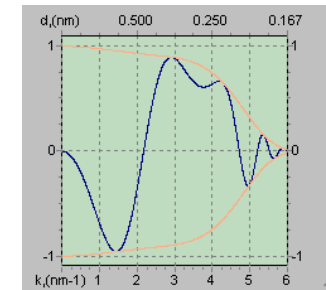
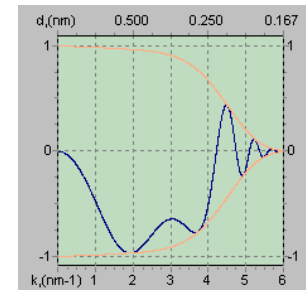
Negative phase contrast ("white atoms")

Simulation of images

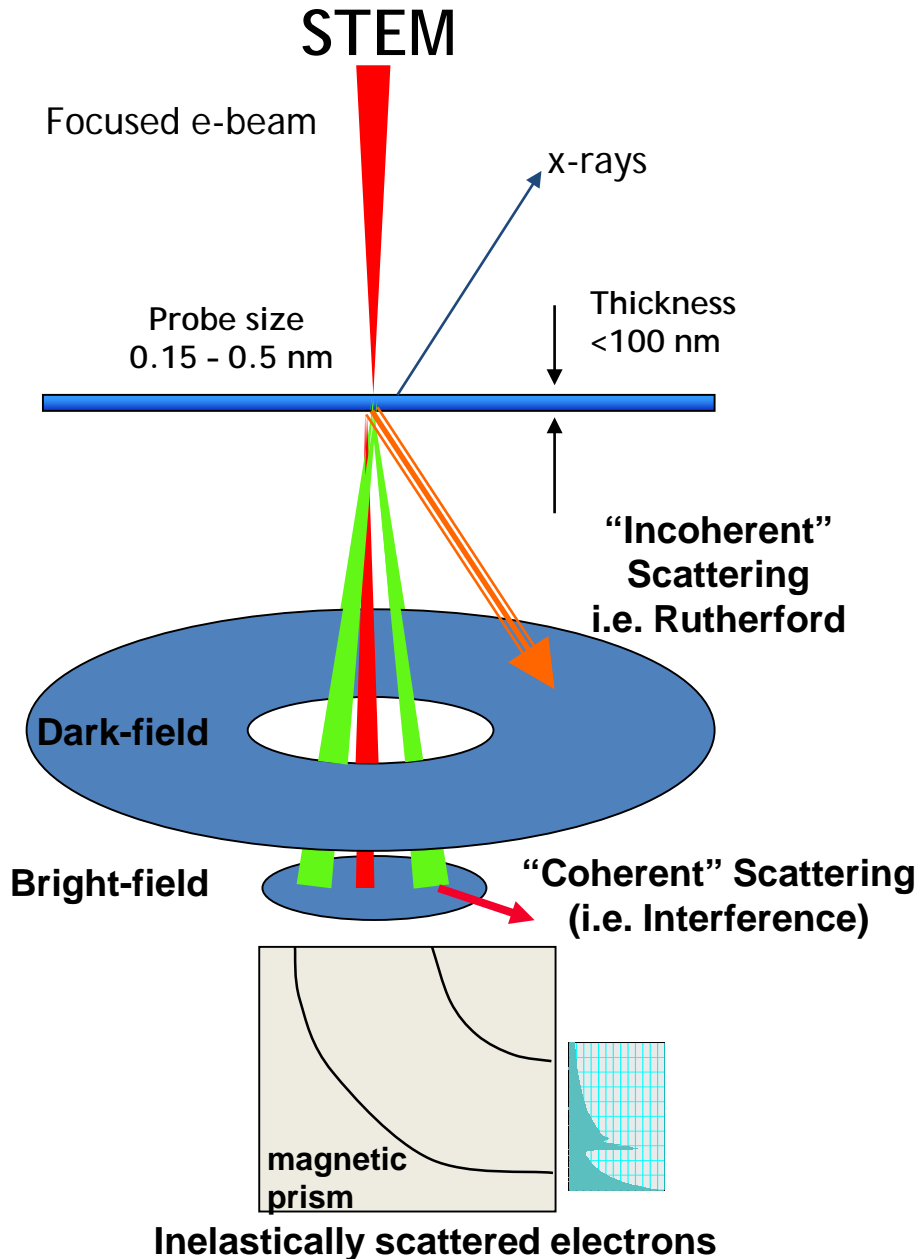
Software: Web-EMAPS (UIUC)
MacTempas

Contrast transfer function

J.G. Wen



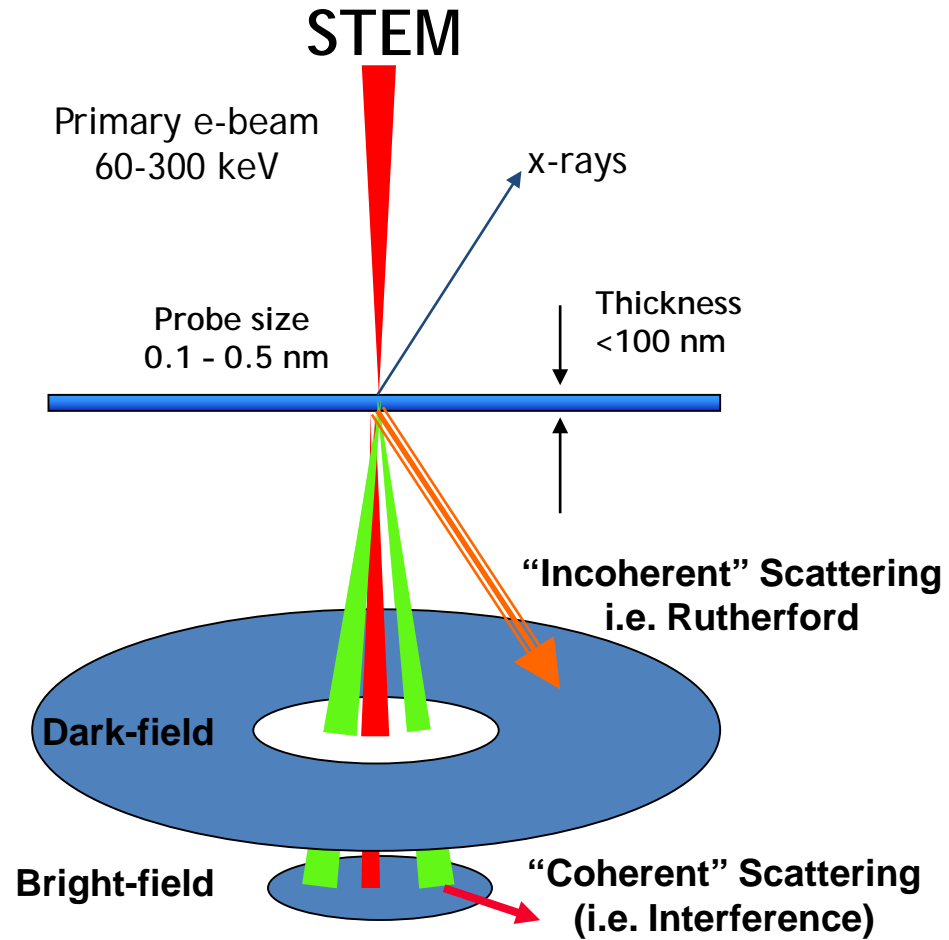
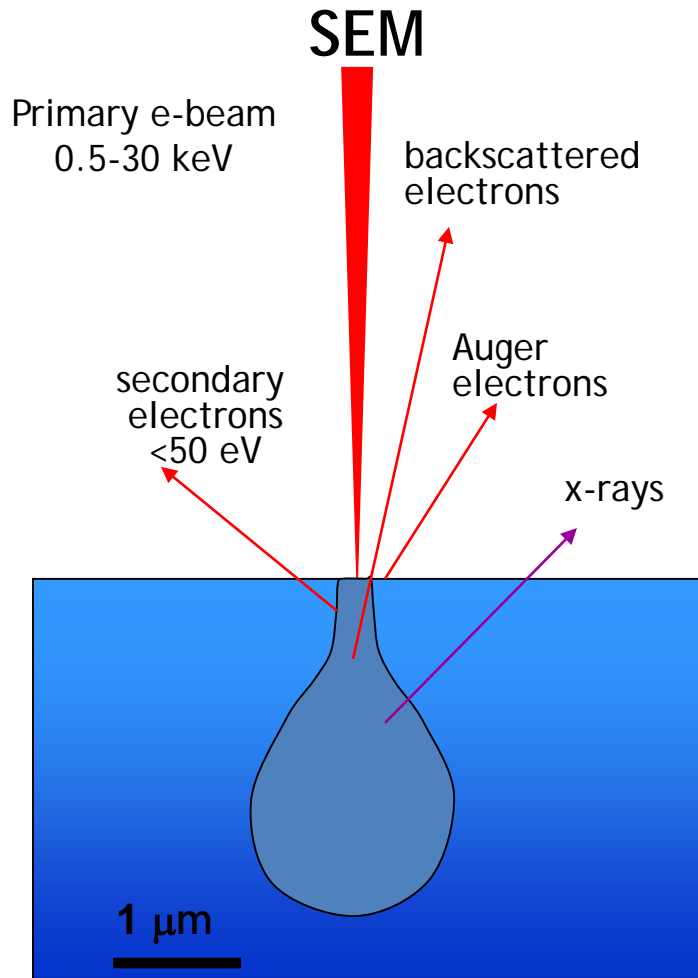
Technique



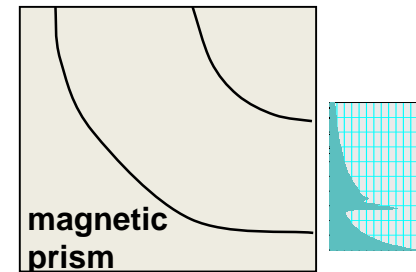
1. Raster a converged probe across and collect the integrated signal on an **Annular** detector (**Dark Field**) or a circular detector (**Bright Field**).
2. An incoherent image is chemically sensitive (Z-contrast) under certain collection angles
3. Annular Dark Field (ADF) STEM is directly interpretable and does not have contrast reversals or delocalization effects like HRTEM
4. STEM resolution is determined by the probe size, which is typically 0.15 to 0.5 nm for a modern S-FEG STEM.
5. Since STEM images are collected serially, the resolution is typically limited by vibrations and stray fields



SEM vs STEM



STEM technique is similar to SEM, except the specimen is much thinner and we collect the transmitted electrons rather than the reflected electrons.



Inelastically scattered electrons

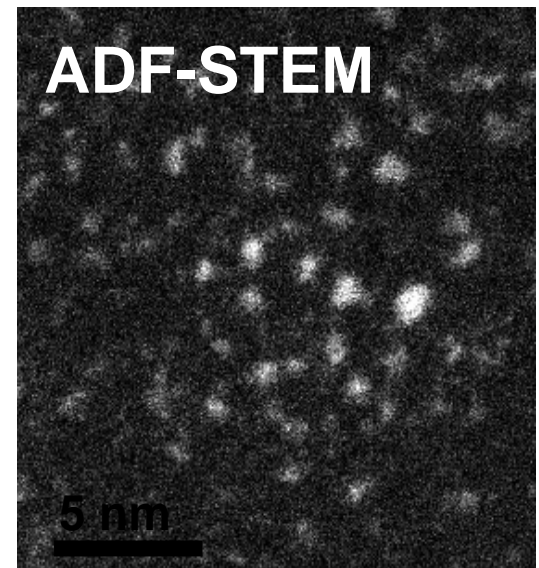
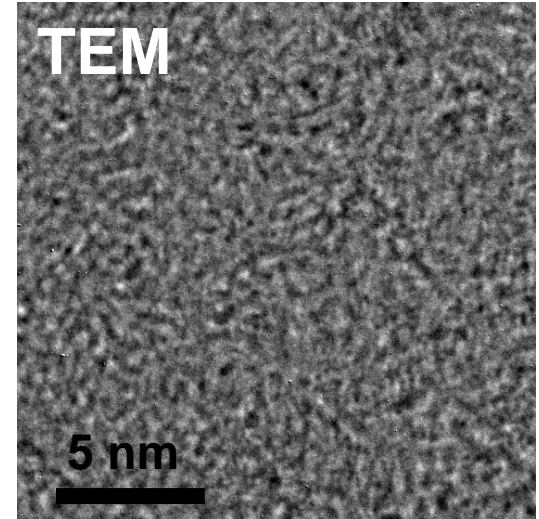
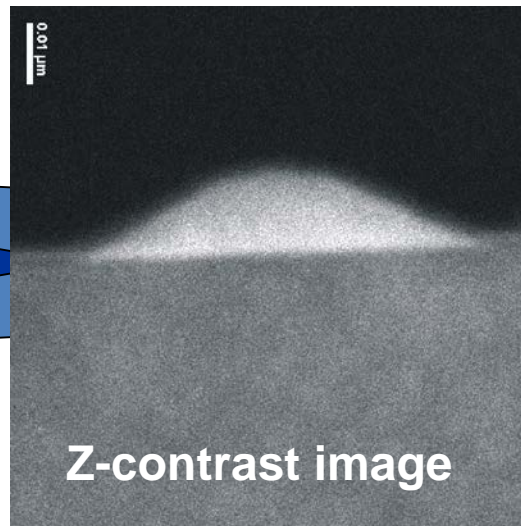
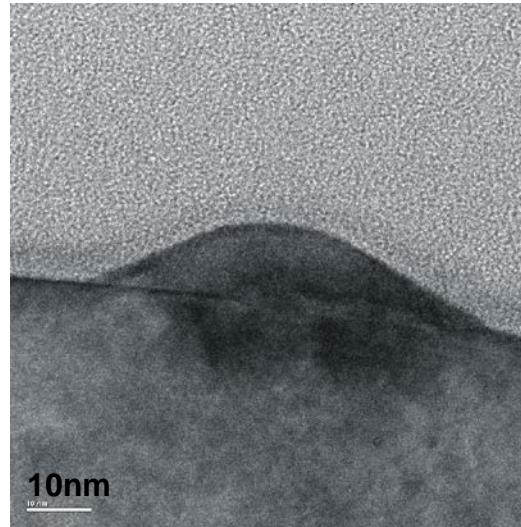
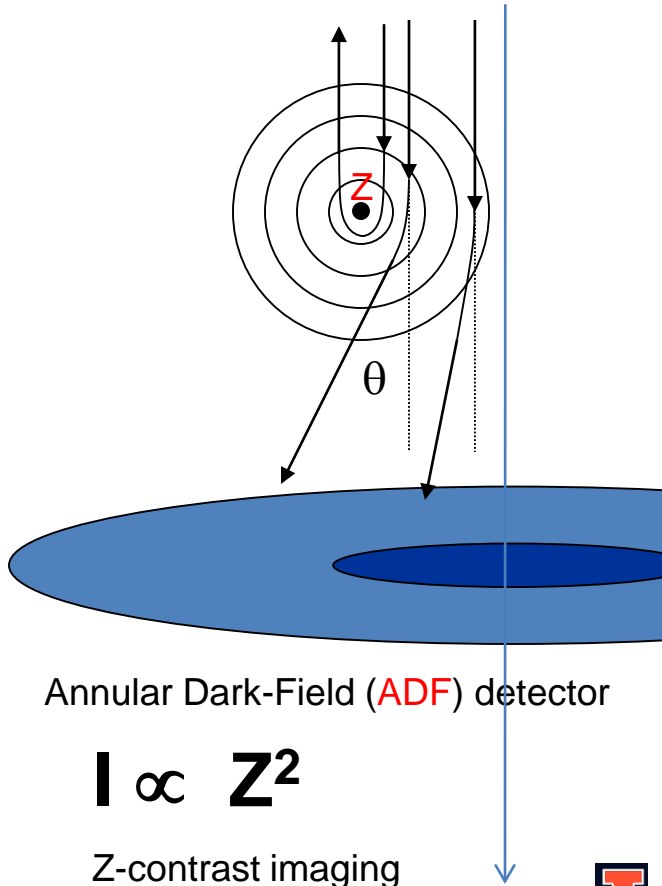


TEM vs ADF-STEM

Ge quantum dots on Si substrate

Ir nanoparticles

1. STEM imaging gives better contrast
2. STEM images show Z-contrast

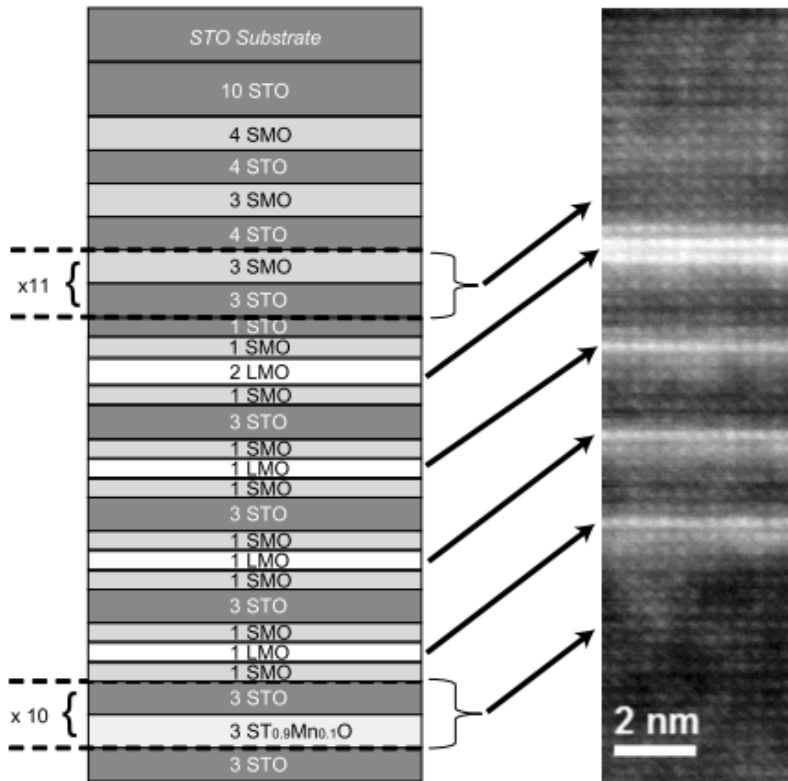


J.G. Wen

L. Long

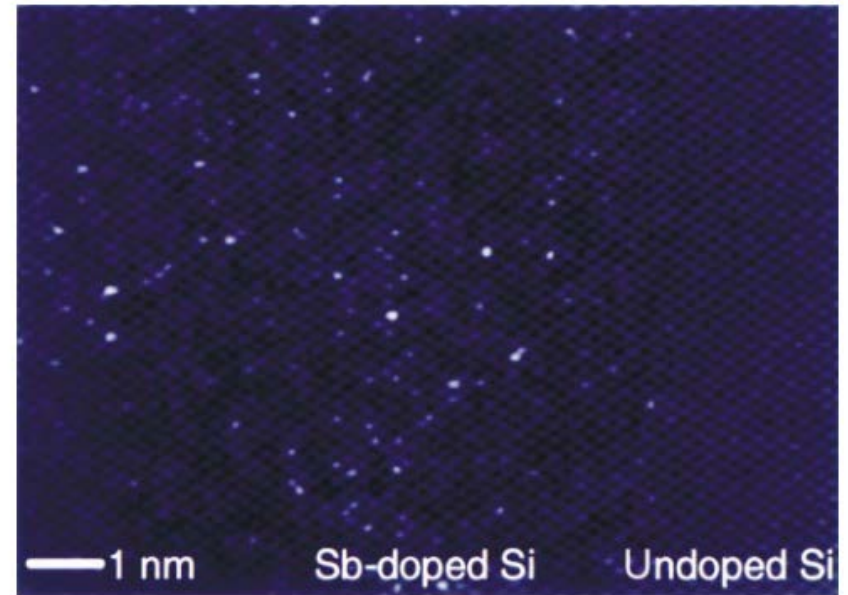


Superlattice of LaMnO_3 - SrMnO_3 - SrTiO_3



A. B. Shah et al., 2008

Dopant atoms in Si

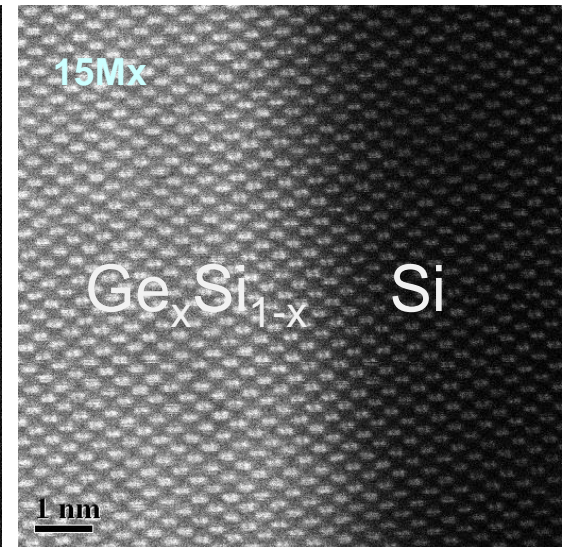
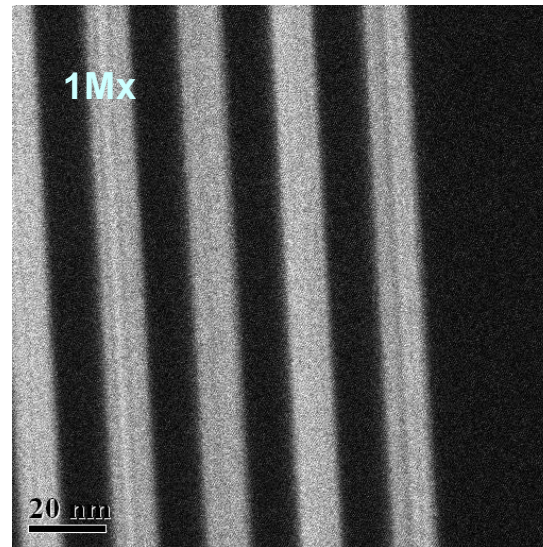
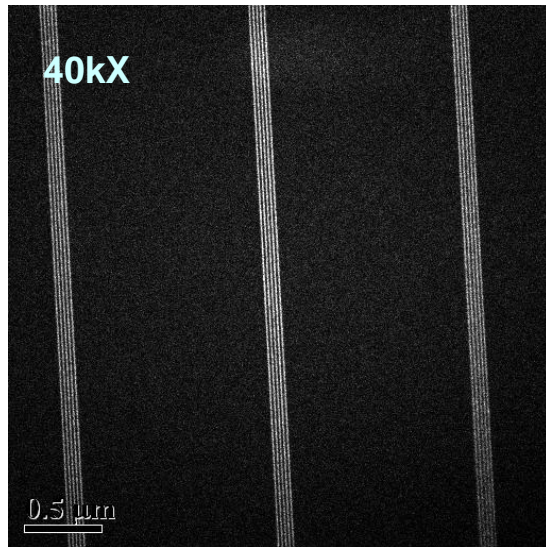
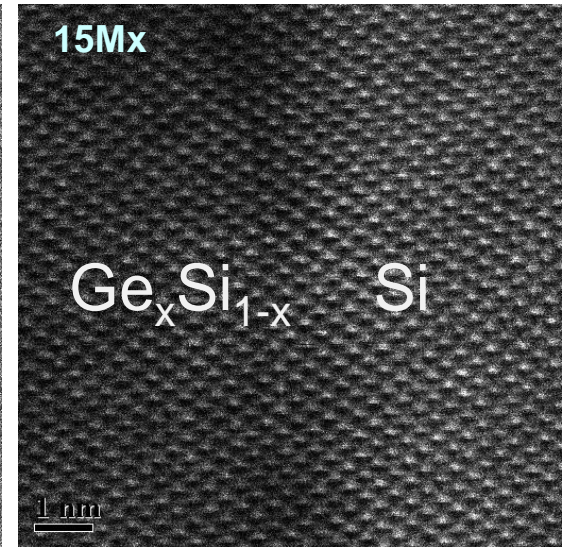
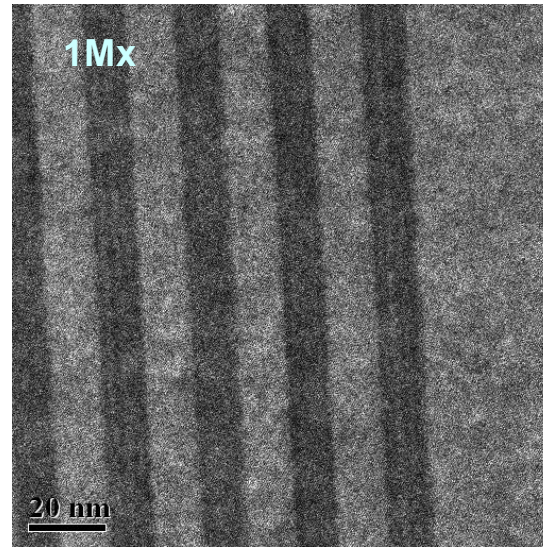
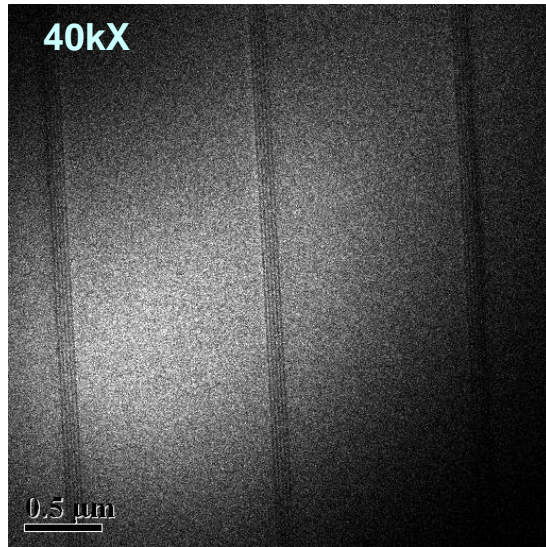


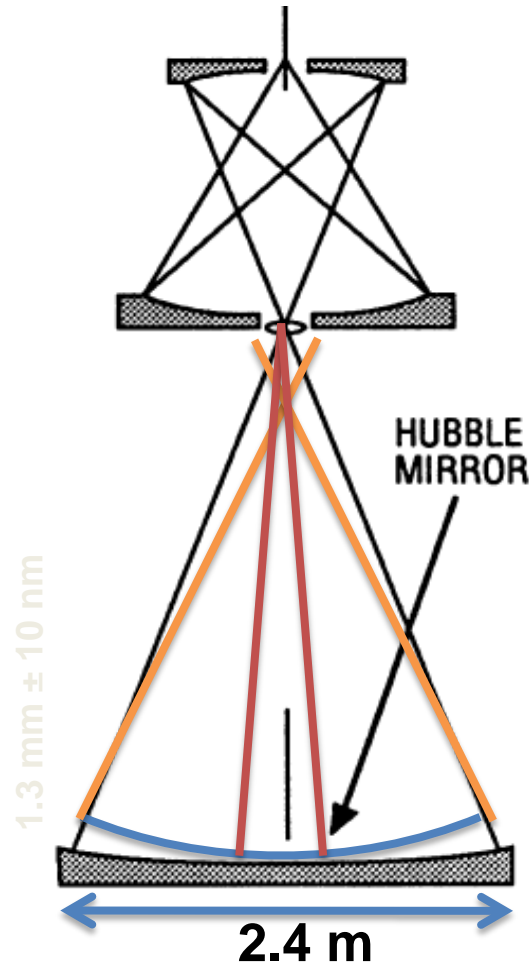
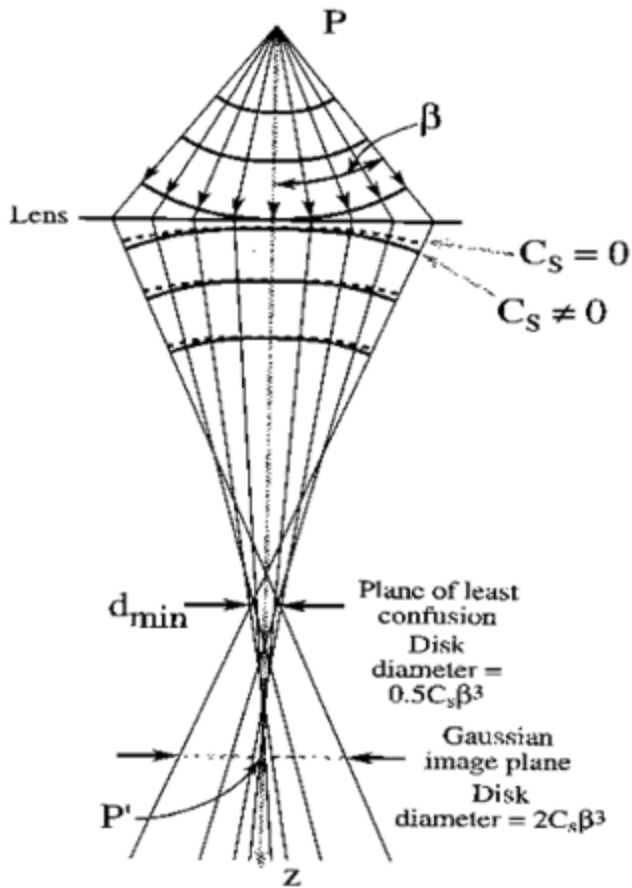
P. M. Voyles et al., 2002



Bright Field STEM vs ADF STEM

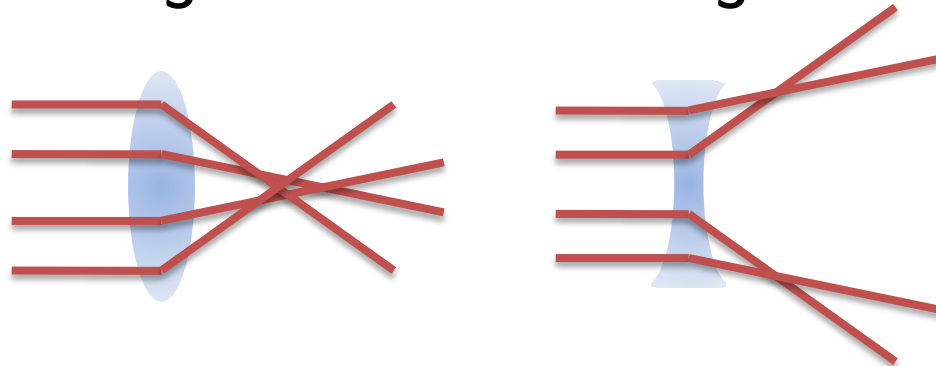
Si – Ge Superlattice





Since 1936, Scherzer proved that spherical and chromatic aberrations would ultimately limit the resolution of the electron microscope. The method to correct aberrations was well known, but experimental aberration correctors were not successful until ~1998 due to complexities in alignment and lack of computing power.

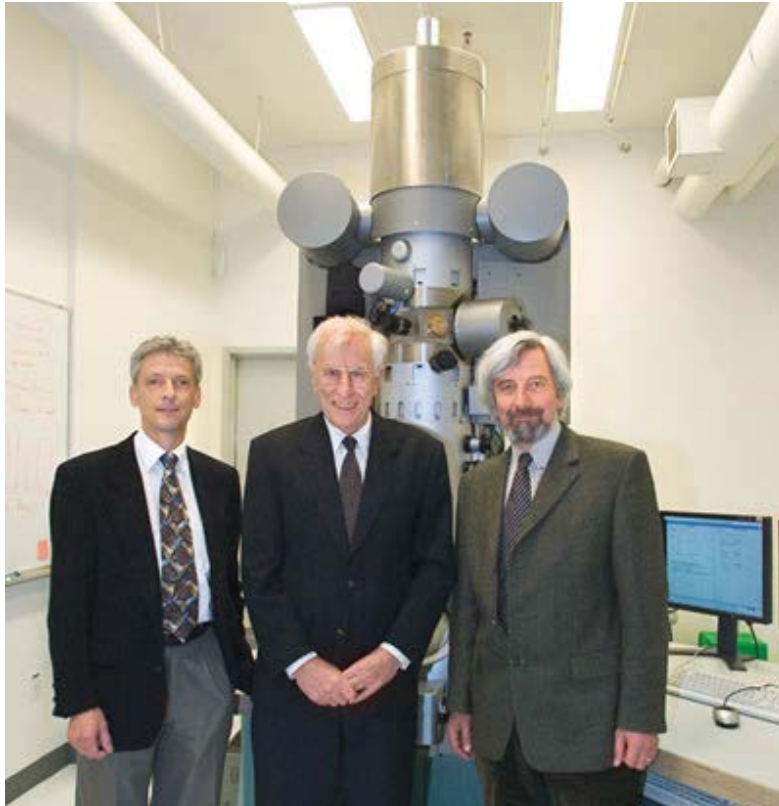
$$C_s + (-C_s) = 0$$



Before correction



After correction

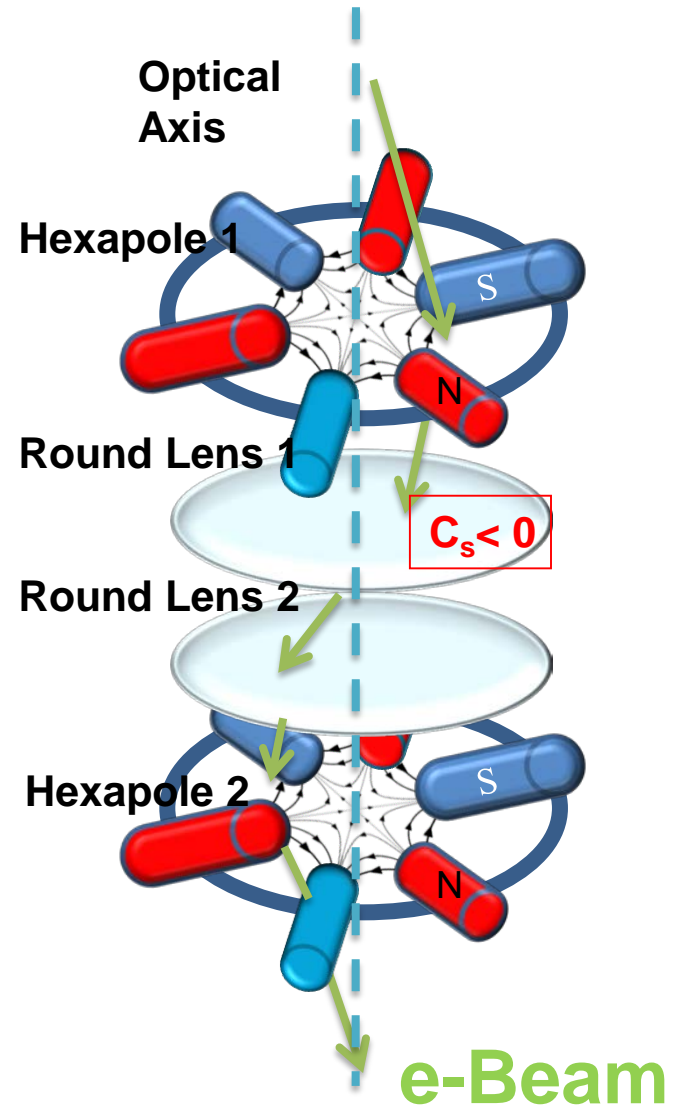


Uli Dahmen
NCEM

Max Haider
CEOS, Germany

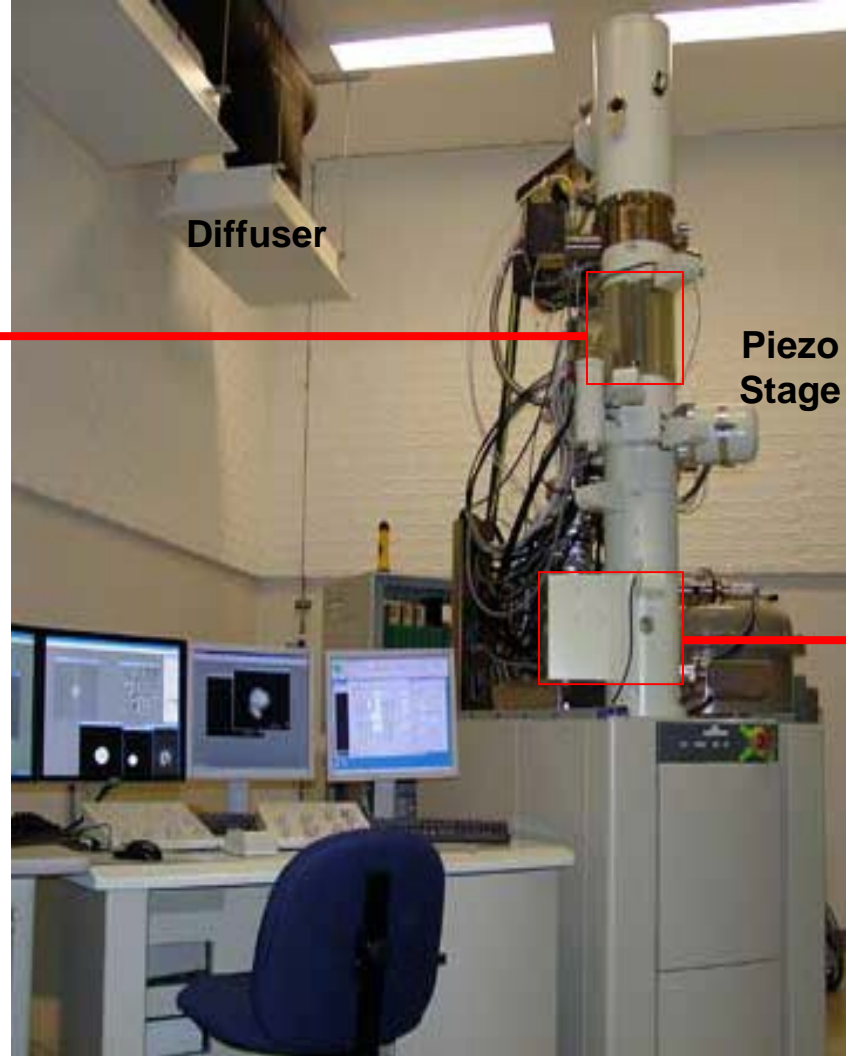
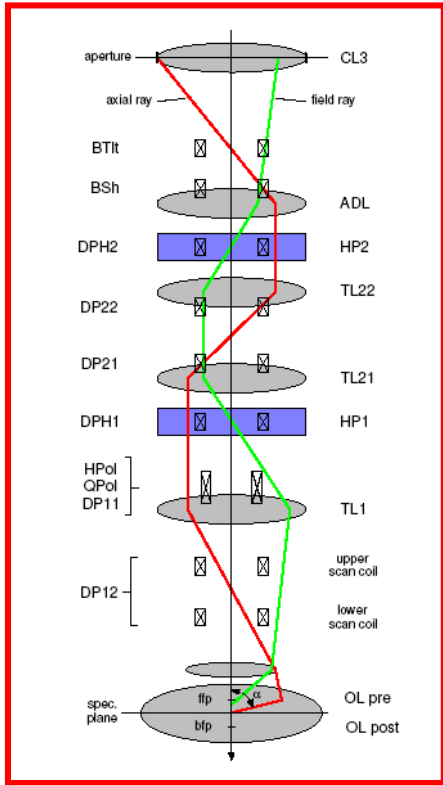
Harald Rose
Univ. of Tech. Darmstadt

Hexapole C_s Corrector

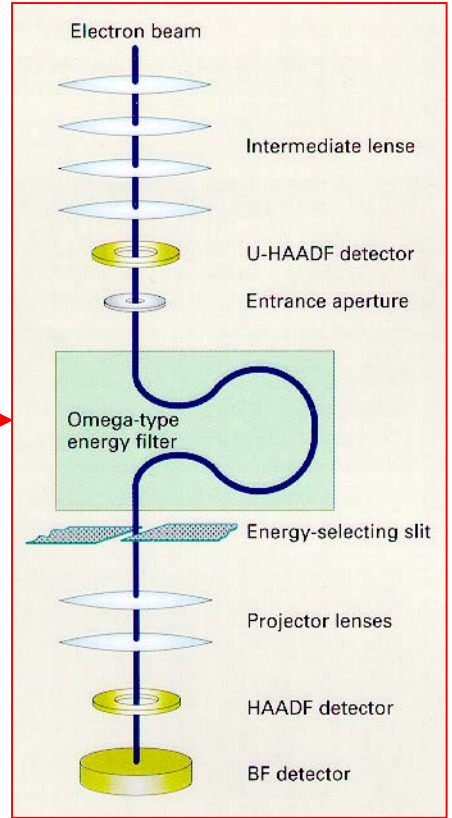




JEOL JEM2200FS with Probe Corrector @ UIUC



The STEM can obtain 1 Å spatial resolution



Only if the instabilities of the room are controlled





Spherical Aberration Correction

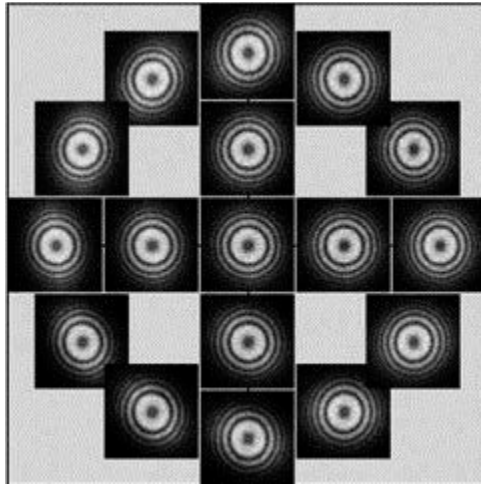
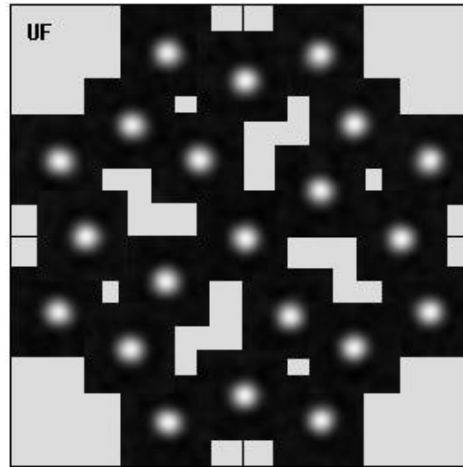
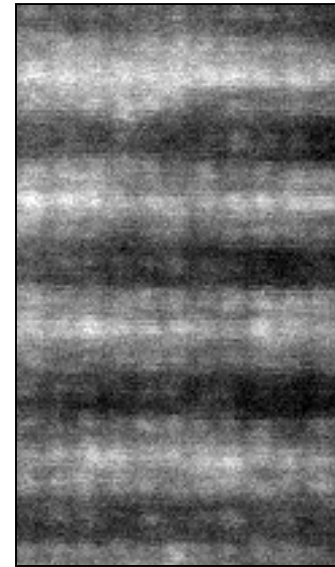


Image corrector

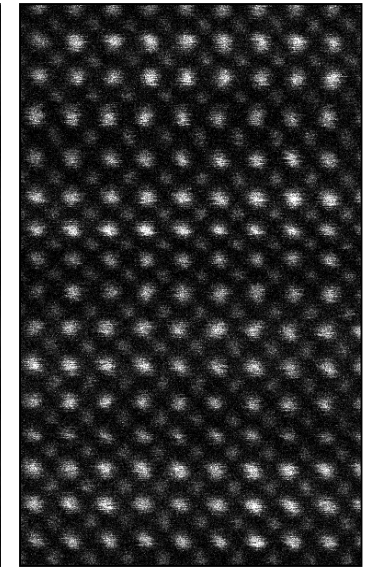


Probe corrector



JEOL 2010F
 $C_s = 1 \text{ mm}$

Probe size
0.3 nm



JEOL 2200FS
with probe corrector

Probe size
0.1 nm

```

#20 C1: 15.32nm A1: 10.3nm / -157deg
#21 C1: 10.08nm A1: 8.85nm / -112.7deg
#22 C1: 20.04nm A1: 6.14nm / +135.8deg
dTime: 3840s Date: Tue Sep 18 16:48:00
1st order measured! (not used:)
Sall: 6.785nm Sused: 6.785nm (1.661%)
C1: 14.91nm (95%: 8.08nm)
A1: 2.851nm / +90.3deg (95%: 10.9nm)
A2: 36.73nm / -40.5deg (95%: 124nm)
B2: 49.49nm / +33.1deg (95%: 107nm)
C3: 1.721um (95%: 8.12um)
A3: 1.137um / +103.8deg (95%: 1.81um)
S3: 1.574um / +115.4deg (95%: 764nm)
A4: 6.573um / -174.2deg (95%: 58.5um)
D4: 31.83um / +69.4deg (95%: 39um)
B4: 29.75um / +40.6deg (95%: 71.4um)
C5: 2.258mm (95%: 9.74mm)
A5: 1.141mm / +101.9deg (95%: 2.1mm)
Btn 'Accept Aberr' pressed.
File /home/cscorr/sm_data/UIUC2200FS/0:

```

$$r_{sch} = 0.66 C_s^{\frac{1}{4}} \lambda^{\frac{3}{4}}$$



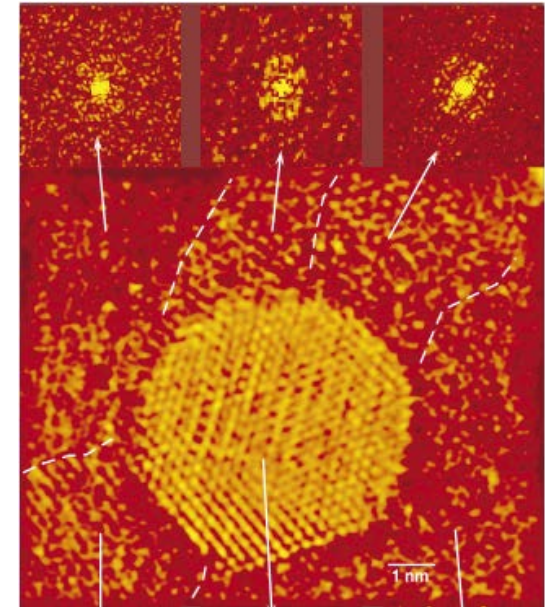
Quadrupole-Octupole C_3 - C_5 corrector



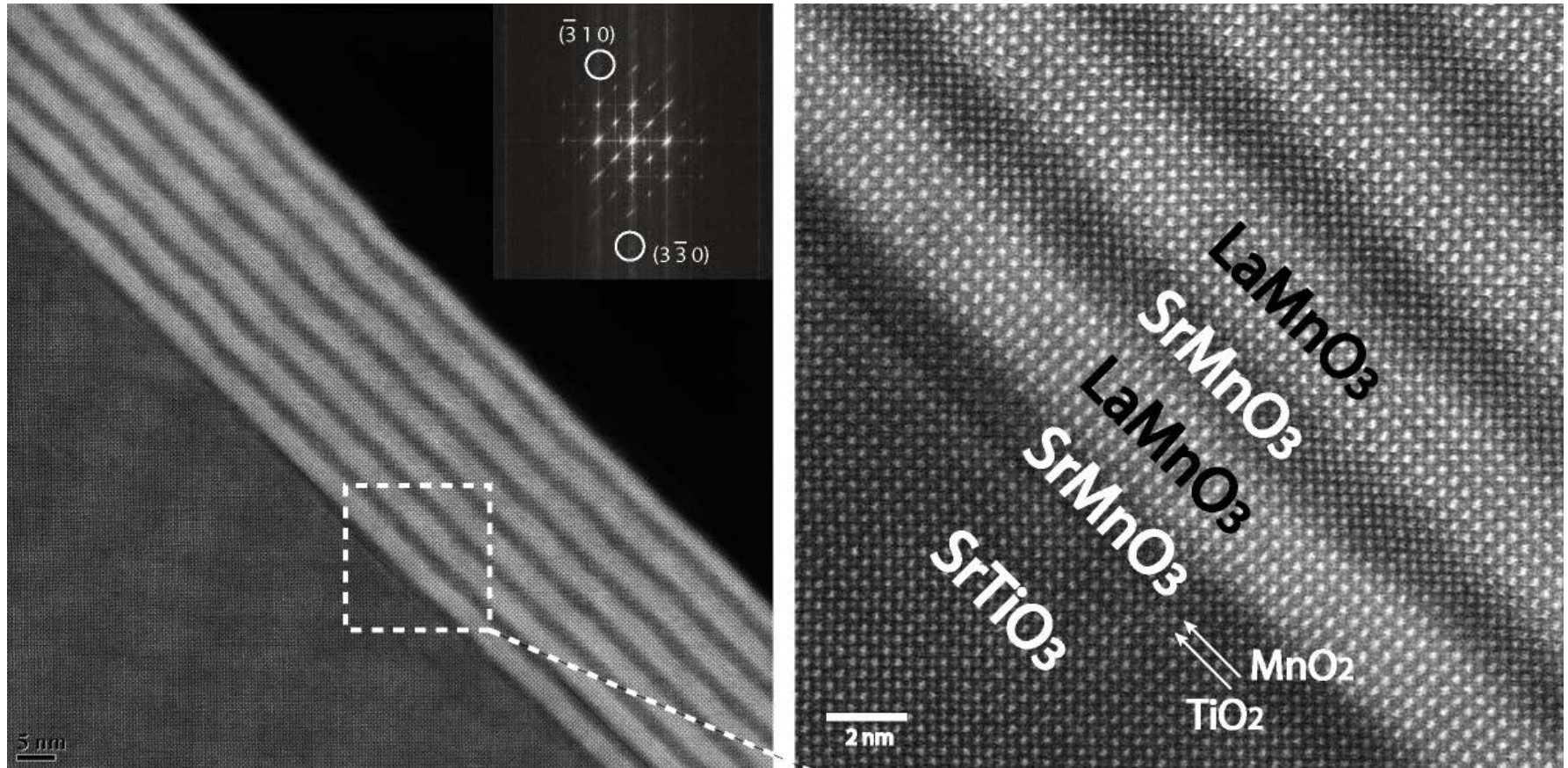
Ondrej Krivanek
Nion Company



First sub-Å image resolved in a STEM



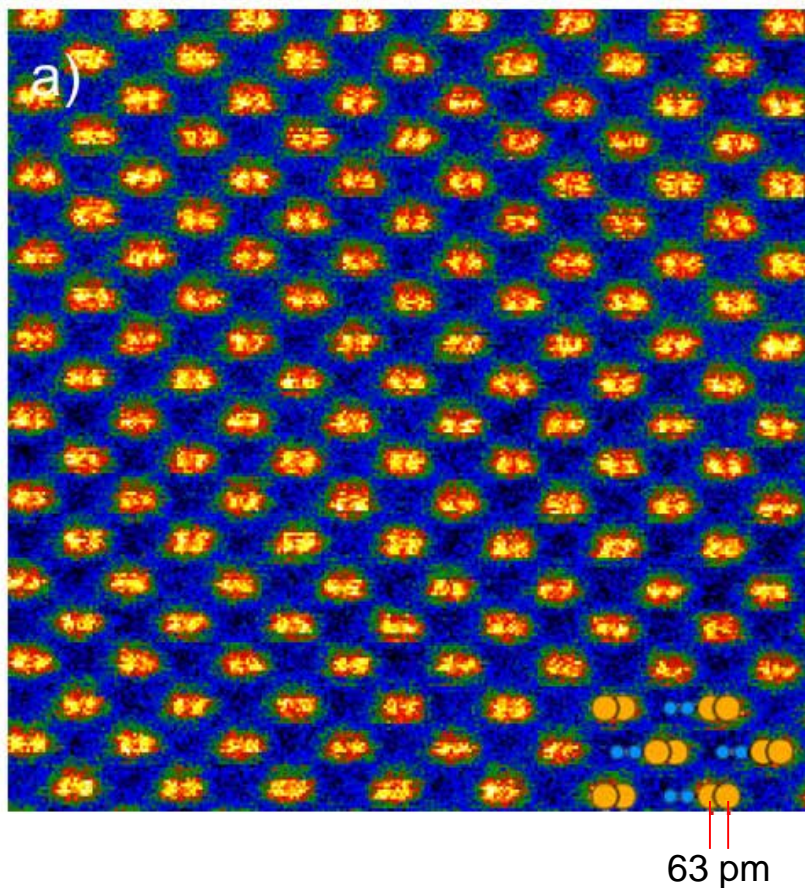
P. E. Batson et al., *Nature*, 2002.



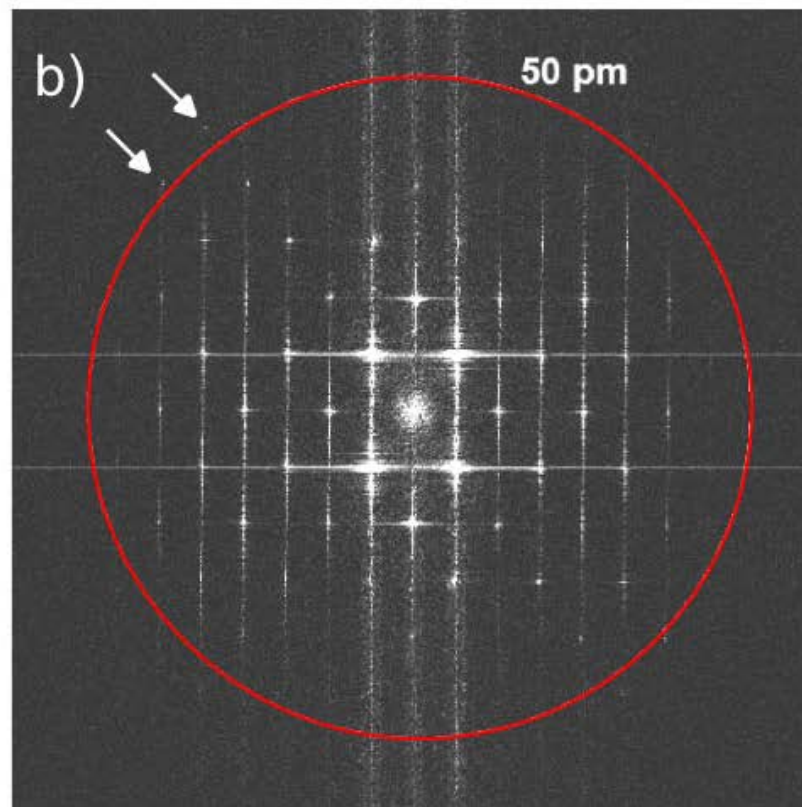
Aberration correction combined with a high stability environment and high quality specimens allow for atomic resolution imaging over a large area. 4k x 4k image shown.

Sub-Å test using GaN film along [211] zone axis

TEAM Microscope at LBNL

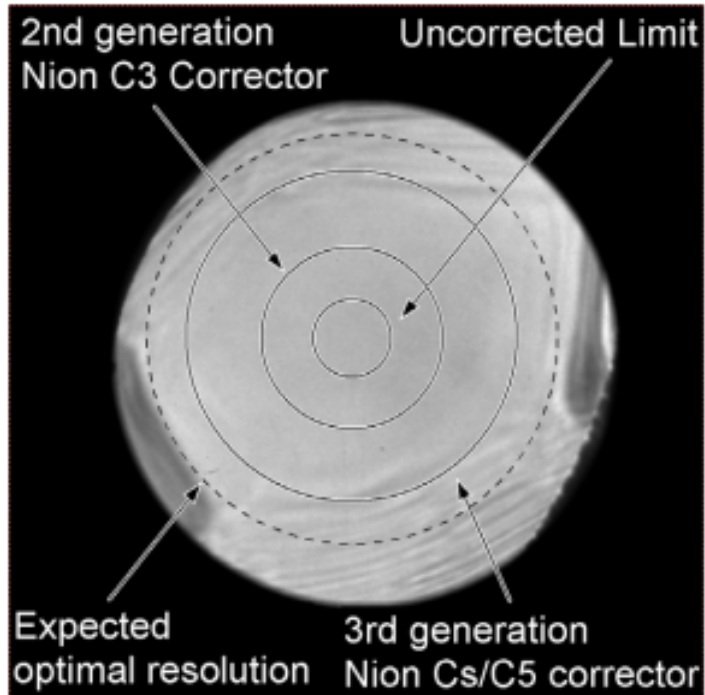


Annular dark field STEM image of hexagonal GaN [211]



Fourier transform of the image; image Fourier components extend to below 50 pm.

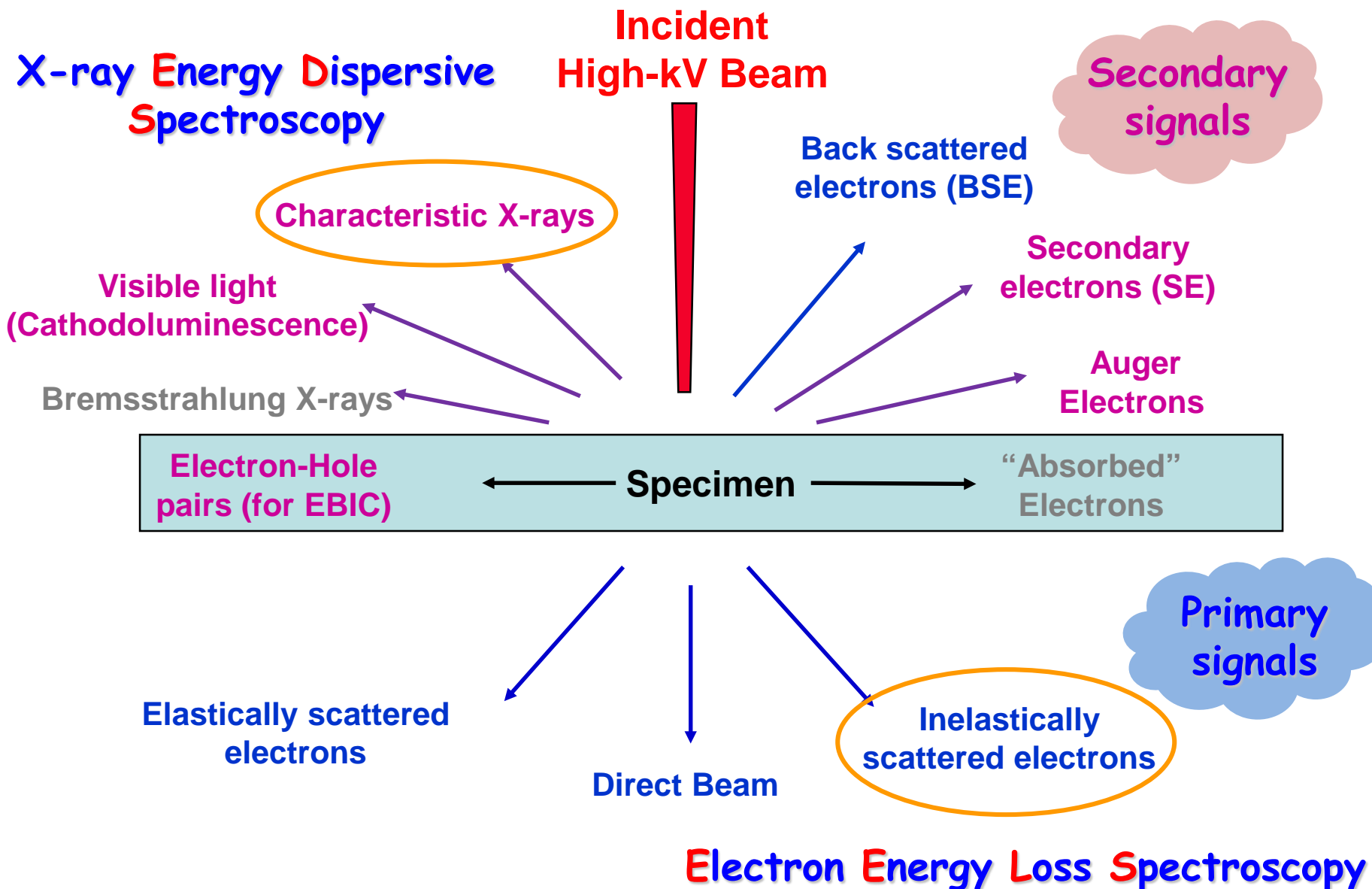
Ronchigram

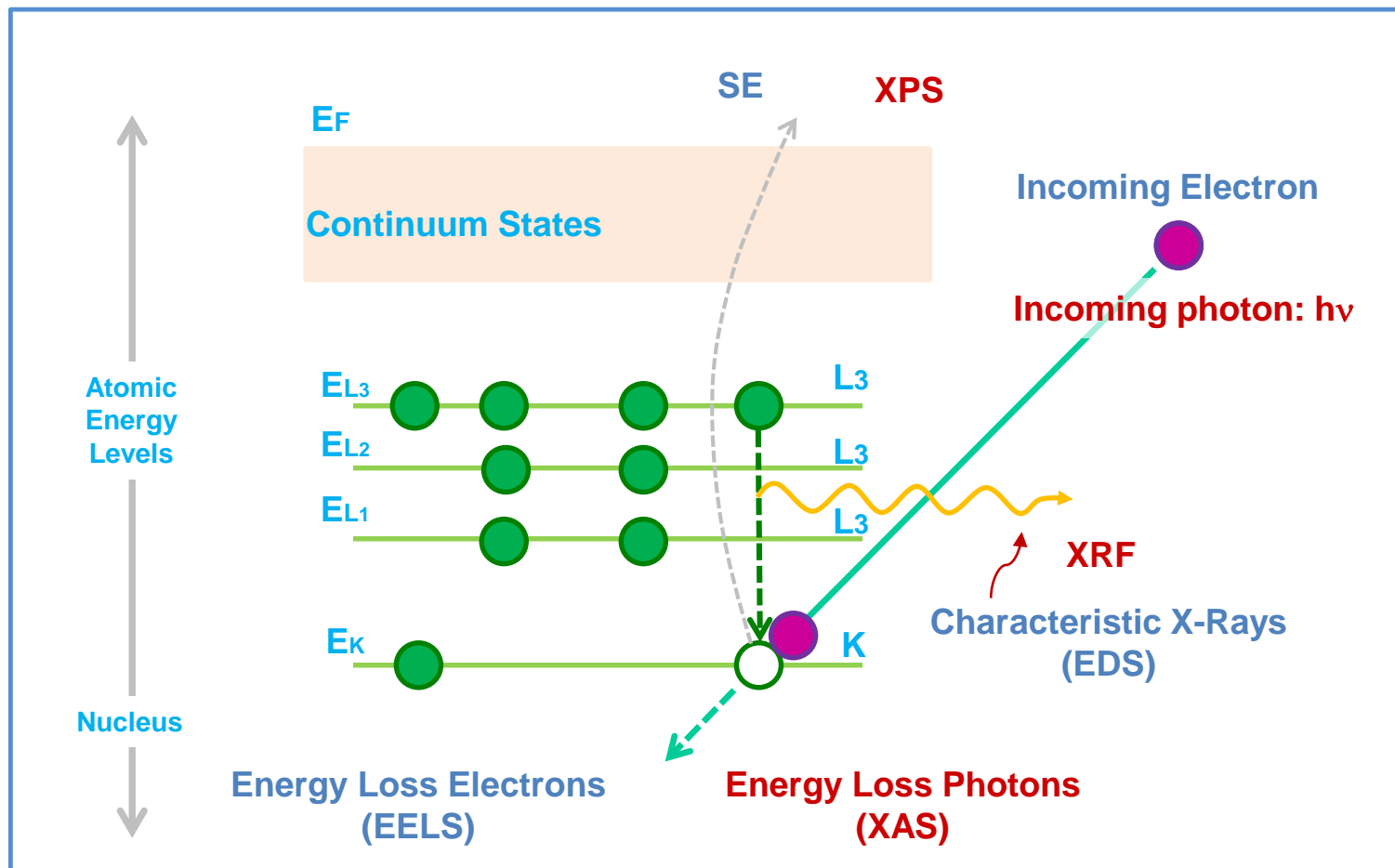


1. **Better Contrast for STEM Imaging with smaller probe**
2. **Reduced delocalization for HRTEM imaging**
3. **Sub-Å resolution imaging at low voltage (60 – 100 kV) for TEM and STEM**
4. **10-20 X more probe current in the STEM for EELS and EDS spectroscopy**



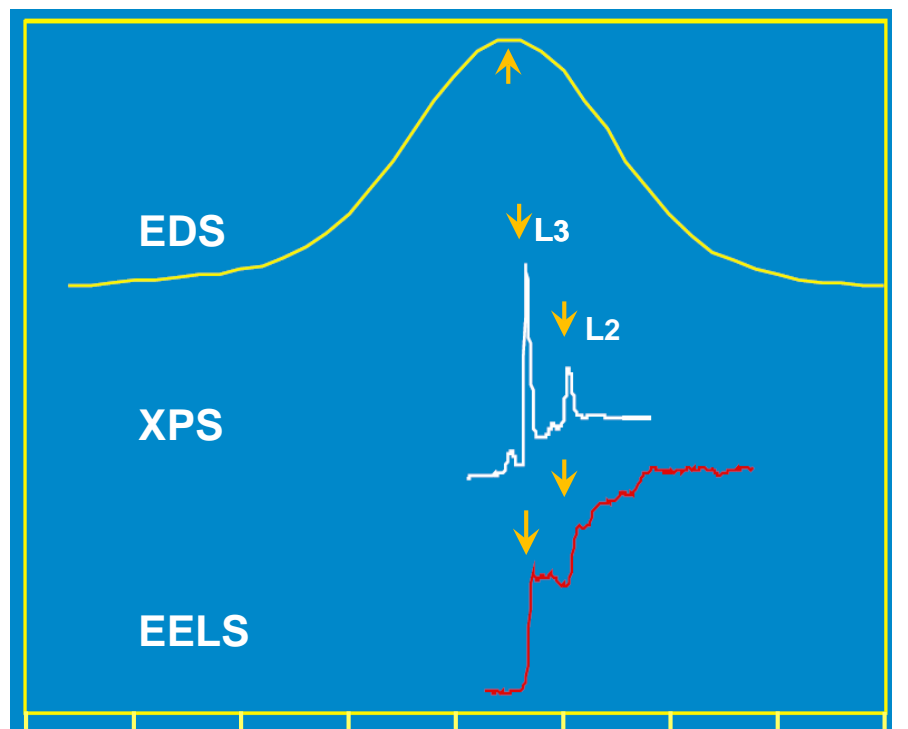
Analytical (Scanning) Transmission Electron Microscopy





The emission of Auger electrons is an alternative to X-ray emission as an ionized atom returns to its ground state

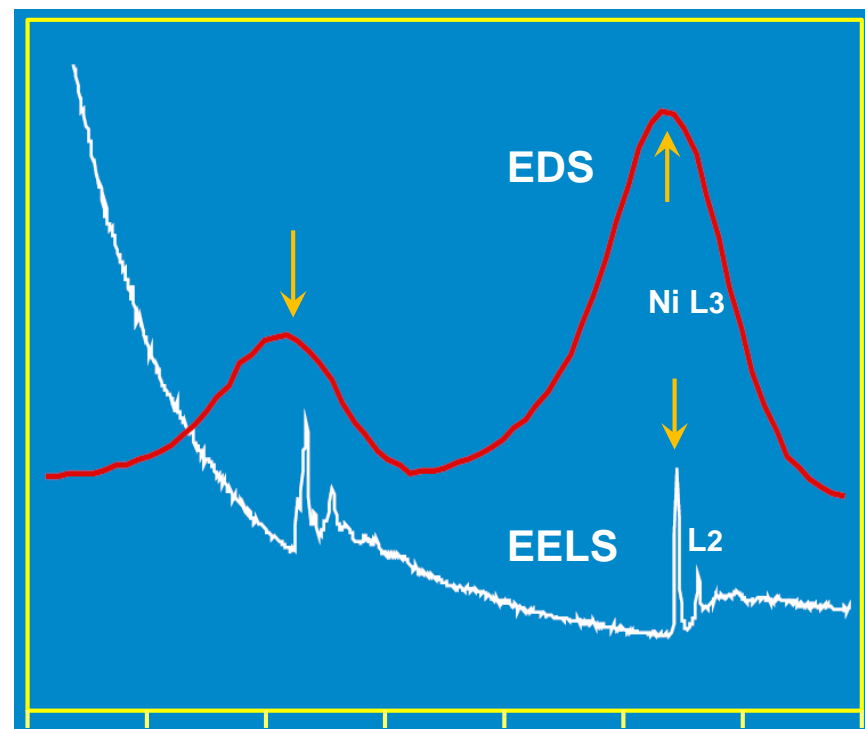
Copper L shell



700 800 900 1000 1100

Energy (eV)

NiO: O K-shell and Ni L shell

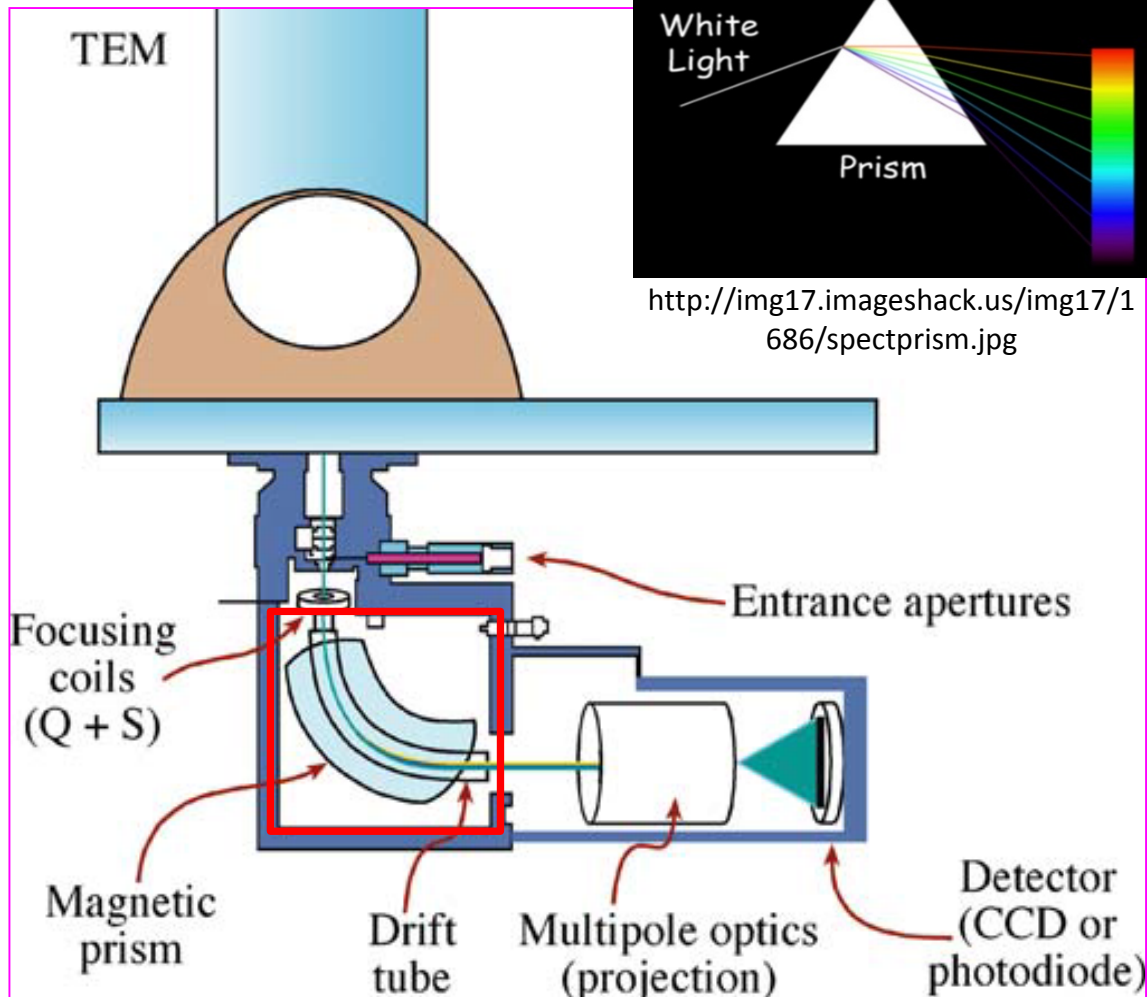


400 600 800 1000

Energy (eV)

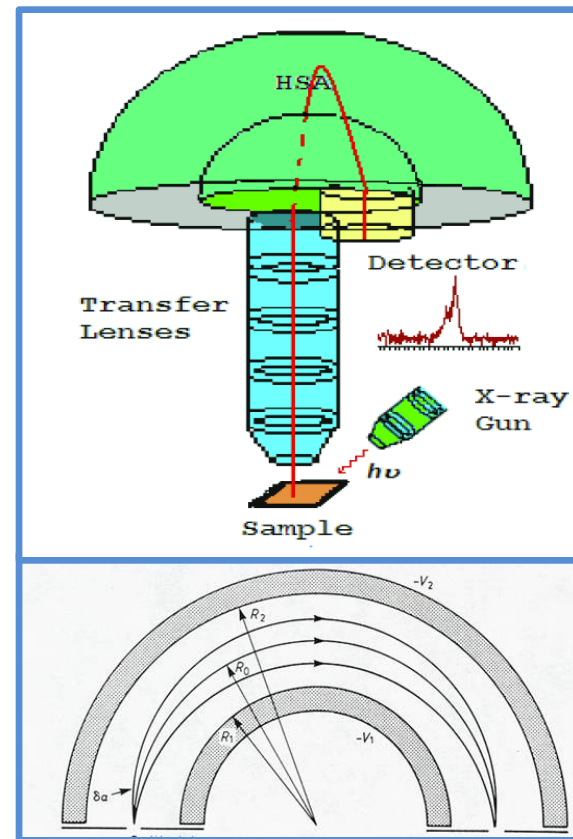
Energy resolution, Spatial resolution, Elements resolving

Post-Column Filter (GIF)



Williams and Carter 2009

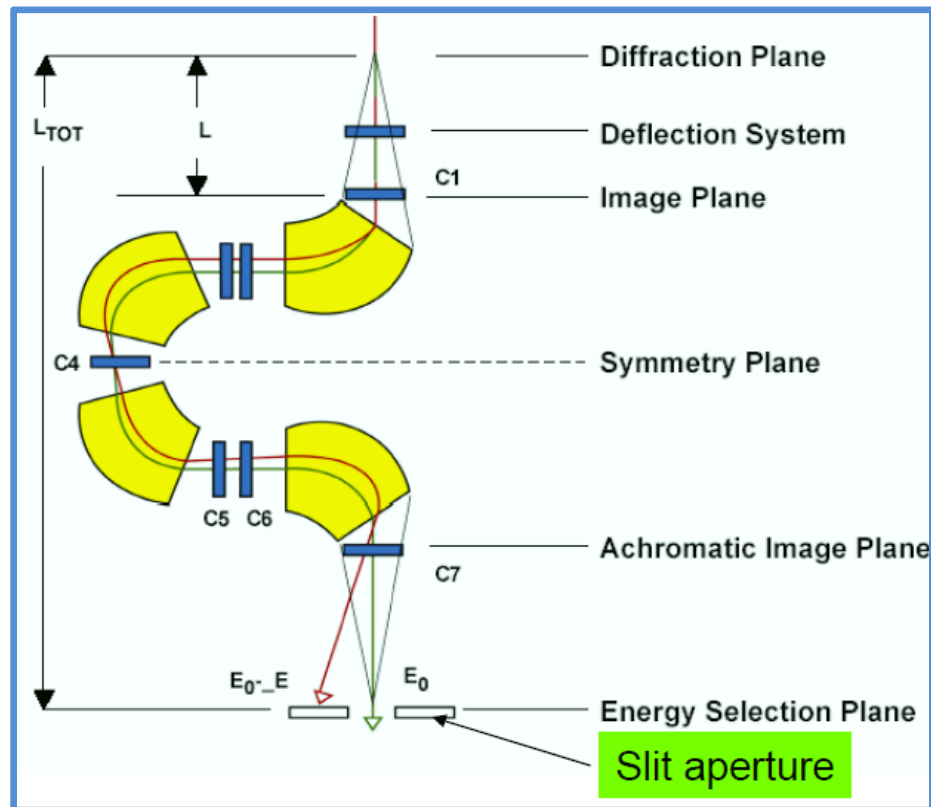
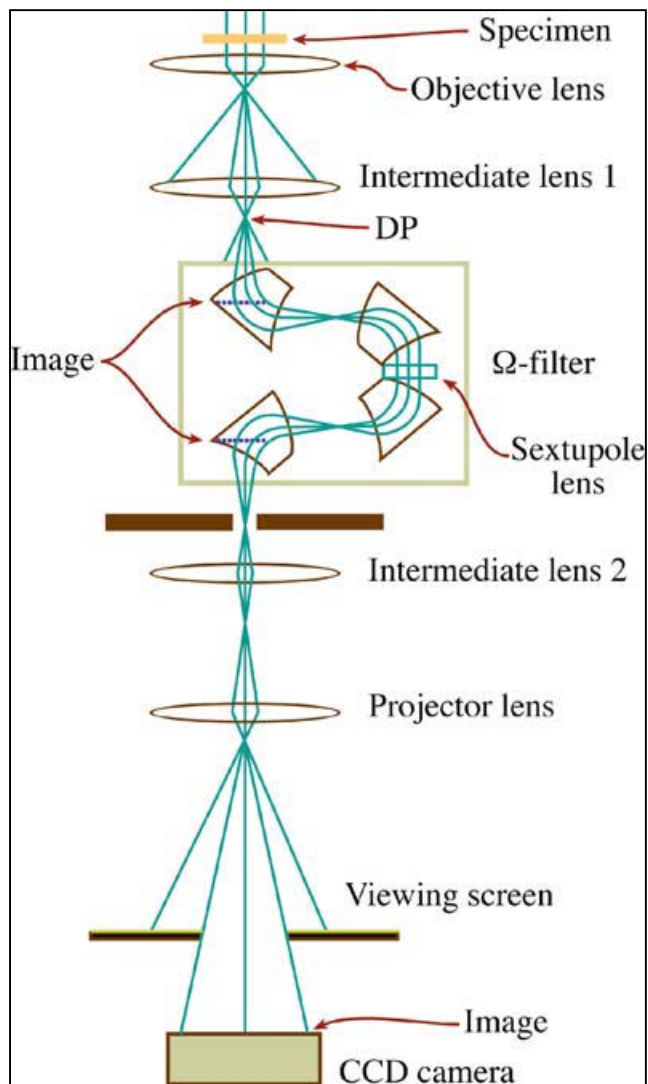
Compare: Hemispherical Electron Energy Analyzer (Surface Analysis)



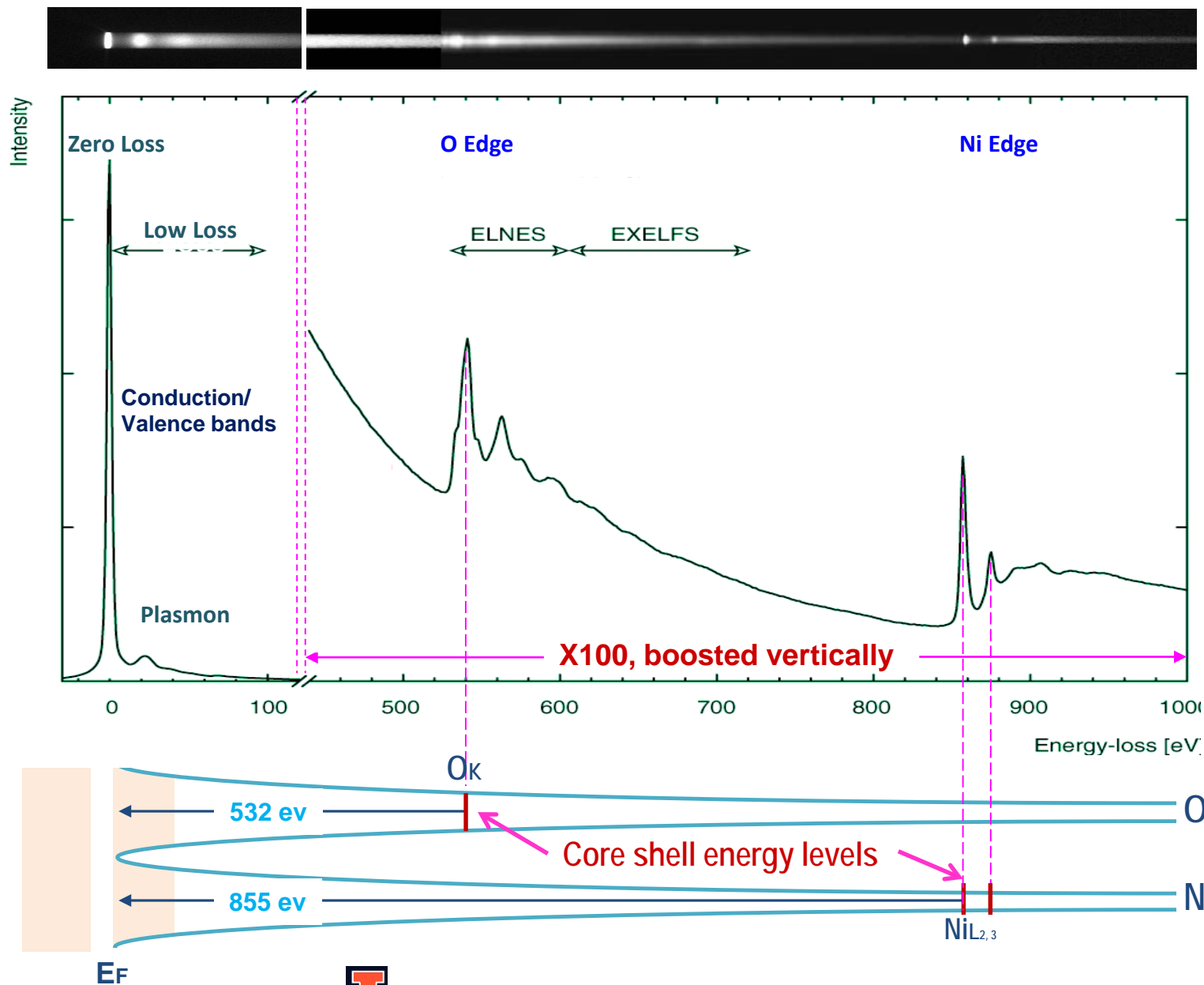
$$V_0 = (V_1 R_1 + V_2 R_2) / 2R_0$$

Casaxps.com

In-Column (Omega) Filter

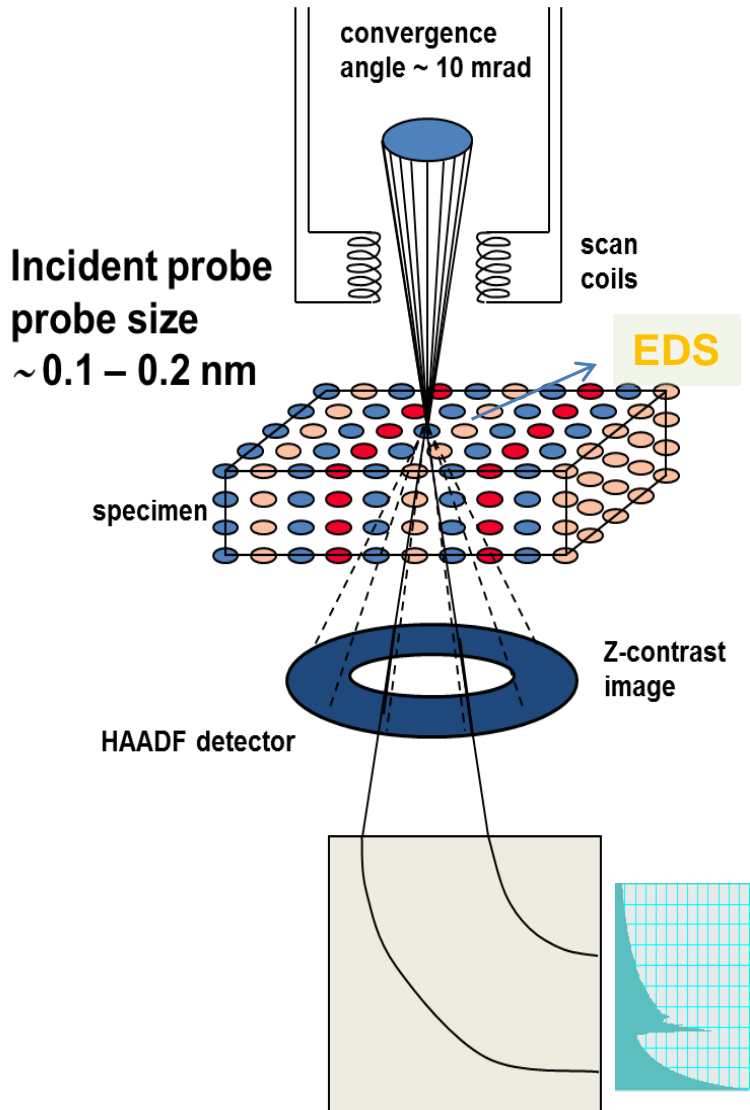


- 4 Dispersive elements
- Integrated into column



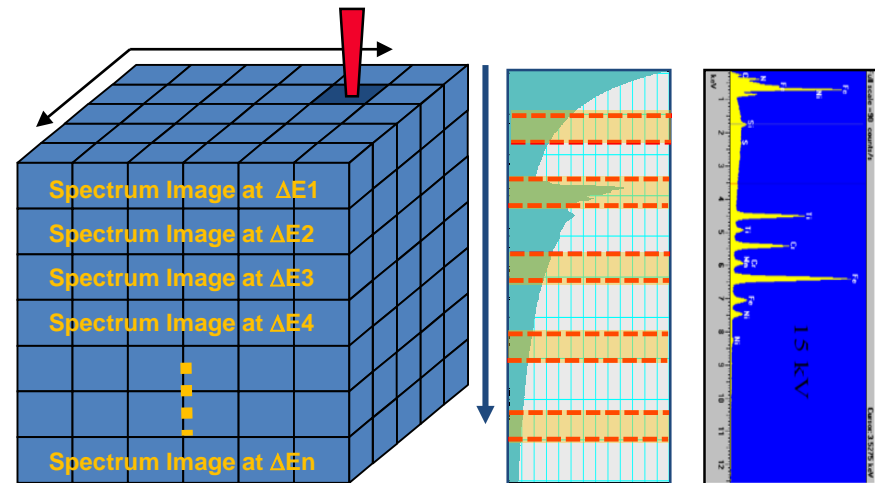


STEM-EELS/EDS Spectrum Imaging: Spatially Resolved Analysis



Spectral Imaging:

- 3D/4D data cube
- x-y image
- z spectrum (EDS/EELS)

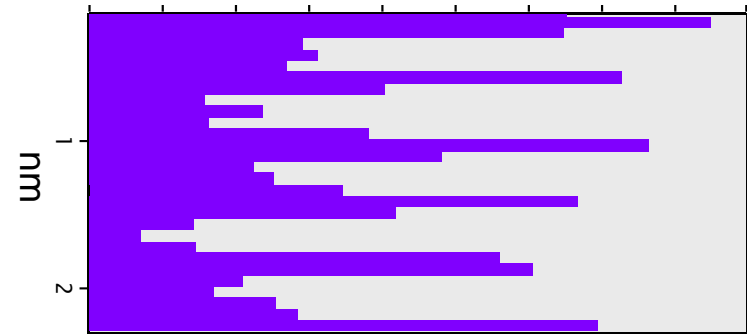
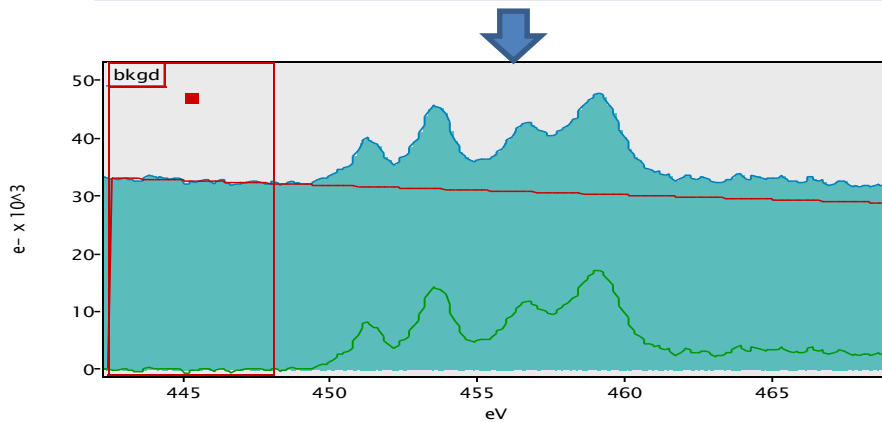
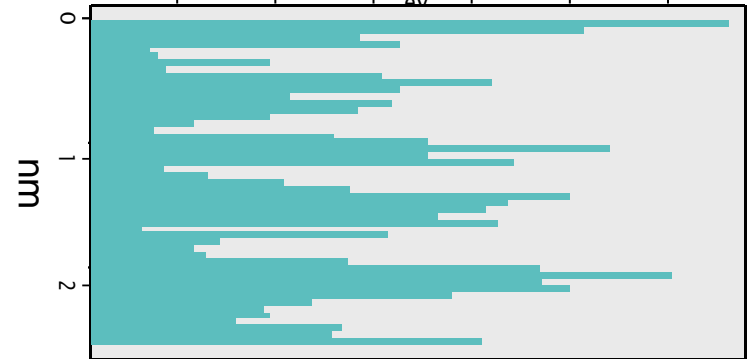
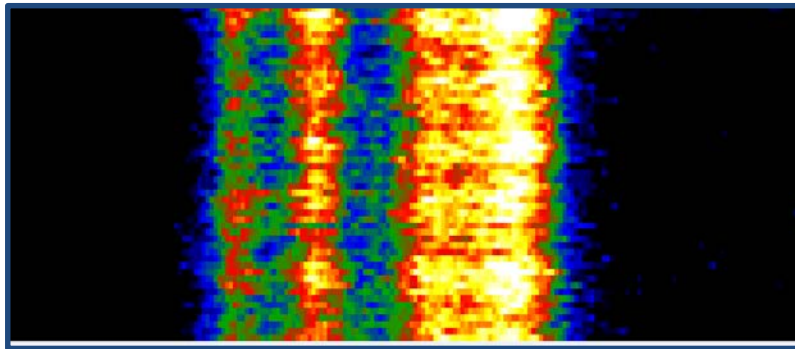
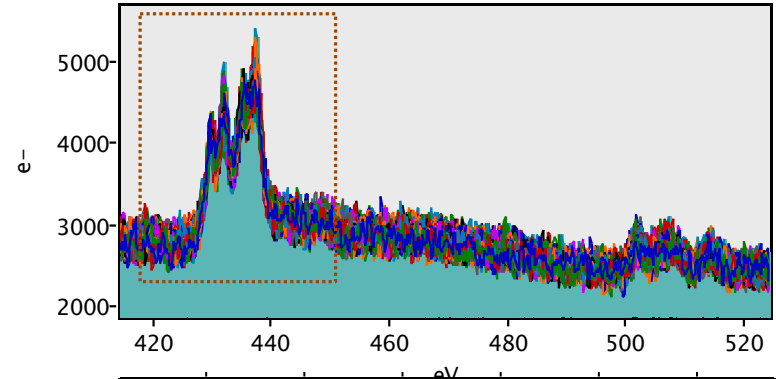
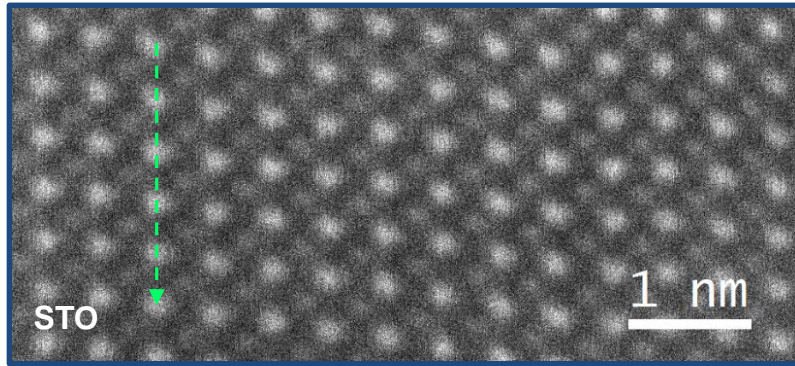


Sub Angstrom in Cs-corrected STEM !





STEM-EELS Spectrum Imaging: Line Scan

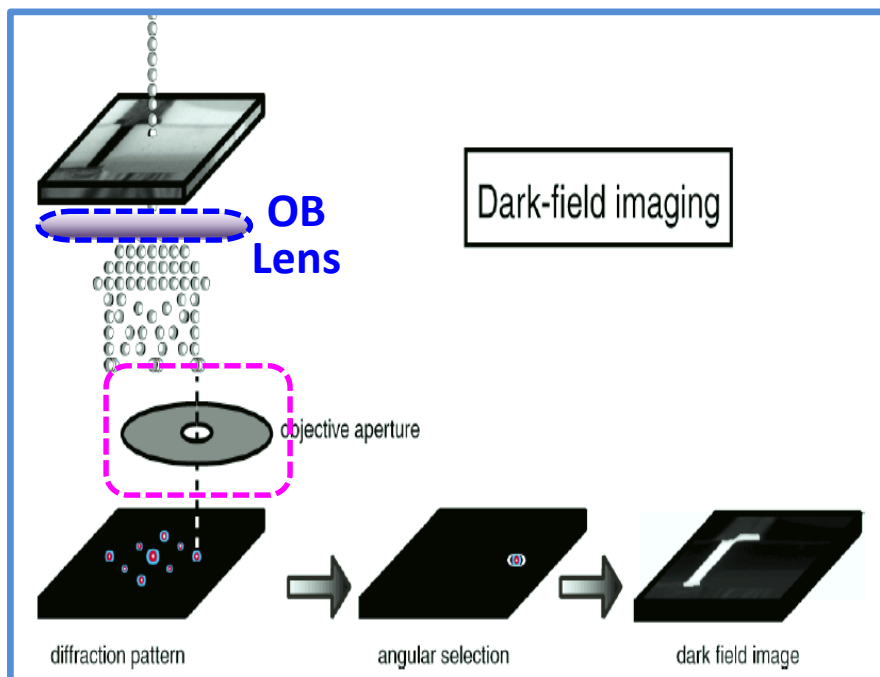


C. Chen, J. Mabon, 2200FS

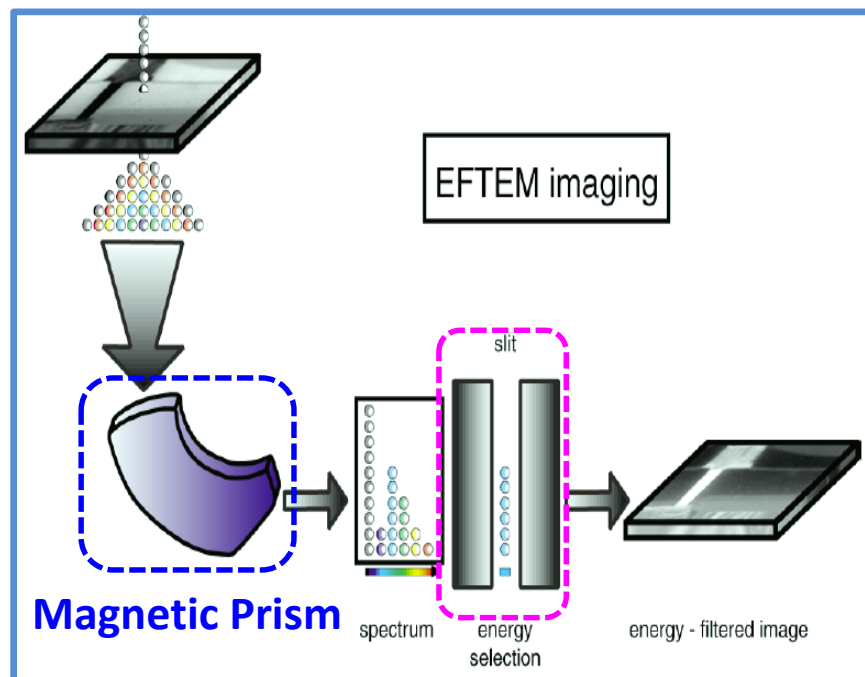


- Use the slit to select electrons of a specific energy
- Allow only those electrons to fall on the screen or CCD
- Analogy to dark-field imaging

Dark-Field TEM

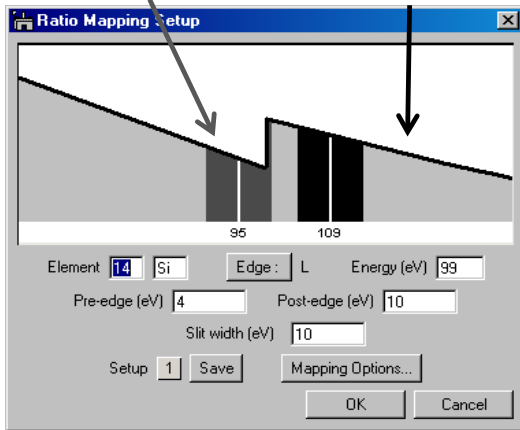


EF-TEM Imaging



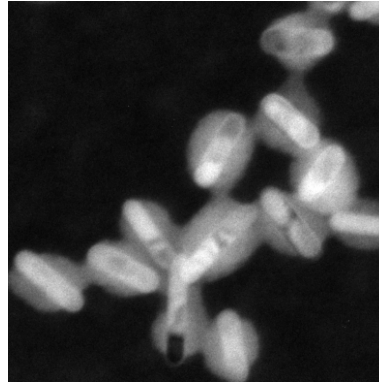
Gatan Review of EFTEM Fundamentals

Pre-edge image Post-edge image

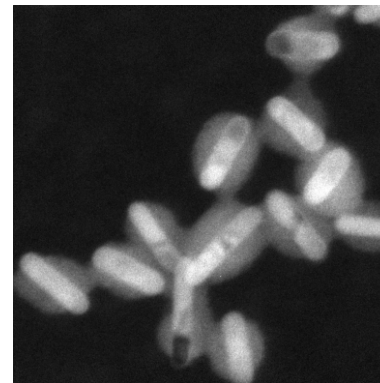


Jump Ratio Imaging

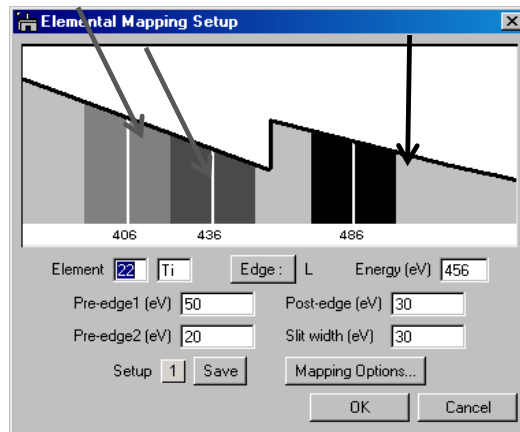
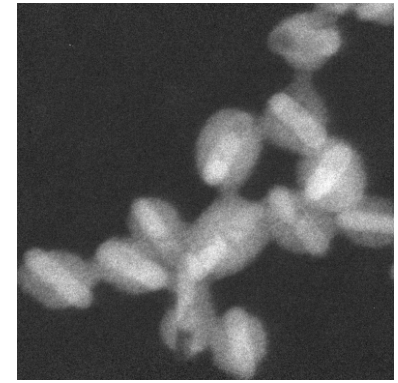
Post-edge 1



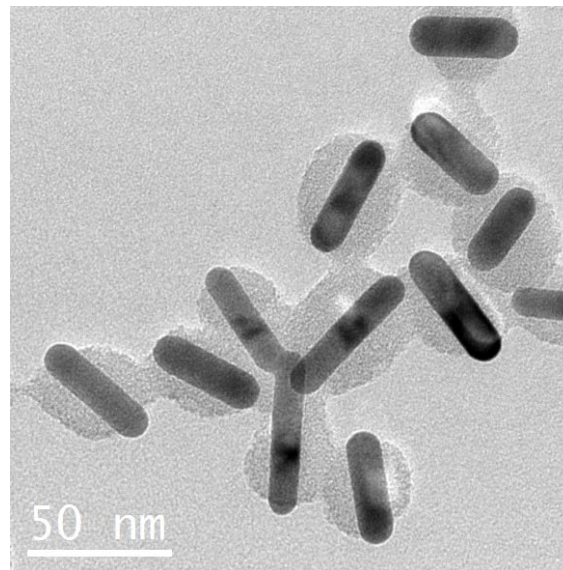
Post-edge 2



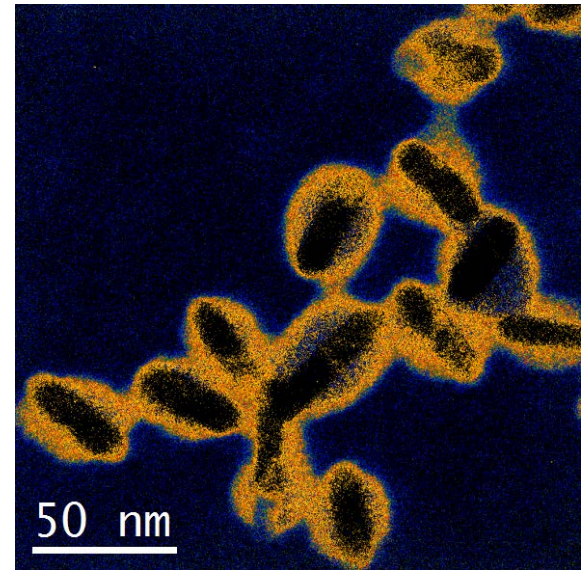
Post-edge



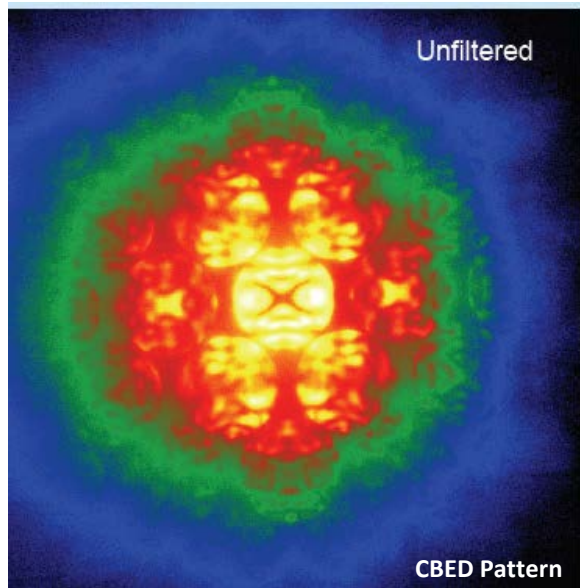
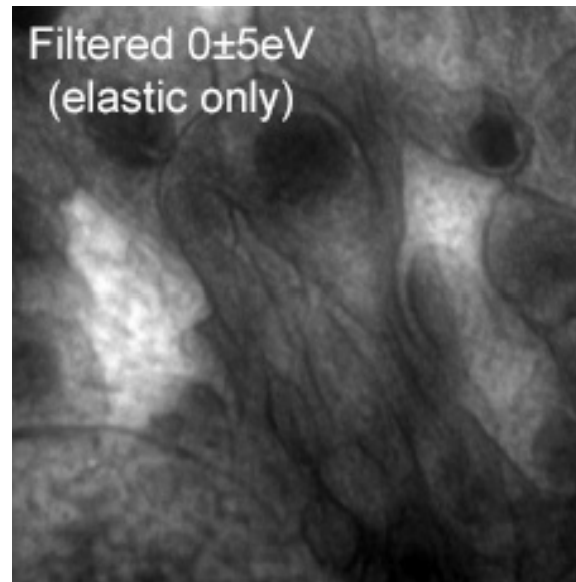
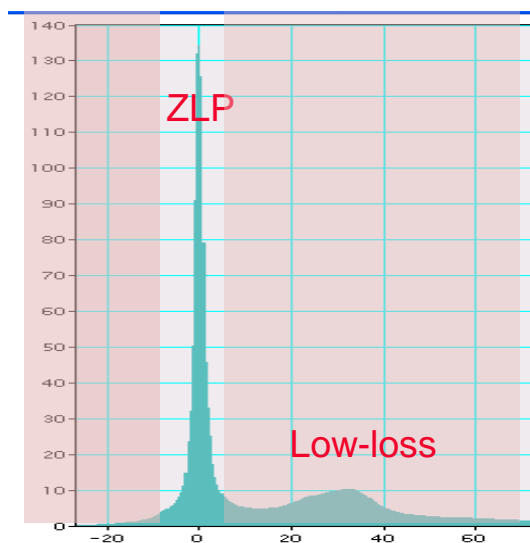
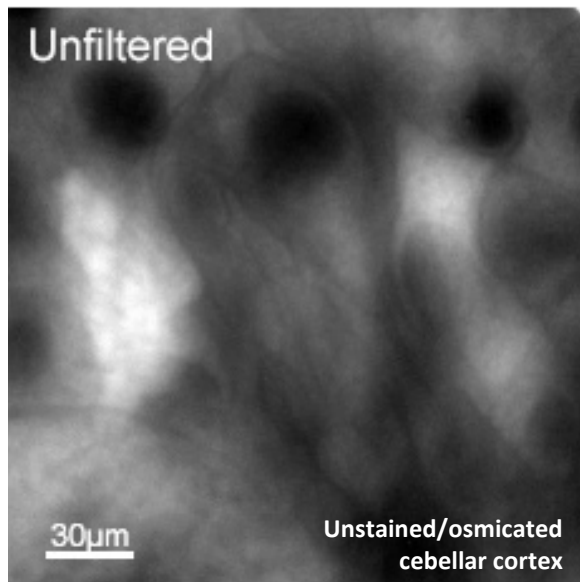
Three Window Mapping



Fast and Easy!

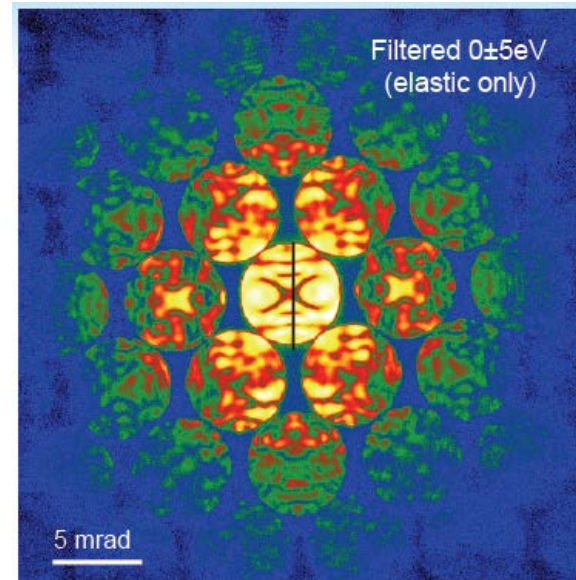


C. Chen, on 2010F, MRL



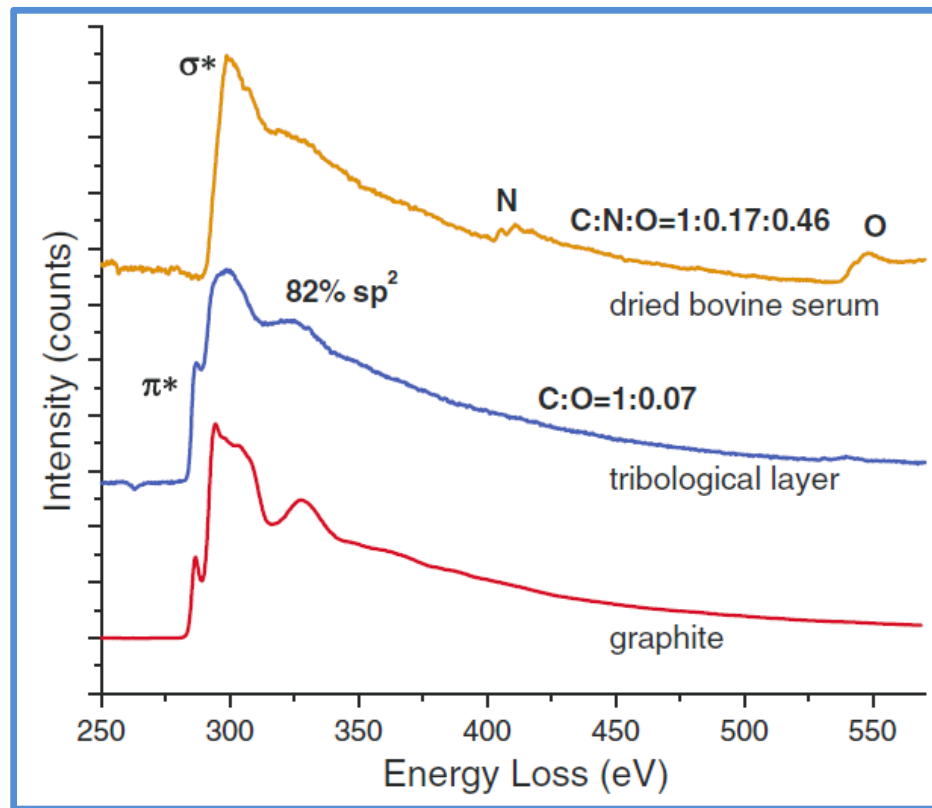
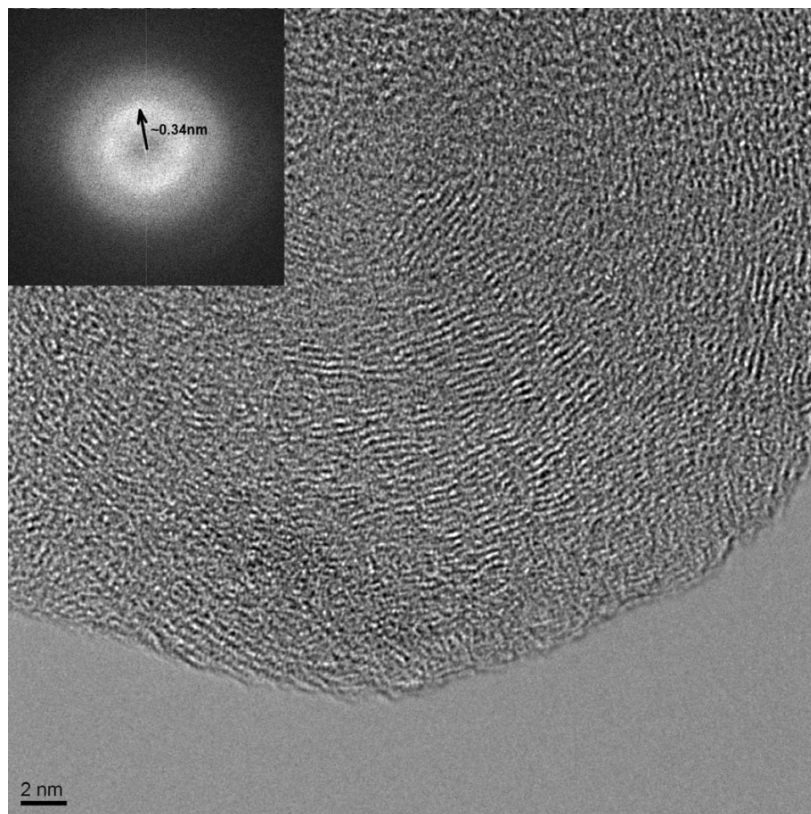
- Elastic electrons only
“Inelastic fog” removed
- Contrast enhanced
(Good for medium thick samples)

Fast and easy!





Graphitic Tribological Layers in M-on-M Hip Replacements



Science, 334, 1687, 2011

HREM image and EELS spectrum showing the graphitic nature of a thin surface layer

- EDS

$$\frac{C_A}{C_B} = k_{AB} \frac{I_A}{I_B}$$

Cliff-Lorimer equation for thin film EDS

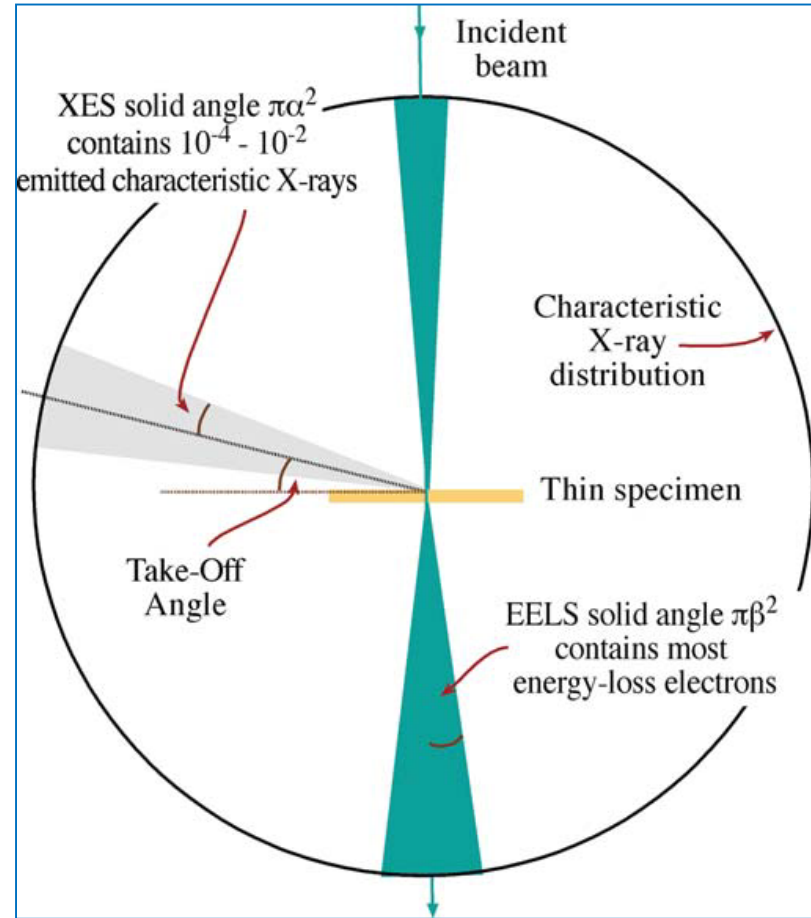
- EELS (Ratio)

$$\frac{N_A}{N_B} = \frac{I_K^A(\beta\Delta) \sigma_K^B(\beta\Delta)}{I_K^B(\beta\Delta) \sigma_K^A(\beta\Delta)}$$

- Absolute quantification (atoms / nm²)

$$N = \frac{I_K(\beta\Delta)}{I_1(\beta\Delta) \sigma_K(\beta\Delta)}$$

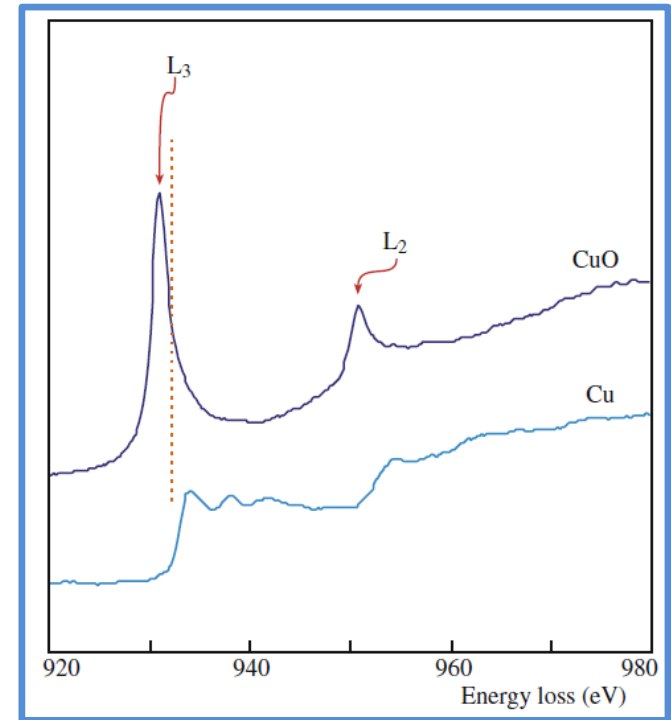
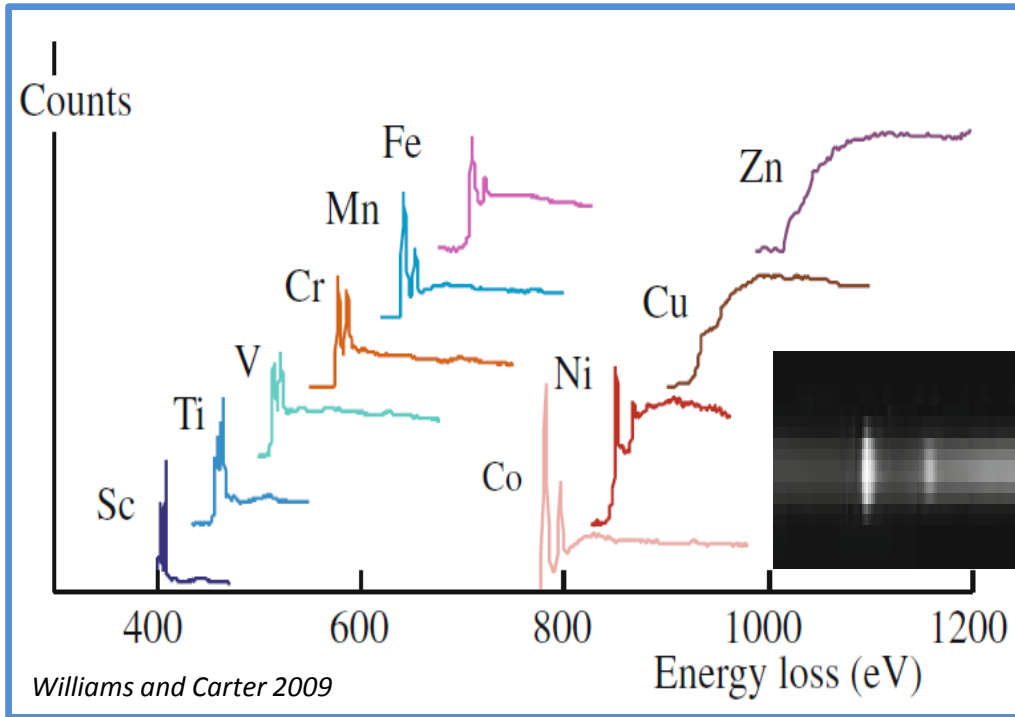
I_k : sum of counts in edge k ,
 I_L : total intensity (including zero loss),
 σ_k : partial cross-section for ionization.
 Δ integration window, β collection angle



Williams and Carter 2009



EELS Near Edge Fine Structure (ELNES): White Lines



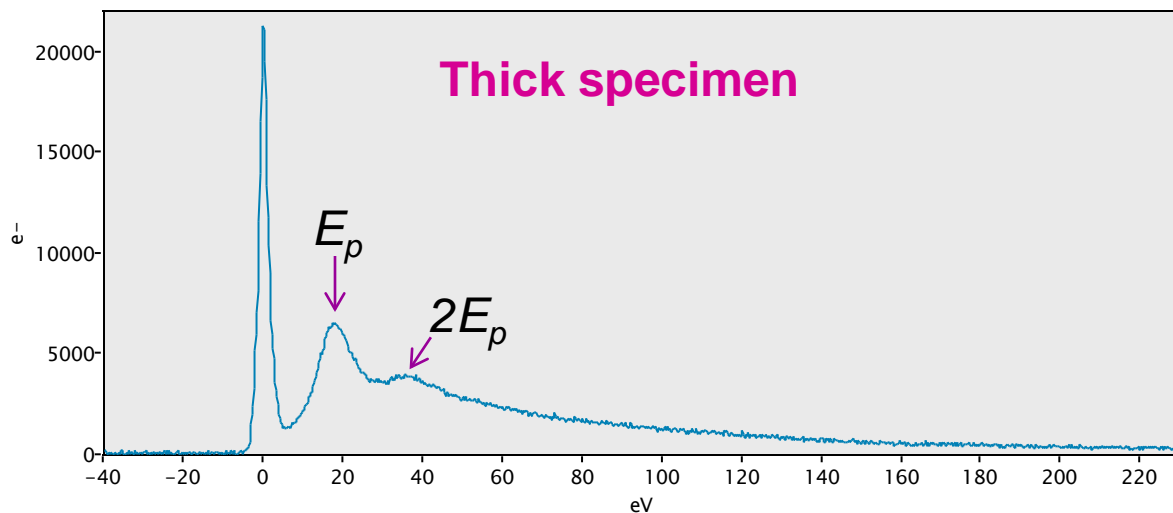
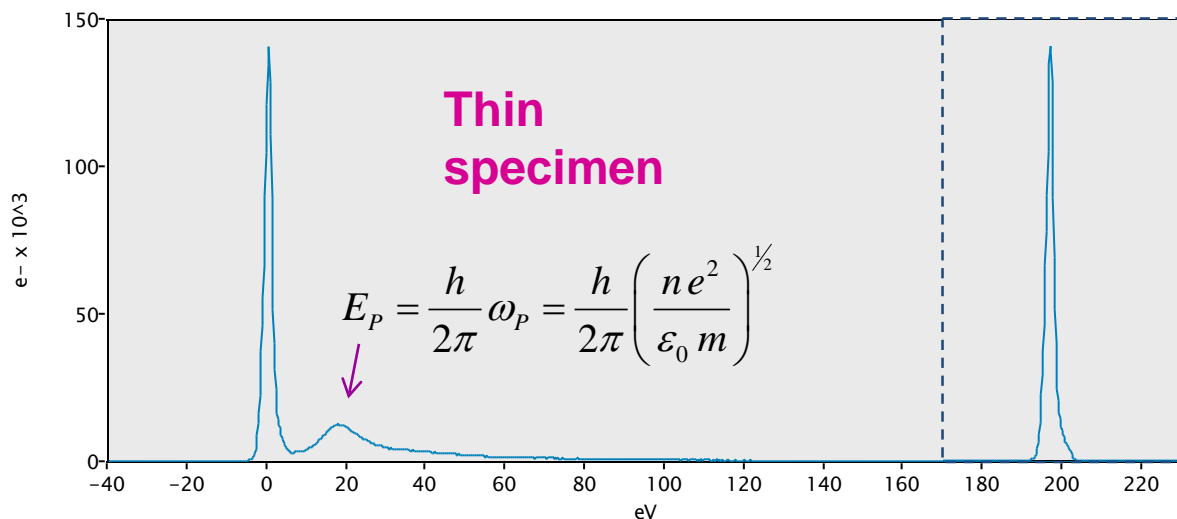
White lines in transition metals

Changes in the Cu L_{2,3} edge with oxidation:
ELNES Finger-Printing





STEM-EELS Measurement of Local Thickness



Log-ratio method

$$t = \lambda_p \times \ln(I_o / I_T)$$

t = thickness

λ_p = Plasmon MFP,

I_o = zero-loss peak

I_T = total spectrum

Relative thickness:

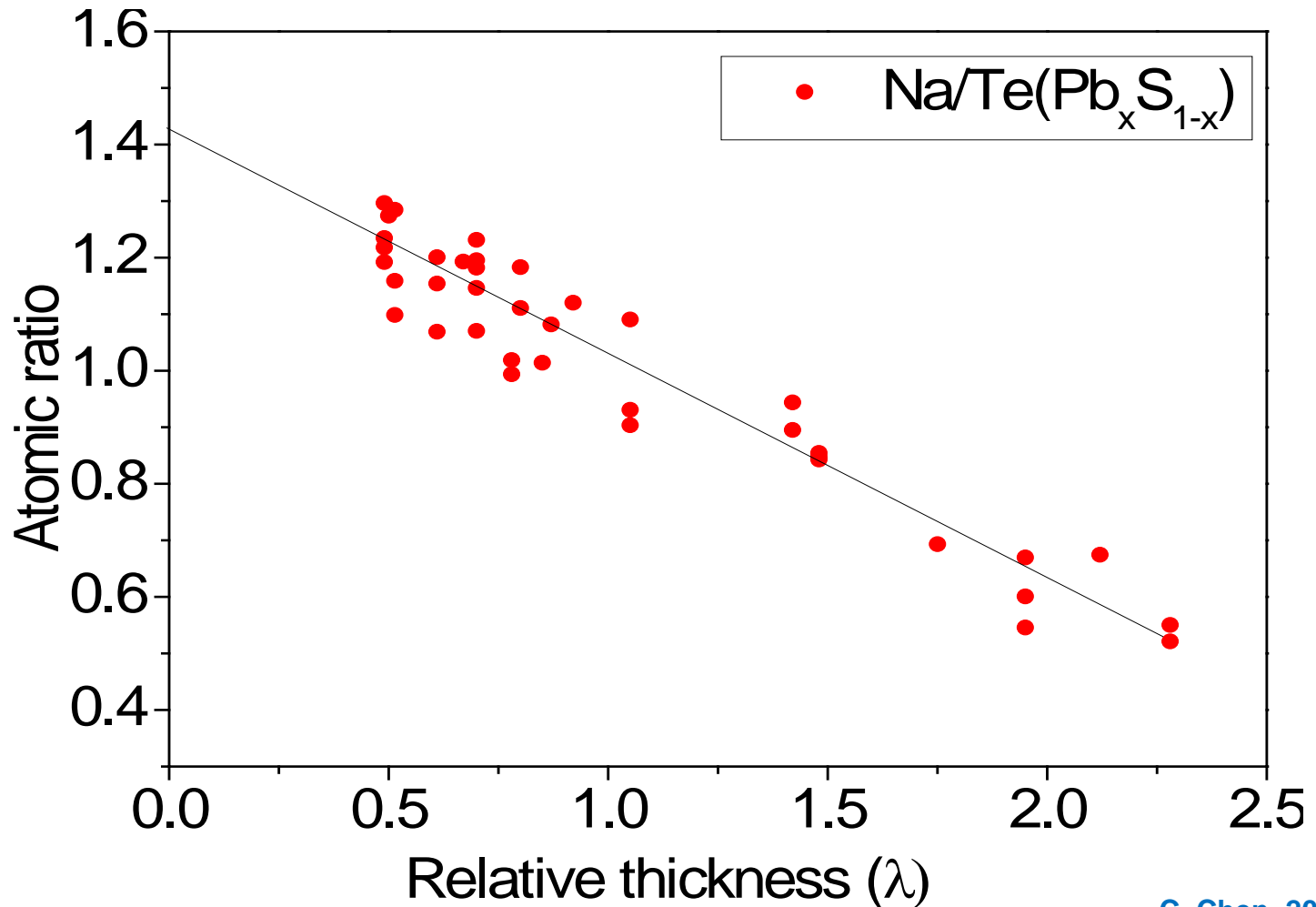
Reliable,

Fast and online,

High spatial resolution



Combine STEM-EDS & STEM-EELS



C. Chen, 2013





Comparison of EELS and EDS

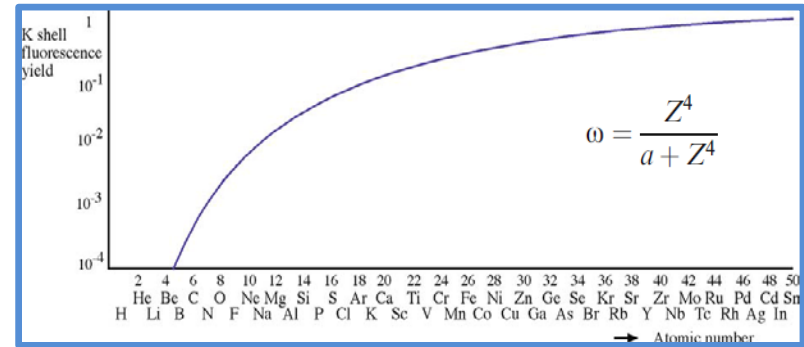
EELS (primary)	EDS (Secondary)
<ul style="list-style-type: none">• Atomic composition• Chemical bonding• Electronic properties• Surface properties• ...	<ul style="list-style-type: none">• Atomic composition only
<ul style="list-style-type: none">• Energy resolution: $\sim 0.15\text{-}1\text{ eV}$	<ul style="list-style-type: none">• Energy resolution: $\sim 130\text{ eV}$ (Mn K_{α})
<ul style="list-style-type: none">• Spatial resolution: $0.1 - 1\text{ nm}$	<ul style="list-style-type: none">• Spatial resolution: $0.1\text{ nm} - 10\text{ nm}$
<ul style="list-style-type: none">• Relatively complicated to use and to interpret	<ul style="list-style-type: none">• Easy to use• Easy to interpret
<ul style="list-style-type: none">• High collection efficiency• (close to 100 %)	<ul style="list-style-type: none">• Low collection efficiency• (1-3%)
<ul style="list-style-type: none">• Sensitive to lighter elements• Signal weak in high loss region	<ul style="list-style-type: none">• Sensitive to heavier elements• Low yield for light elements





Comparison of EELS and EDS

- EDS: low x-ray yield for lower Z
- EDS: Low energy x-ray below detection limit
- EDS: higher energy favorable (>1KV ideally)
- EELS: Lower loss favorable (<1KV ideally)



Primary vs Secondary:

- EELS: Events causing ionization
- EDS: Events after Ionization

One Ionization Event (~EELS)



Several Relaxation Events (~EDS/AES)

$$E_{\text{loss}} > E_c > E_{\text{EDS}}$$

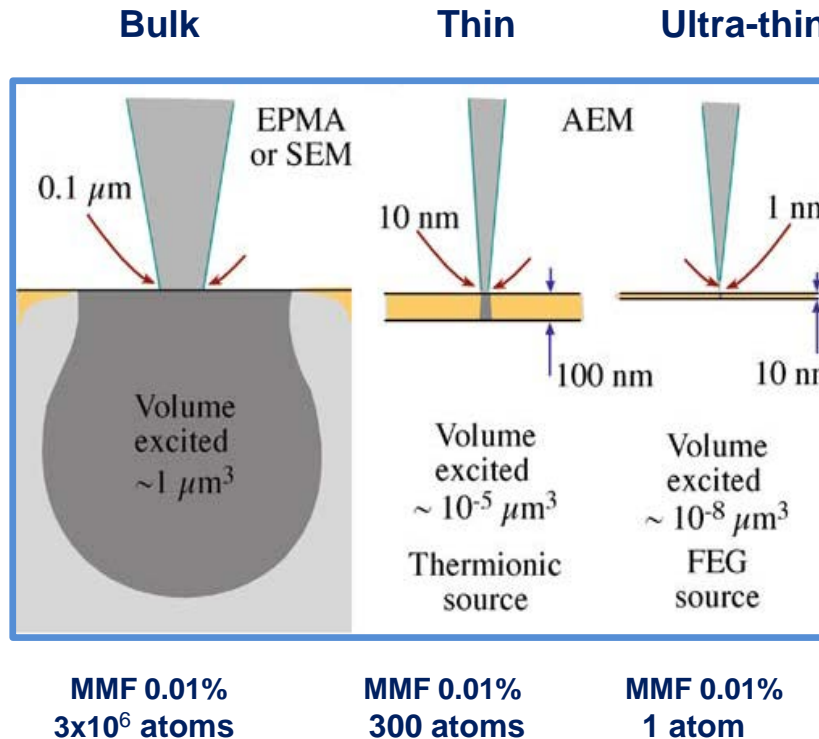
TABLE 4.2 Difference Between E_c and E_K

Element	Critical ionization energy E_c (keV)	X-ray energy E_K (keV)
C	0.282	0.277
Al	1.562	1.487
Ca	4.034	3.692
Cu	8.993	8.048
Ag	25.531	22.163

Note that the energies may be affected by bonding states but shifts will only be a few eV.

Williams and Carter 2009





Beam diameter & spreading

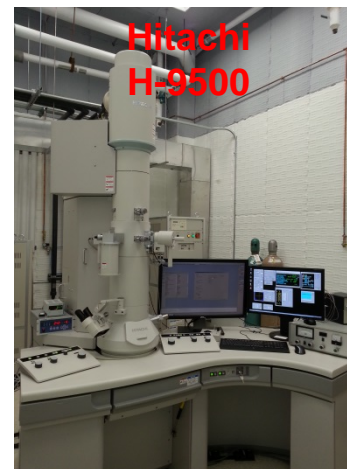
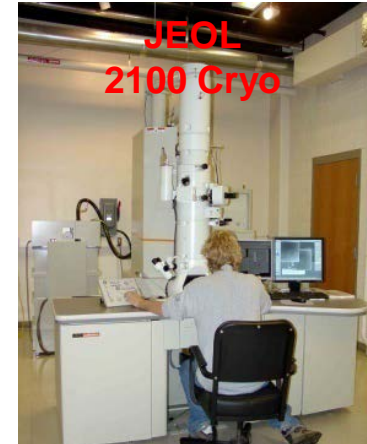
$$b = 8 \times 10^{-12} \frac{Z}{E_0} (N_v)^{1/2} t^{3/2}$$

E_0 energy, t thickness, Z atomic number, N number of atoms per volume

- **Thin foil: better R,**
- **Thin foil: worse MMF**
- **Typical MMF: 0.1–1%**
- **C_s correction improves both**
- **Achieving atomic resolution**
- **Approaching atomic level detection**

Williams and Carter 2009

1. JEOL JEM 2010 LaB6 TEM
 - TEM, low dose, NBD, HRTEM, in-situ experiments
2. JEOL JEM 2100 LaB6 (Cryo-TEM)
 - TEM, Low dose, special cryo-shielding
3. Hitachi H-9500 TEM (LaB6, 300 kV)
 - Environmental TEM (in-situ heating and gas reaction)
 - Gatan K2 camera (400 fps, or 1600 fps at reduced size)
 - Dynamic TEM (developing)
3. JEOL JEM 2010 F Analytical (S)TEM
 - EDS, STEM, Z-contrast imaging
4. JEOL JEM 2200 FS C_s corrected (S)TEM
 - Ultra high resolution Z-contrast STEM, BF STEM, NBD, CBED, EDS, EELS, EFTEM
6. Hitachi H-600 TEM (W)
 - Biological samples, staff assisted only
6. ThermoFisher Scientific Themis Z STEM/TEM

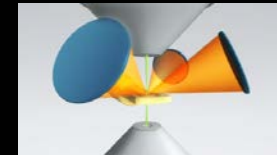
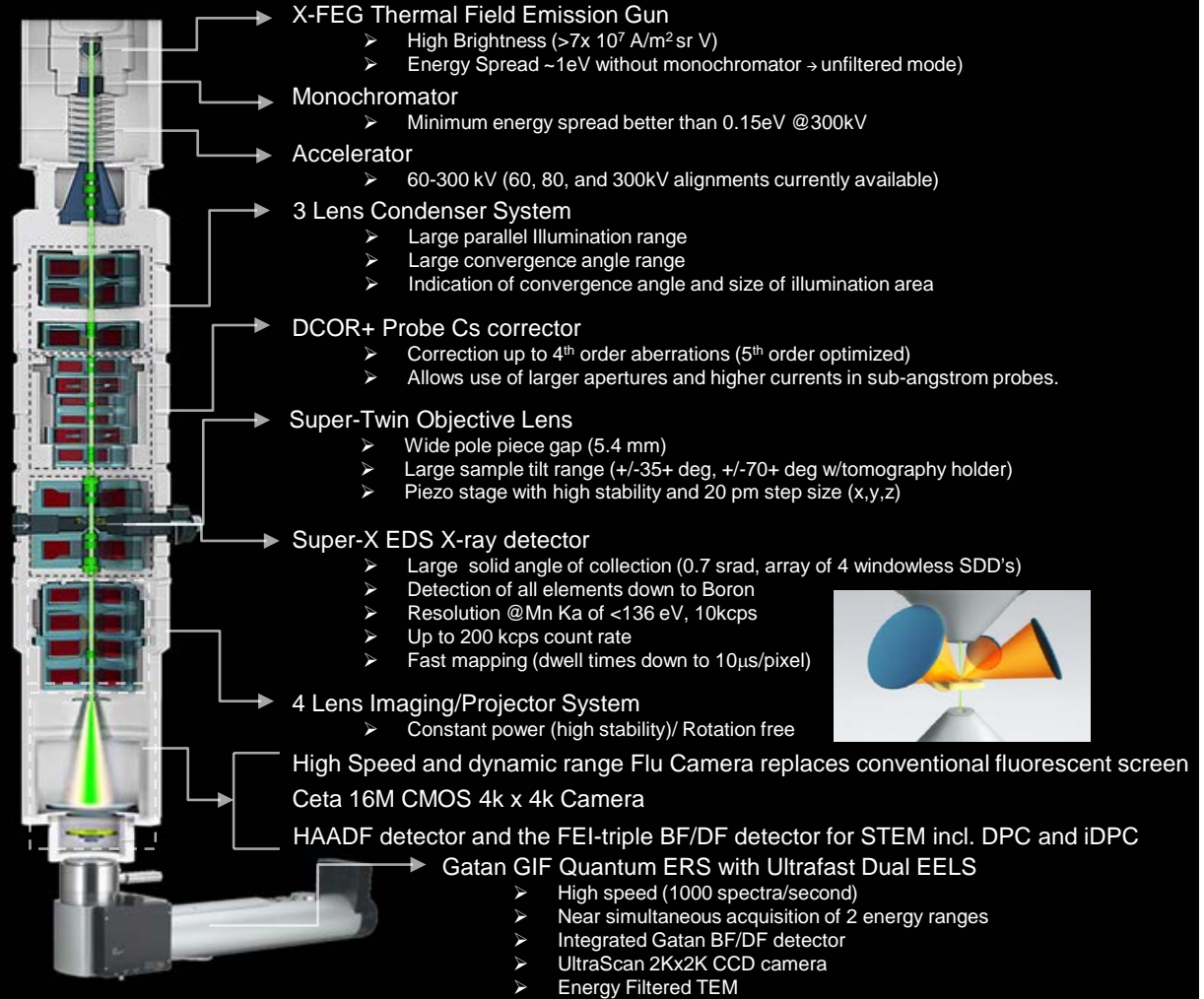
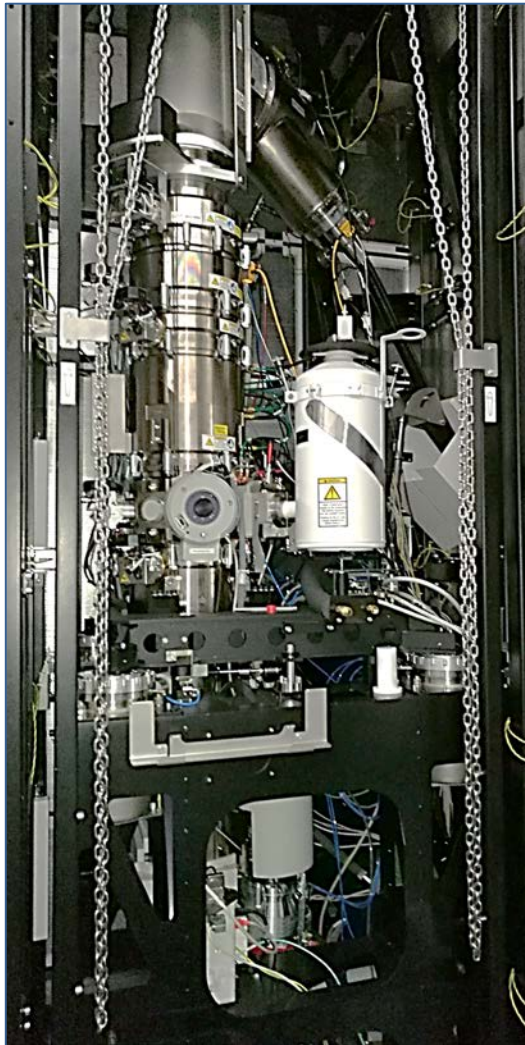


60 – 300 kV Ultra-High Resolution Analytical STEM and TEM

- **X-FEG** high brightness electron source with energy **monochromator**
- Advanced **spherical aberration probe corrector** for STEM
 - <60 pm STEM resolution attainable @300kV
 - <110 pm STEM attainable @ 80 kV
 - <120 pm STEM attainable @ 60kV
- TEM mode attainable information transfer of: 300kV-60 pm (<0.2nm point-point), 200kV-80 pm, 60kV-100pm (Young's fringe information limit method).
- Chemical mapping down to atomic resolution in 2D and 3D
 - EELS - Ultra-fast Dual EELS detector for detection of light elements, mapping bonding states
 - EDS - 4-detector EDX for fast and atomic or nanoscale chemical analysis
- Monochromator for high energy resolution EELS
 - Mapping of plasmonic modes, fine structure for local chemical and electronic states
 - Measurement of local bandgap in semiconductors
 - Reduced chromatic aberration for imaging (in particular low kV's)
- Lower kV operation (60 and 80 kV) for 2D electronic materials and low dimensional molecular structures
- STEM/TEM Tomography acquisition
 - 3D imaging (down to ~1 nm resolution)
 - 3D chemical mapping (EDS)
 - Diffraction tomography
- OptiSTEM+: Automated fine tuning low order aberrations (C1\A1, A2\B2)
- OptiMono: Automated Monochromator tuning
- iDPC: Integrated differential phase contrast (a new ABF) for imaging light elements simultaneous with heavy element (more linear with Z) at low dose



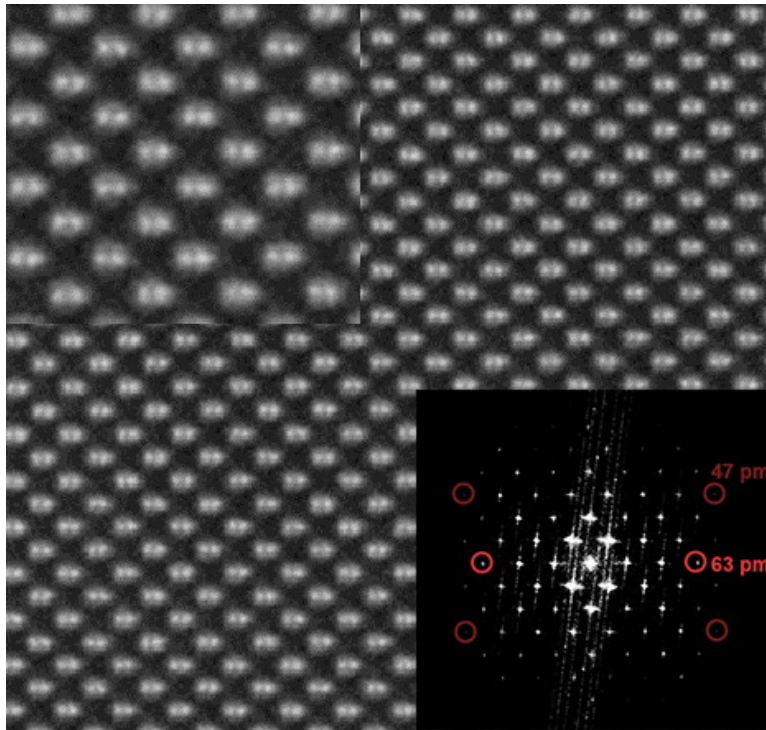
ThermoFisher Scientific Themis Z STEM/TEM:



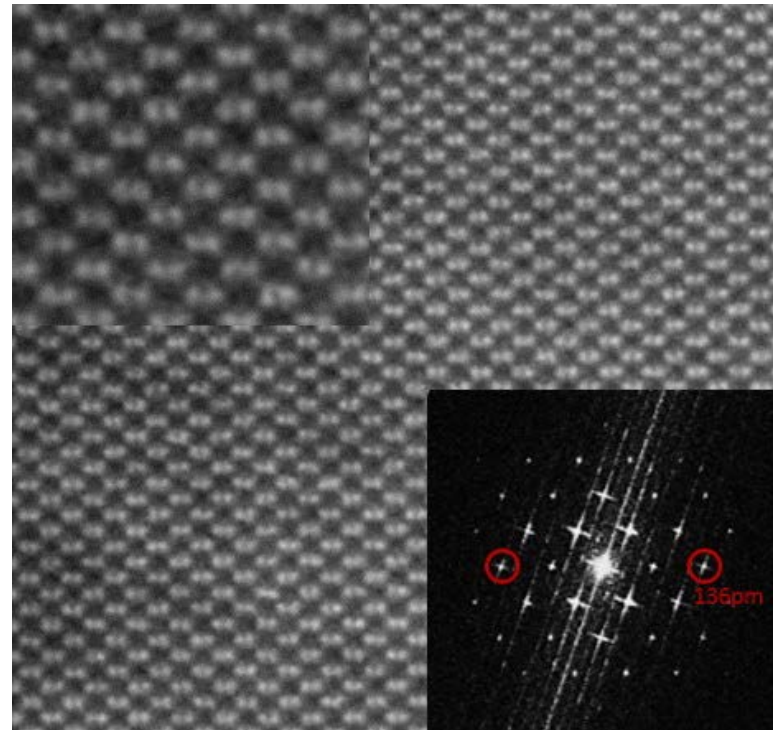


Imaging Performance: Themis Z STEM:

GaN [211] imaged at 300 kV
showing <63 pm resolution



Si [110] imaged at 60 kV showing
<136 pm resolution

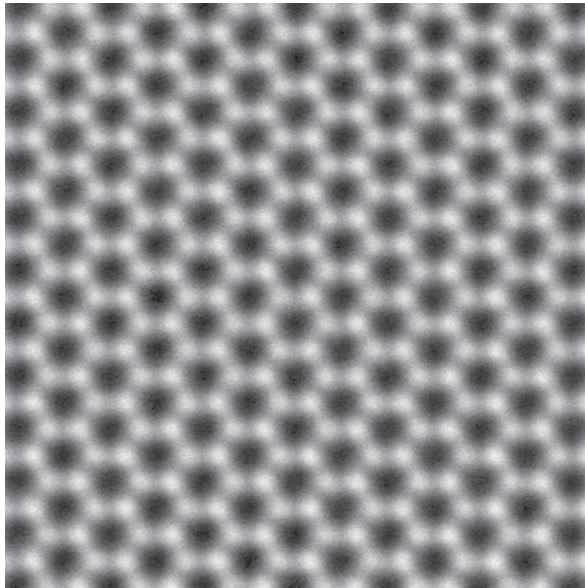


Images - Thermo Fisher Scientific
<https://www.fei.com/products/tem/themis-z-for-materials-science/>

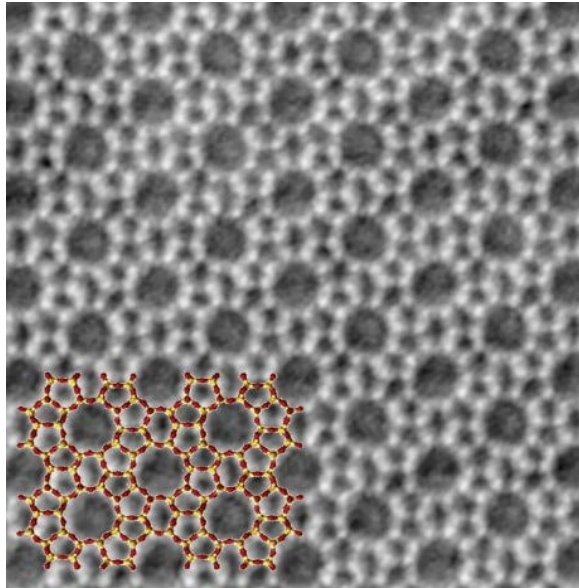


- Low kV operation (60/80 kV) for knock-on damage sensitive materials
- Low dose sensitivity for dose sensitive materials
- Low atomic number imaging sensitivity with iDPC

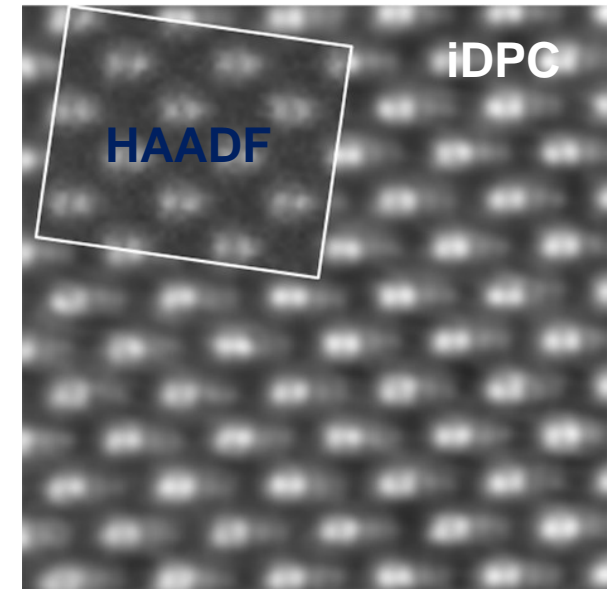
HAADF STEM image of a graphene lattice imaged at 60kV.



Zeolite imaged at 300kV and <math><1\text{pA}</math> with iDPC. Oxygen atoms are visible with extreme low doses.



GaN [211] imaged at 300 kV with iDPC Ga and N dumbbells are clearly visible.

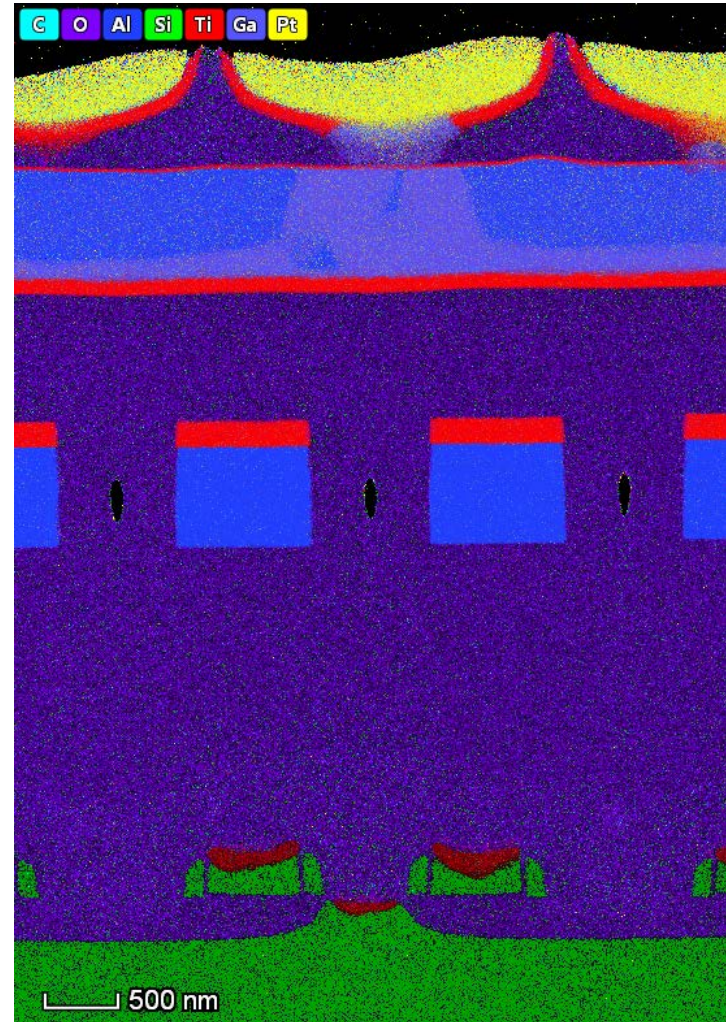
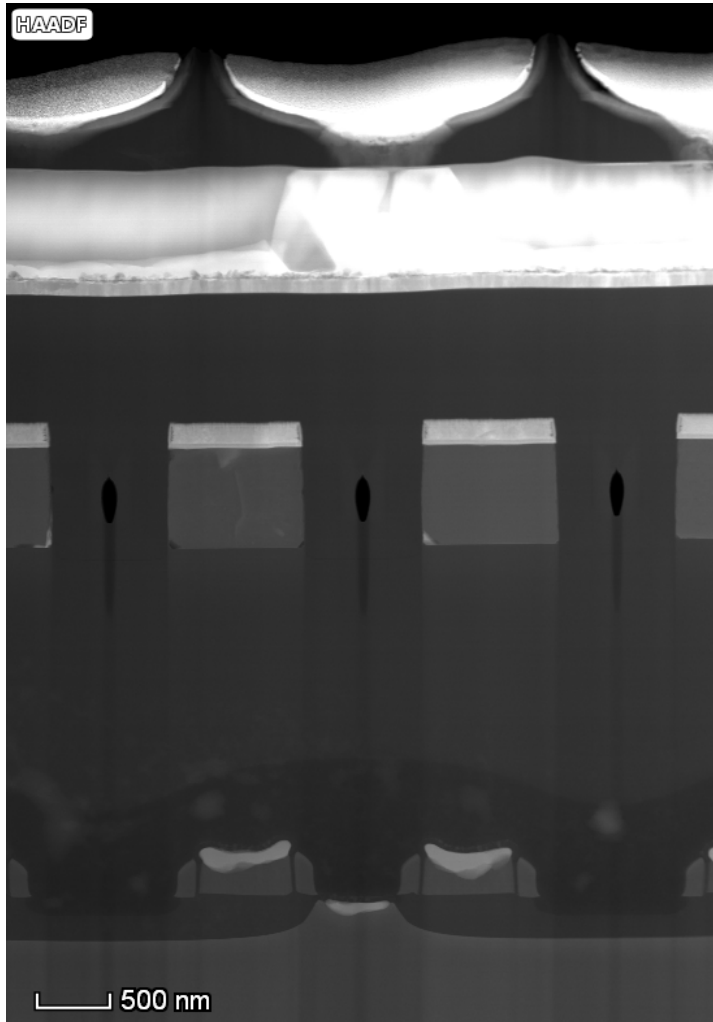


Images - Thermo Fisher Scientific

<https://www.fei.com/products/tem/themis-z-for-materials-science/>



High throughput spectrum imaging: Microprocessor X-TEM EDS



300KV, 1.2nA, 40K cps, 12 minutes

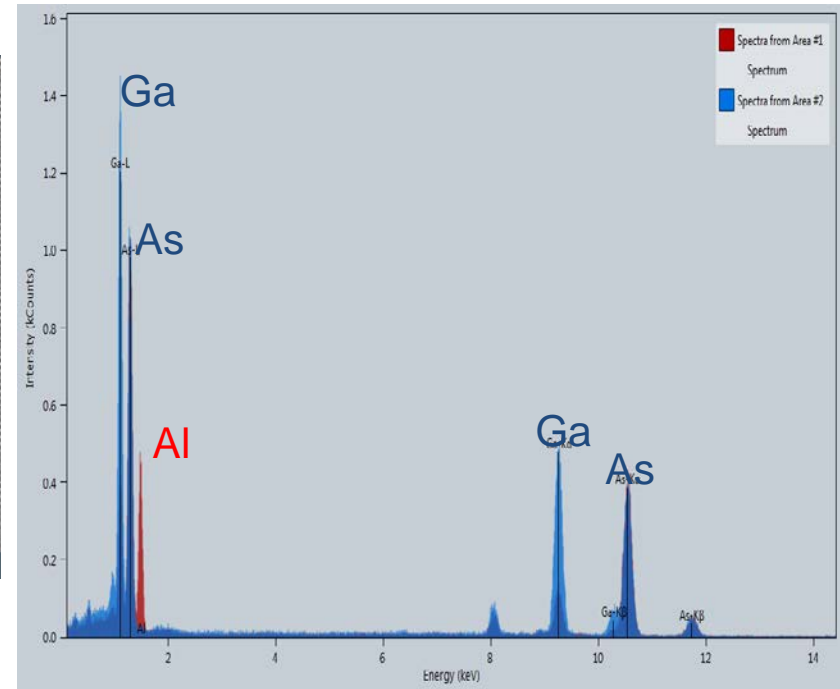
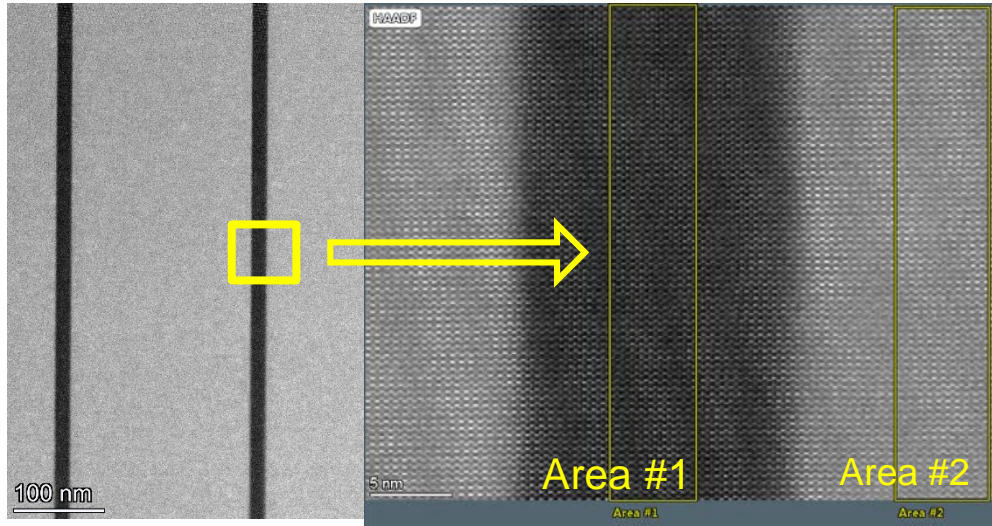
J. Mabon, C. Chen - Themis Z, MRL



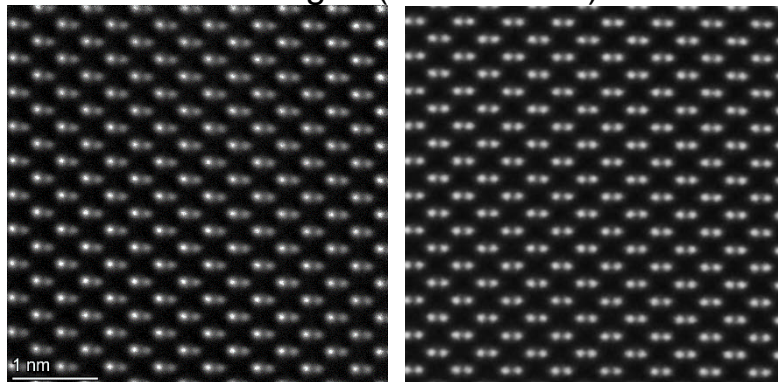


EDS Spectrum Imaging and Analysis:

AlGaAs – GaAs multilayer



DCFI HAADF images (~20 Frames)



Area #1

Area #2

2019-05-28 09:13:25 Analysis of spectrum: Spectra from Area #1

Z	Element	Family	Atomic Fraction (%)	Atomic Error (%)	Mass Fraction (%)	Mass Error (%)	Fit error (%)
13	Al	K	83.04	5.05	15.26	1.47	2.38
31	Ga	K	12.83	2.57	15.32	2.47	0.39
33	As	K	54.13	10.83	69.42	11.18	0.16

2019-05-28 09:13:25 Analysis of spectrum: Spectra from Area #2

Z	Element	Family	Atomic Fraction (%)	Atomic Error (%)	Mass Fraction (%)	Mass Error (%)	Fit error (%)
13	Al	K	0.00	0.05	0.00	0.02	0.00
31	Ga	K	51.29	10.66	49.49	7.97	0.14
33	As	K	48.71	10.12	50.51	8.12	0.24

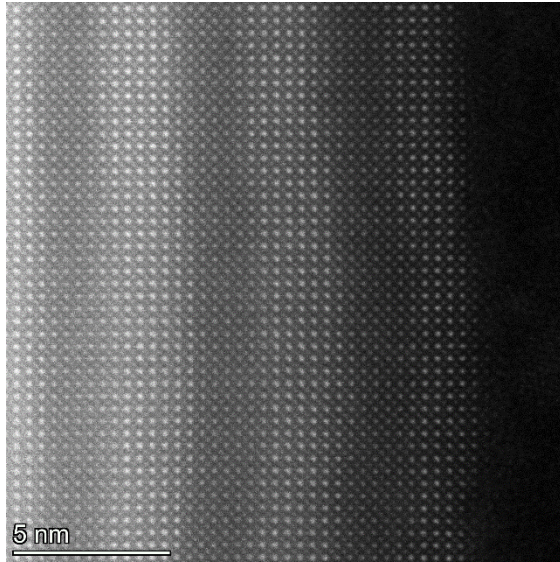
EDS 4 minute acquisition time, 50 pA, 300kV



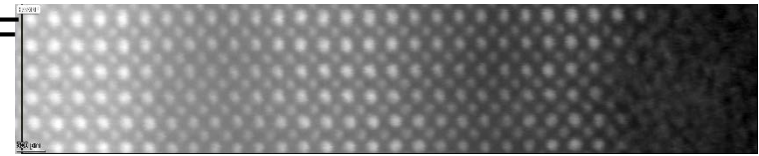


Fast EDS spectrum imaging @ high resolution: LMO/SMO

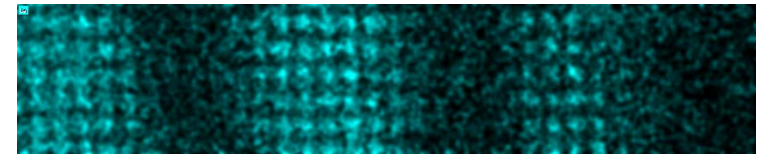
DCFI HAADF



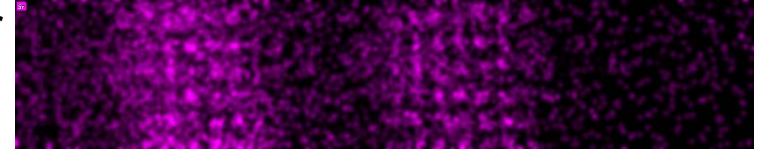
HAADF



La



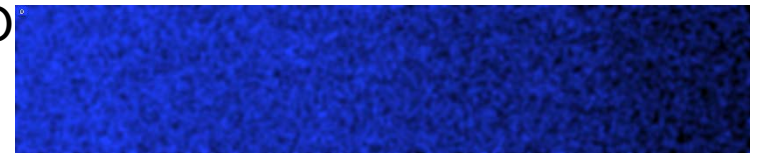
Sr



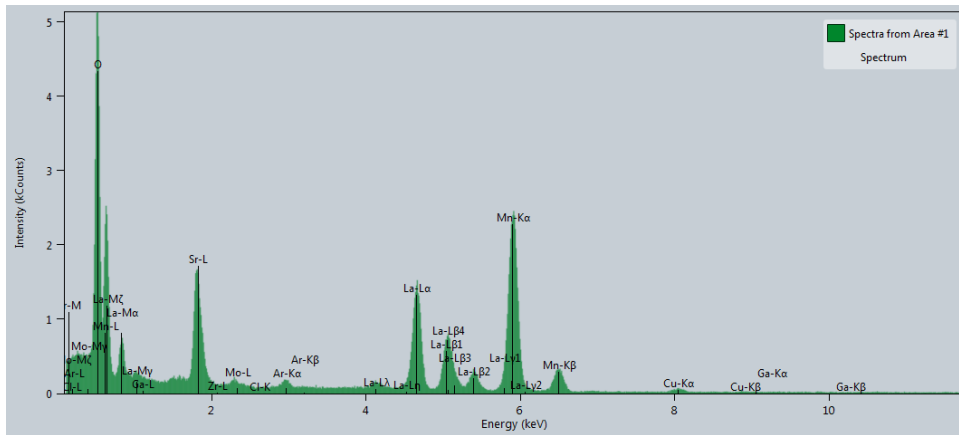
Mn



O



300KV, 140 pA, ~5 minutes



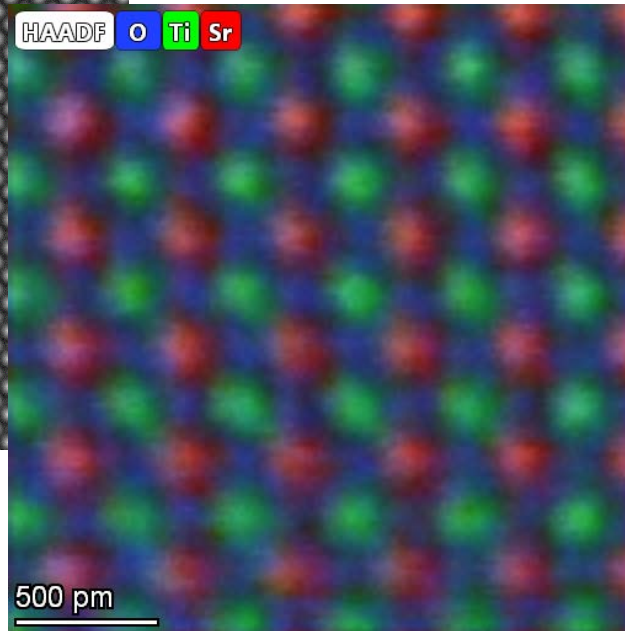
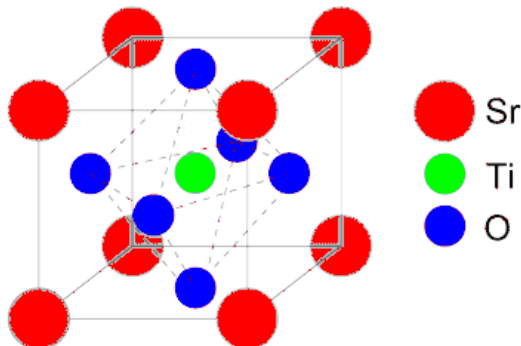
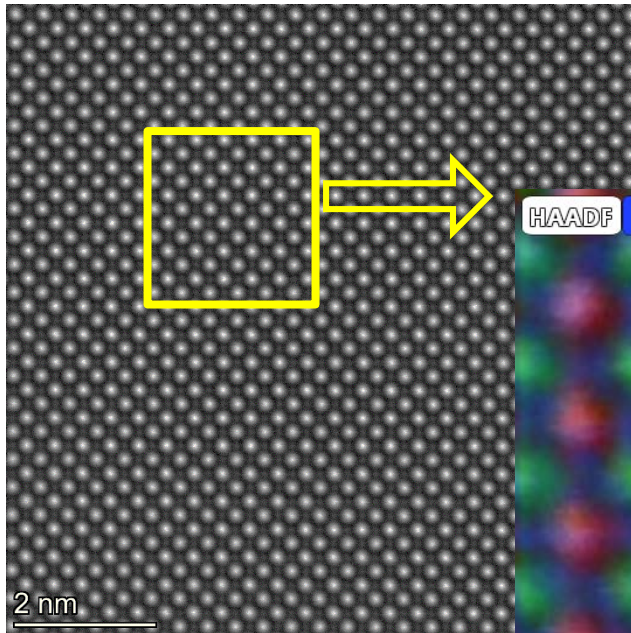
J. Mabon, C. Q. Chen - Themis Z, MRL 68





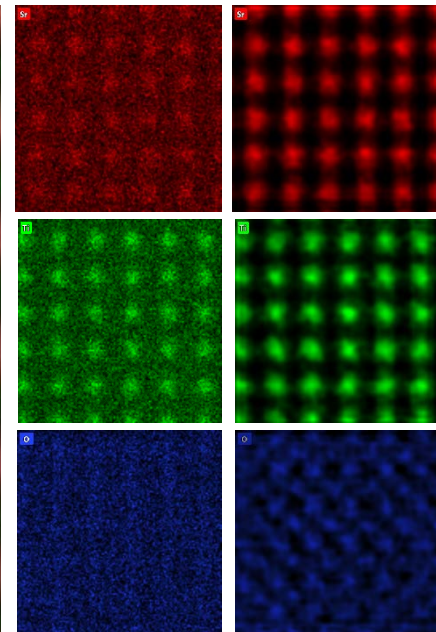
Strontium Titanium Oxide (SrTiO_3)

DCFI HAADF



Raw

Filtered



12 minute acquisition time, 100pA, 300kV

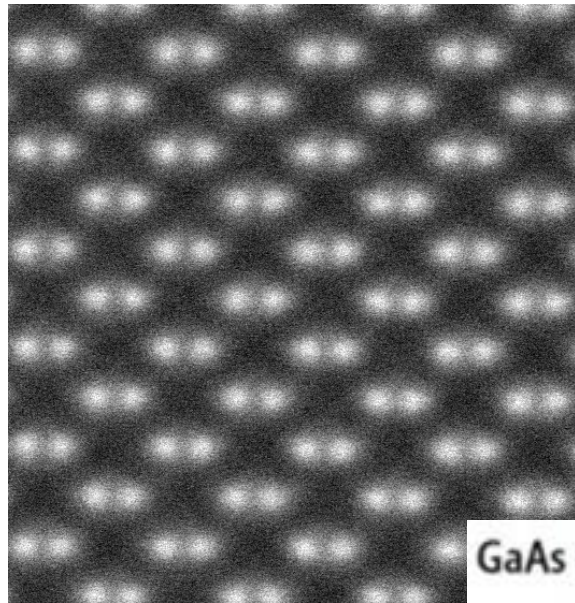
J. Mabon - Themis Z, MRL





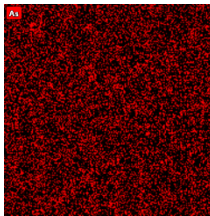
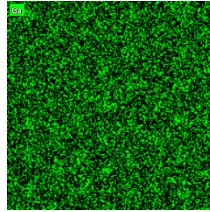
Atomic resolution EDS spectrum imaging - GaAs

HAADF

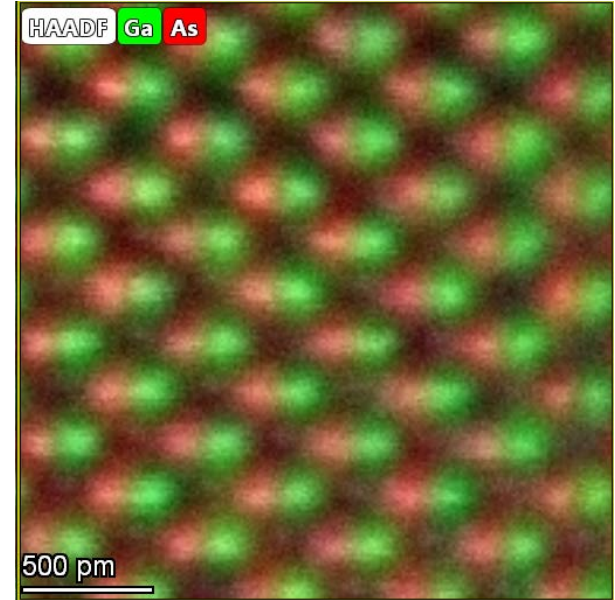
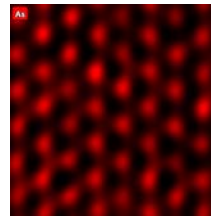
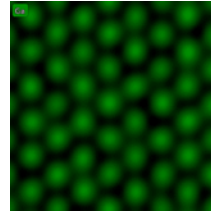


GaAs (110)

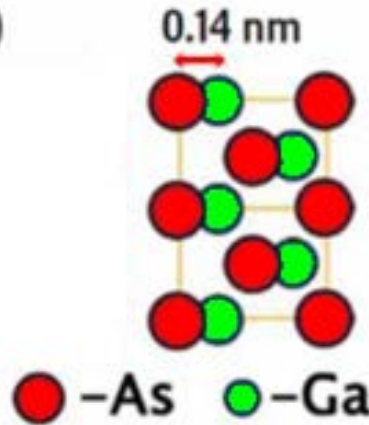
Raw



Filtered (Radial Wiener de-blur)



Overlay of filtered maps on HAADF



J. Mabon - Themis Z, MRL

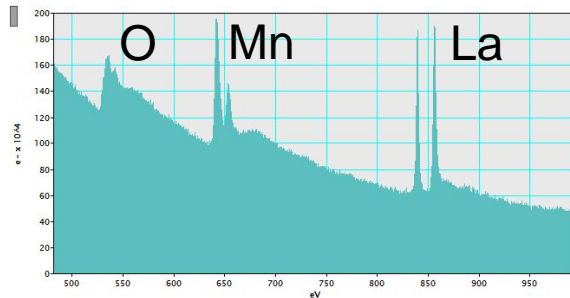
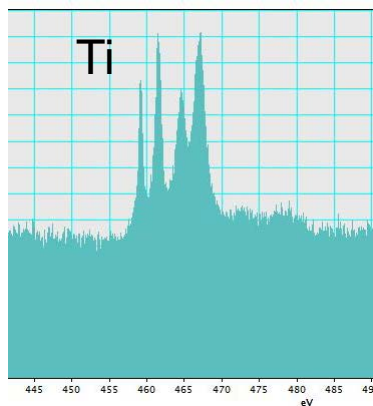
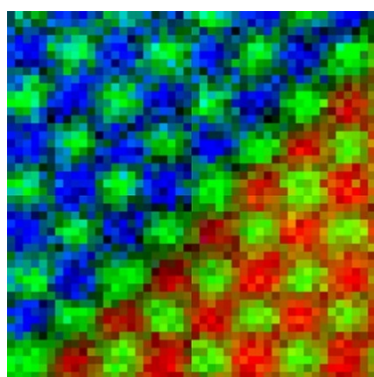
EDS 1.5 minute acquisition time, 50 pA, 300kV



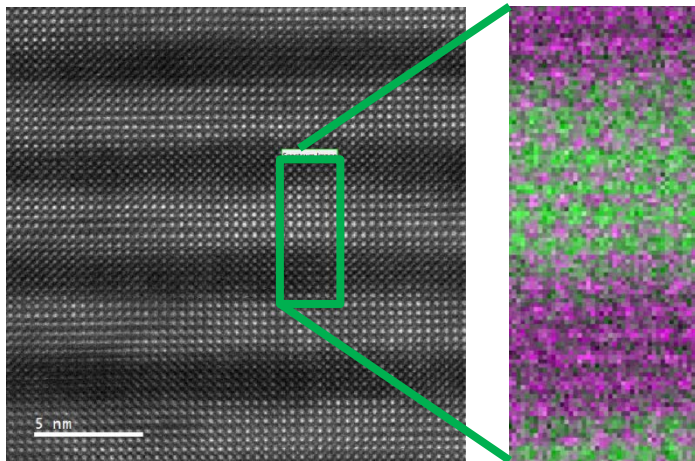


Atomic resolution EELS mapping and analysis (with monochromator):

BaTiO₃/SrTiO₃ interface



DCFI HAADF



La & Mn

Lanthanum Manganese Oxide/
Strontium Manganese Oxide Multilayer

Mn

Images - ThermoFisher Scientific - U of I Instrument Demonstration and <https://www.fei.com/products/tem/themis-z-for-materials-science/>

EELS Spectra J. Mabon

Also possible:

- Mapping of light elements
- Mapping of bonding, oxidation states
- Measurement of local electronic and optical states
- Mapping of plasmon excitations

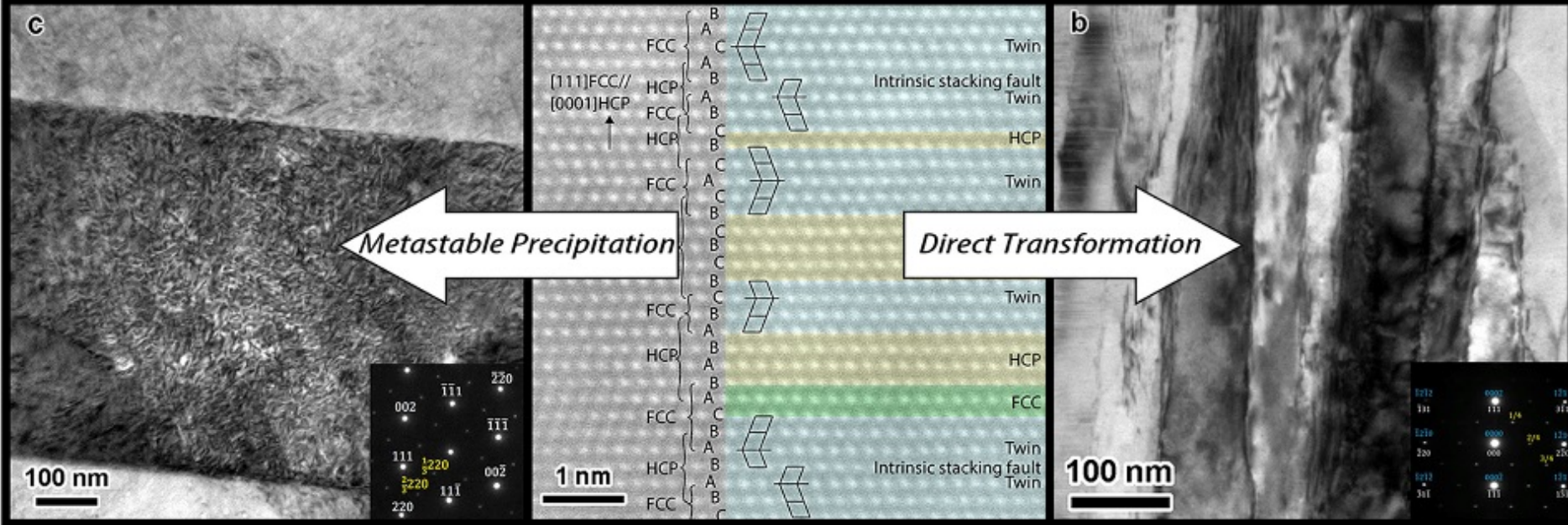




Example: Study of a defects in nanocrystalline alloy

Imaging of planar defects in the nanotwinned, nanocrystalline microstructure of a Ni-25Mo-8Cr superalloy

1066°C/30mins+650°C/48h *As deposited, nanocrystalline, nanotwinned superalloy microstructure* 650°C/48h



The HRSTEM shows the atomic ordering in the side view of a direct current magnetron sputtered film. FCC- and HCP-like ordering behavior are noted on the left; on the right FCC and HCP regions are indicated in green and yellow, and regions that contain nanotwinned FCC are indicated in blue.

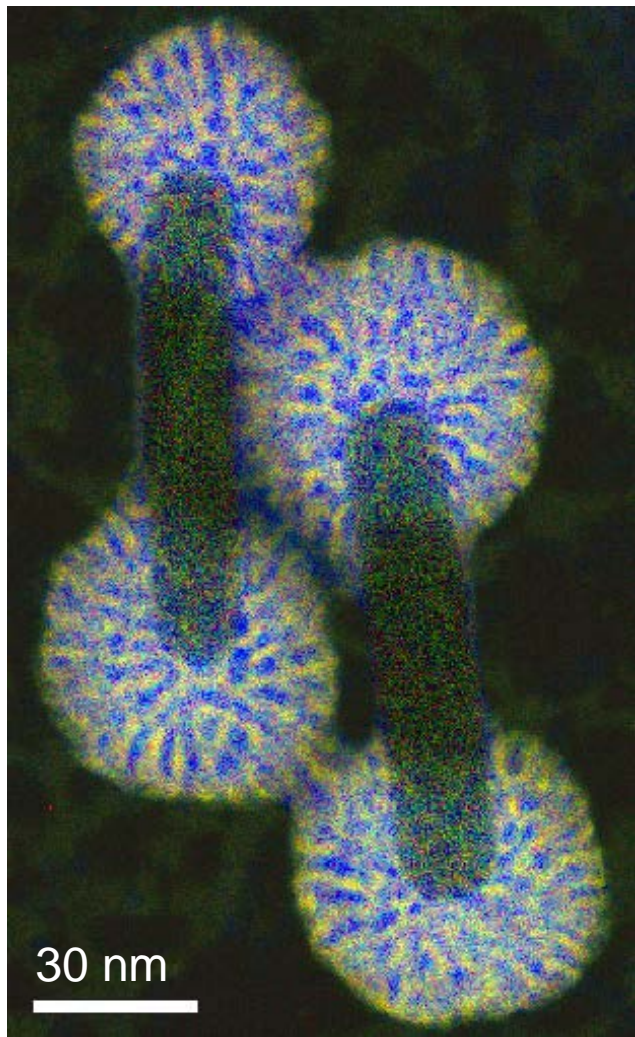
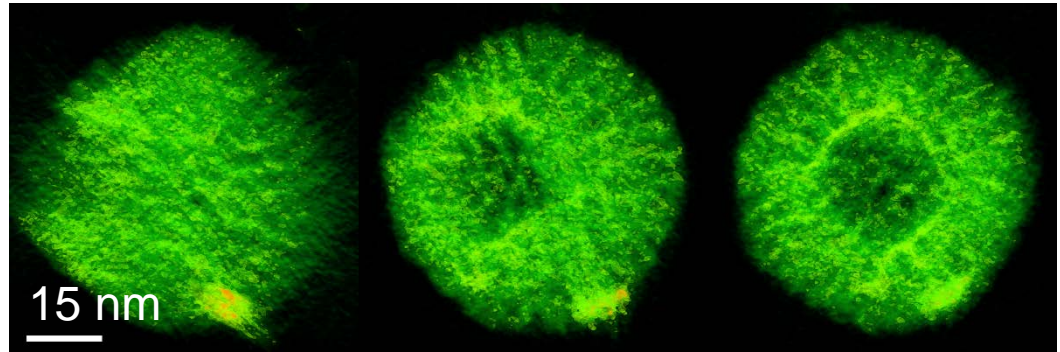
M.G. Emigh, R.D. McAuliffe, C. Chen, J.C. Mabon, T. Weihs, K.J. Hemker, J.A. Krogstad
Influence of a nanotwinned, nanocrystalline microstructure on aging of a Ni-25Mo-8Cr superalloy
Acta Mater., 156 (2018), pp. 411-419





Example: mesoporous silica coating on gold nanorods

Tomographic reconstruction allows visualization of pore size and orientation for applications such as drug delivery.



Chemical mapping at the nanoscale: electron energy loss spectral image (EELS-SI) of a mesoporous silica coating on gold nanorods. Carbon is confined in the pores in mesoporous silica.

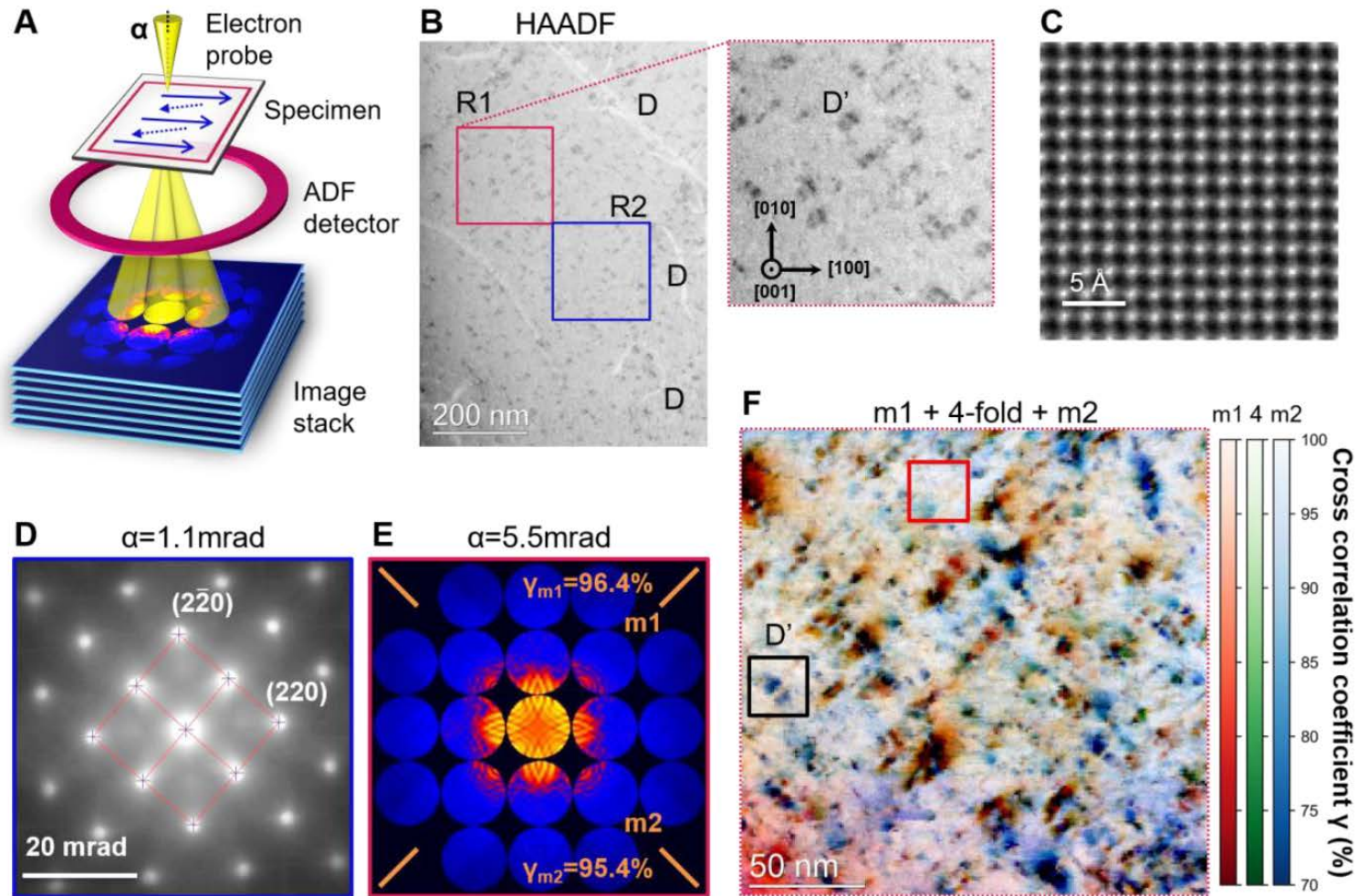
 -Carbon  -Silica

Images acquired by Blanka Janicek (Professor P. Huang Group)





Study of lattice distortions in an fcc High Entropy Alloy, Al_{0.1}CrFeCoNi

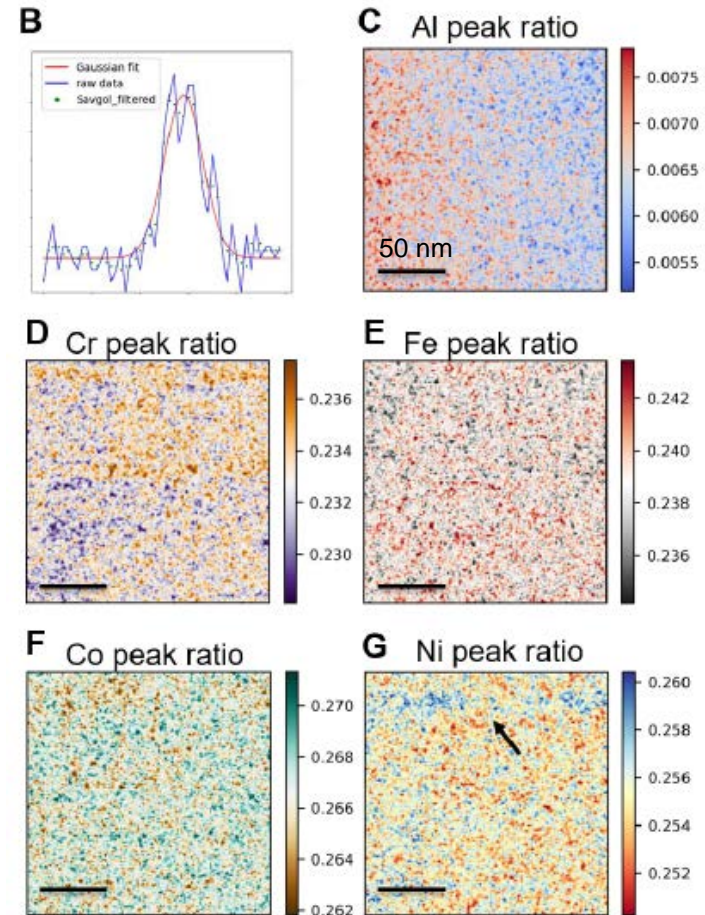
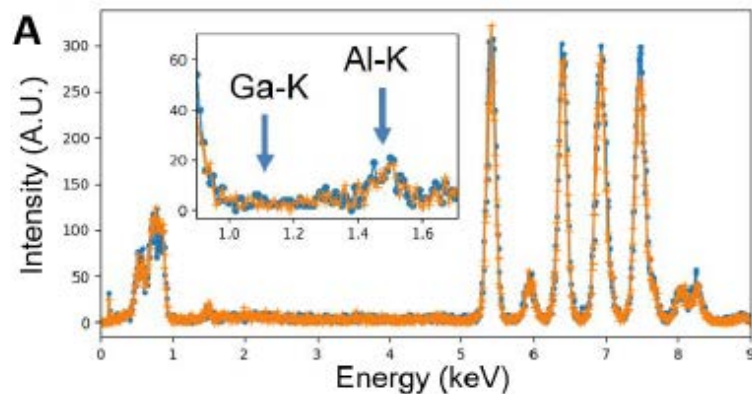


Yu-Tsun Shao, Renliang Yuan, Yang Hu, Qun Yang, Jian-Min Zuo. (2019). The Paracrystalline Nature of Lattice Distortion in a High Entropy Alloy

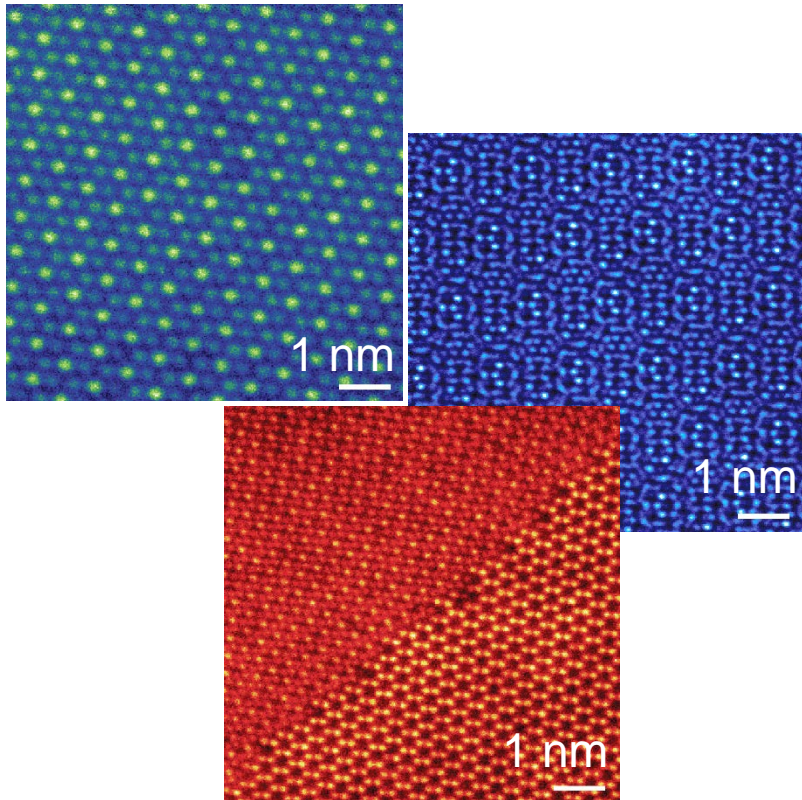


EDS elemental X-ray analysis of Al_{0.1}CrFeCoNi HEA

EDS spectrum image 180x180 pixels with step sizes of 1nm and dwell of 1s acquired about the same region as for SCBED. Total acquisition time of ~11hrs for detection of Al rich inclusions and fluctuation of composition at length scales of a few to tens of nm



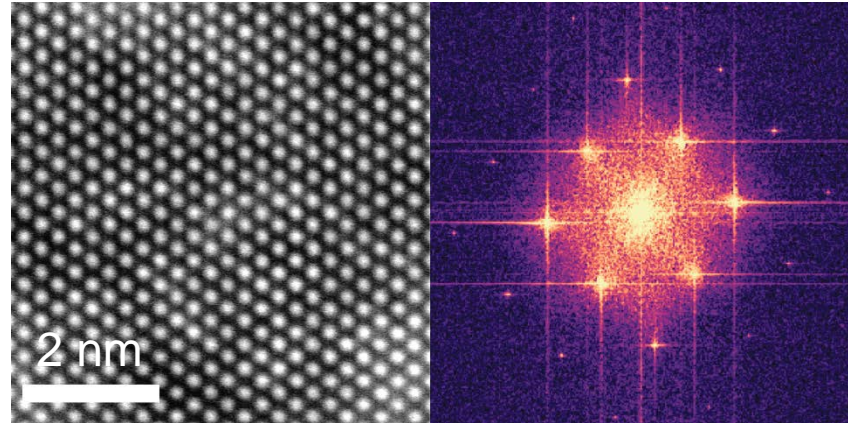
Yu-Tsun Shao, Renliang Yuan, Yang Hu, Qun Yang, Jian-Min Zuo. (2019). The Paracrystalline Nature of Lattice Distortion in a High Entropy Alloy



False-colored atomic-resolution scanning transmission electron microscope images of WSe_2

- A) Two atomic layers of WSe_2 . The two layers are rotationally aligned with one another but shifted, forming the 3R structure
- B) Moiré pattern in twisted bilayer WSe_2 where the two layers are rotated by an angle of 17 degrees
- C) A grain boundary of in bilayer WSe_2 results in a change in stacking orders across the diagonal

Images acquired by Chia-hao Lee (Professor P. Huang Group)



STEM image and FFT of cubic boron arsenide.

This material represents the experimental realization of new class of high thermal conductivity materials.

S. Li et al. High thermal conductivity in cubic boron arsenide crystals, Science 8982 (2018).

Image acquired by Yinchuan Lv (Professor P. Huang Group)

For more information start with the following resources:

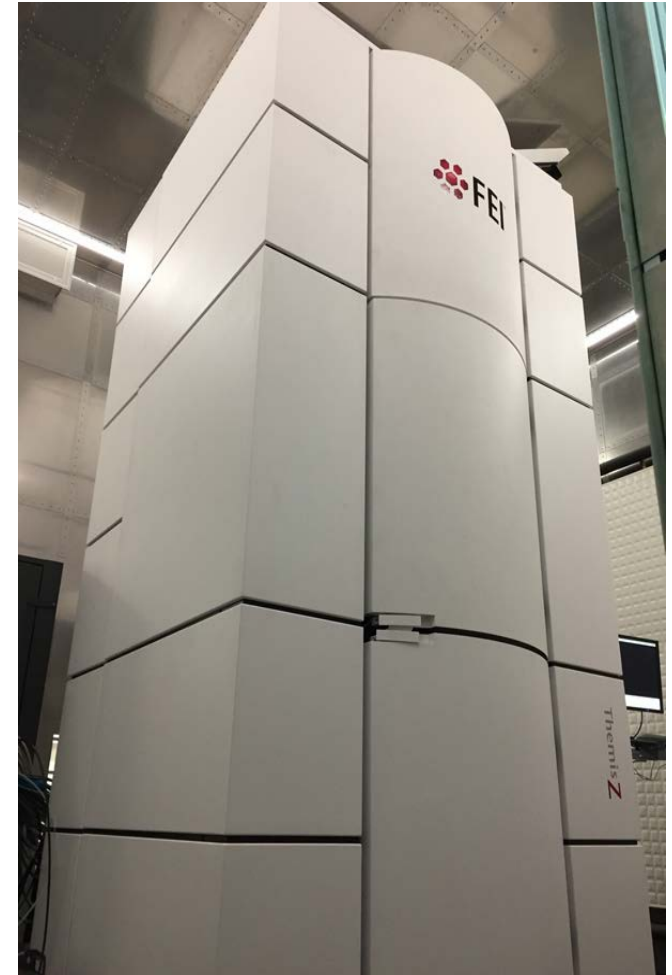
<http://mrl.illinois.edu/facilities/equipment/f-ei-themis-z-advanced-probe-aberration-corrected-analytical-temstem>

<https://www.fei.com/products/tem/themis-z-for-materials-science/>

Or

See MRL Facility Staff Members:

Dr. Jim Mabon or Dr. C.Q. Chen



Thanks to our sponsors!

PLATINUM SPONSORS



SPONSORS



LIVE STREAMING SPONSOR





The End!

Thank you!
Questions?